Biofilm formation in *Bacillus thuringiensis*

Functional analysis of three putative cyclic di-GMP signaling proteins and a potential downstream effector

Veronica Krogstad

Department of Pharmaceutical Biosciences,
School of Pharmacy

Faculty of Mathematics and Natural Sciences

UNIVERSITY OF OSLO

15/5-2012

2012

Biofilm formation in *Bacillus thuringiensis* – Functional analysis of three putative cyclic di-GMP signaling proteins and a potential downstream effector

Veronica Krogstad

http://www.duo.uio.no/

Trykk: Reprosentralen, Universitetet i Oslo

ACKNOWLEDGEMENTS

The work for this thesis was carried out at the Department of Pharmaceutical Biosciences, School of Pharmacy, University of Oslo in the time period March 2011 to May 2012 supervised by Associate professor Ole Andreas Økstad and post-doc Annette Fagerlund.

First, I would like to express my gratitude to my excellent supervisor, Associate professor Ole Andreas Økstad, who has been extremely helpful and supportive during my laboratory work period, as well as during the writing process. Thank you for being so friendly and encouraging and for allowing me to take part in your research project. The past year has been exciting and educational.

I would also like to give a big thank you to my second brilliant supervisor, post-doc Annette Fagerlund, who followed me closely from the beginning of my laboratory work period with patience and friendliness. Thank you for sharing your impressive knowledge and skill and for providing me with invaluable guidance concerning both practical and theoretical matters.

I am also indebted to all of the other people working at the Department of Biosciences, including Ewa, Veronika, Aniko, Elisabeth and professor Anne Brit Kolstø, who have all been exceptionally helpful and welcoming. You have played a major role in making my stay here so enjoyable.

Finally, I would like to thank my family and friends for all their valuable support throughout the last year.

Oslo, May 15th, 2012

Veronica Krogstad

ABSTRACT

Biofilms are communities of microorganisms establishing on surfaces like minerals, air-liquid interfaces or living material like plants or humans. Bacteria living within biofilms are protected from environmental factors like mechanical stress, antimicrobial compounds and constituents of the human immune system and may thus cause serious problems in for example medicine and in the food industry.

Bis-(3'-5')-cyclic dimeric guanosine monophosphate, also known as cyclic di-GMP (c-di-GMP), is a second messenger shown to play a central role in controlling the transition from a motile, planktonic to a sedentary biofilm-associated lifestyle in various bacteria, mostly characterized in Gram-negative species. Increased levels of c-di-GMP have been found to stimulate formation of biofilms and reduce motility. c-di-GMP is synthesized by diguanylate cyclase (DGC) enzymes containing GGDEF domains, and degraded by phosphodiesterase (PDE) enzymes containing EAL domains.

Bacillus cereus, *Bacillus thuringiensis* and *Bacillus anthracis* are members of the *B. cereus* group of Gram-positive, rod-shaped spore forming bacteria and have shown to be of great economical and medical importance. Their chromosomes exhibit a close similarity and genes encoding species-specific virulence factors are mostly plasmid-borne. While *B. anthracis* is the cause of anthrax, an acute and possible lethal disease in mammals, *B. cereus* is an important cause of food poisoning in humans, and *B. thuringiensis* a commercially utilized insect pathogen. *B. thuringiensis* 407 (Bt407) is a model strain used for studying the genetics of *B. thuringiensis*. The genome of Bt407 carries ten genes predicted to encode proteins with GGDEF and/or EAL domains. In this thesis, three of these proteins were functionally characterized: Cdg135 (containing a GGDEF and an EAL domain, both with conserved active sites required for enzymatic activity), Cdg141 (containing a GGDEF domain predicted to lack DGC activity) and Cdg113 (containing a predicted enzymatically inactive EAL domain).

Results from the current thesis indicate that Cdg135 is probably involved in controlling biofilm formation and motility in Bt407, possibly by exhibiting DGC activity and catalyzing the synthesis of c-di-GMP. Cdg135 was shown to positively affect the transcription of a gene encoding a predicted cell wall bound adhesion protein. This gene, an ortholog to the *B. cereus* ATCC 14579 gene with locus tag BC_1060, referred to as *bspA* (*Bacillus* surface protein A) in the current thesis, is located downstream of a c-di-GMP-sensitive "on-riboswitch", and the corresponding BspA gene product was shown to stimulate biofilm formation in Bt407. The

effects of BspA are, however, not essential for the ability of Bt407 to form biofilms, as Cdg135 over-expression could compensate for *bspA* loss. Cdg141 did not seem to influence biofilm formation in Bt407, but excessive amounts of Cdg141 in the cell probably results in toxic effects, as the over-expression strain was deficient in growth. Results from biofilm assays indicated that Cdg113 has positive effects on biofilm formation in Bt407. As Cdg113 is predicted to lack DGC activity, it could function as an effector molecule, regulating biofilm formation upon binding c-di-GMP.

CONTENTS

ACKNOWLEDGEMENTS 4

ABSTRACT 5

CONTENTS 7

CHAPTER 1: INTRODUCTION 12

1.1 The *Bacillus cereus* group of bacteria 12

1.2 Biofilms 13

1.3 Biofilm formation 15

1.4 Regulation of biofilm formation 16

1.5 Regulation of biofilm formation in Gram-positive bacteria 17

1.5.1 SinI/SinR system 17

1.5.2 Regulation of flagellar motility 18

1.5.3 Regulation of biofilm formation in the *B. cereus* group 19

1.6 Cyclic di-GMP 21

1.6.1 Production and degradation of c-di-GMP 22

1.6.2 Signal inputs 23

1.6.3 Effector components 23

CHAPTER 2: BACKGROUND AND AIM OF THE THESIS 25

2.1 Background for the thesis 25

2.2 Aim of the thesis 26

CHAPTER 3: MATERIALS 28

3.1 Bacterial strains 28

3.2 Vectors 28

3.3 Primers 29

3.4 Enzymes 29

3.5 Molecular weight standards 30

3.6 Reagents and solutions provided 30
3.7 Solutions prepared at the lab 33
3.8 Growth media 36
3.9 Commercial kits 38
3.10 Various equipment 39
CHAPTER 4: METHODS 41
4.1 Growth of bacteria 41
4.1.1 *B. thuringiensis* 407 41
4.1.2 *E. coli* XL1-Blue 41
4.2 Genomic DNA (gDNA) preparations 41
4.3 Polymerase chain reaction (PCR) 42
4.4 Preparation of RNA 43
4.5 Isolation and precipitation of plasmids 44
4.5.1 Isolation of plasmids 44
4.5.2 Ethanol precipitation of DNA 45
4.6 Restriction digests 45
4.7 Agarose gel electrophoresis 46
4.8 Spectrophotometry 47
4.9 Transformation 47
4.9.1 Preparing electrocompetent *B. thuringiensis* cells 47
4.9.2 Electroporation 47
4.10 Biofilm screening assay 48
4.11 Microarray analysis 48
4.11.1 Precipitation of RNA 50
4.11.2 cDNA preparation 50
4.11.3 Resuspension of Cy3 and Cy5 51
4.11.4 NHS-Ester Containing Dye Coupling Reaction 51

4.11.5 Dye-Coupled cDNA purification 51
4.11.6 Concentration of labeled cDNA 51
4.11.7 Prehybridization 52
4.11.8 Hybridization 52
4.11.9 Analysis 54
4.12 Reverse transcriptase quantitative PCR (RT-qPCR) 54
4.12.1 DNase-treatment and cDNA synthesis 55
4.12.2 Determination of E and r^2 for the primer pairs 56
4.12.3 Negative controls 56
4.12.4 Analyzing expression of target genes 57
4.13 Designing primers 57
CHAPTER 5: RESULTS 58
5.1 Characterization of the *cdg135* deletion mutant (Bt407Δ135) 58
5.1.1 Identification 58
5.1.2 Growth curves with observations for motility 59
5.1.3 RNA isolation from Bt407 wild type and *cdg135* deletion mutant 60
5.1.4 Transcriptional analysis using microarrays 61
5.1.5 RT-qPCR to confirm up-regulation of genes 63
5.2 Characterization of interaction between BspA and Cdg135 67
5.2.1 Preparation and/or confirmation of strains to be tested for growth, motility and biofilm formation 68
5.2.2 Growth curves with observations for motility 72
5.2.3 Biofilm formation 73
5.3 Characterization of the *cdg141* deletion mutant (Bt407Δ141) 76
5.3.1 Identification 76
5.3.2 Growth curves with observations for motility 77
5.3.3 RNA isolation from Bt407 wild type and *cdg141* deletion mutant 78

5.3.4 Transcriptional analysis using microarrays 79
5.4 Characterization of Cdg141 80
5.4.1 Preparation and/or confirmation of strains to be tested for growth, motility and biofilm formation 81
5.4.2 Growth curves with observations for motility 82
5.4.3 Biofilm assays 85
5.5 Characterization of Cdg113 87
5.5.1 Preparation and/or confirmation of strains to be tested for growth, motility and biofilm formation 88
5.5.2 Growth curves with observations for motility 89
5.5.3 Biofilm assays 90
CHAPTER 6: DISCUSSION 92
6.1 Role of Cdg135 in biofilm formation in Bt407 92
6.1.1 Function in biofilm formation and motility 92
6.1.2 Identification of genes differentially expressed in a *cdg135* deletion mutant 93
6.2 Role of BspA in biofilm formation in Bt407 95
6.2.1 BspA 95
6.2.2 Interaction between Cdg135 and BspA 96
6.3 Role of aldo/keto reductases and MFS transporters 96
6.4 Role of Cdg141 in biofilm formation in Bt407 97
6.5 Role of Cdg113 in biofilm formation in Bt407 98
6.6 Conclusions 99
6.7 Future perspectives 99
APPENDICES 101
Appendix 1: Analysis of microarray experiment comparing *cdg135* deletion mutant and wild type 101
Appendix 2: Analysis of microarray experiment comparing *cdg141* deletion mutant and wild type 103

REFERENCES 105

CHAPTER 1: INTRODUCTION

1.1 The *Bacillus cereus* group of bacteria

The *Bacillus- cereus* group of bacteria comprises seven species of rod shaped facultative aerobic Gram-positive spore formers: *B. cereus sensu stricto*, *Bacillus anthracis*, *Bacillus thuringiensis, Bacillus mycoides*, *Bacillus pseudomycoides*, *Bacillus weihenstephanensis* and *Bacillus cytotoxicus* [1-3]. *B. anthracis*, *B. cereus* and *B. thuringiensis* have proven to be of great economic and medical importance and their genetics have therefore been thoroughly investigated. Their chromosomes exhibit a close similarity and they can therefore be considered to be part of the same species [4]. However, their characteristics, including their potential to cause disease in animals and humans, differ strongly between the species. The chromosome carries genes encoding various virulence factors and enterotoxins, while the genes encoding species-specific virulence factors are mostly plasmid-borne [4].

B. anthracis causes anthrax in mammals, an acute and potentially lethal disease. The bacterium causes disease through skin lesions, by accessing the gastrointestinal (GI) tract or by inhalation [5]. *B. anthracis* contains two large plasmids essential for its virulence, pXO1 of 182 kb and pXO2 of 95 kb [6, 7]. pXO1 encodes the anthrax toxin subunits including protective antigen (PA), lethal factor (LF) and edema factor (EF). pXO2 encodes a polyglutamate capsule protecting the bacterium from phagocytes. Research on *B. anthracis* has intensified following the terror attacks taking place in the United States in 2001 where spores were spread by letters, infecting 17 people of which five died [8]. The spores of *B. anthracis,* and *Bacillus* species in general, are extremely resistant to environmental influences like heat, pressure and chemical agents. *B. anthracis* bacteria can be released to the soil from decomposed animals that suffered from anthrax, and sporulate upon contact with air. Ingestion by a host leads to germination, production of virulence factors and development of disease in the host [1].

B. cereus sensu stricto is an opportunistic pathogen found ubiquitously in nature, and the spores germinate when they come in contact with organic material or land inside an insect or animal host [9]. This germination process usually begins in response to specific nutrients like amino acids, sugars and derivates of purine stimulating germinant receptors [10]. *B. cereus* is an important cause of food poisoning in humans, and can lead to two different clinical syndromes [2]. The diarrheal syndrome gives profuse diarrhea combined with abdominal pain

and cramps beginning 8 to 16 hours after ingestion of the contamination source, often proteinaceous foods. These symptoms are caused by enterotoxins, and recovery is usually observed within 12 hours. The emetic syndrome is characterized by nausea, vomiting, abdominal cramps, and in some cases diarrhea. The emetic toxin, cereulide, is produced by a non-ribosomal peptide synthetase encoded by the *ces* gene cluster located on a large plasmid [11] and gives rise to symptoms after an incubation period of 1 to 5 hours. The rapid onset indicates that the disease is an intoxication caused by toxin preformed in foods. The contaminated foods are often based on rice or pasta and symptoms usually disappear within 24 hours [2]. There has, however, been deaths in children due to this particular toxin [12, 13]. It is important to note that *B. cereus* is also a symbiont that can colonize intestinal systems of certain hosts asymptomatically [8]. *B. cereus* can also cause several non-gastrointestinal diseases, most often in individuals with weakened immune system, including neonates, intravenous drug abusers, patients with wounds from trauma or surgery and patients with indwelling catheters [9]. These diseases include ocular infections, septicemia, endocarditis, central nervous system infections and respiratory tract infections [2].

B. thuringiensis is an insect pathogen used commercially as a biopesticide. Upon sporulation, it forms intracellular protein crystals [1]. After ingestion by insect larvae, these crystals solubilize due to the alkaline pH in the insect gut, and are cleaved by gut proteases produced by the larvae itself. Active toxin is then released that creates pores in the midgut epithelial cell membranes of the larvae. The cells lyse and the larvae's GI-system is disturbed with the consequence that it stops eating and ultimately dies. By lysing the cells, the bacteria also gain access to the larvae's hemocoel [1]. Genes encoding the Bt toxins (Cry and Cyt) are usually located on large plasmids [8]. *B. cereus* principally differs from *B. thuringiensis* only by lacking the ability to form protein crystals during sporulation, and *B. thuringiensis*, like *B. cereus sensu stricto*, can therefore be considered an opportunistic pathogen in animals and humans. The intestinal systems of insects are thought to be the bacteria's natural living reservoir [1, 14].

1.2 Biofilms

There exists no official definition of biofilms, but suggestions are among others "communities of microorganisms attached to a surface" [15] and "a thin coating compromised of living material" [16]. Almost all bacteria are thought to exist in biofilms in their natural habitats [15]. A biofilm can consist of one single microbial species or multiple different species and

biofilms can form on non-living surfaces like minerals and air-liquid interfaces as well as living surfaces like plants, other microbes and animals [16]. Bacteria living in biofilms can cause serious medical problems. They have in certain cases been proven to be up to 1000-fold more resistant to antibiotics when growing in a biofilm compared to planktonic cells and are protected from the immune system of the host [17]. Biofilms can form on medical implants and contact lenses and are also involved in diseases like cystic fibrosis and periodontitis. Biofilms also cause trouble in the food industry as established biofilms are difficult to remove/decontaminate and constitute a possible source of food contamination [18]. The ability to form biofilms has been shown to be a common feature among almost all species of bacteria, although the signals and pathways leading to biofilm formation and disruption vary enormously. However, according to Lemon *et al.*[19], all biofilms seem to have certain features in common:

- Constituent cells are held together by an extracellular matrix.
- Biofilm development occurs in response to extracellular signals, both environmental and self-produced.
- Bacteria living in biofilms are protected from a broad spectrum of environmental influences, including antibiotics and the human immune system.

The biofilm matrix may consist of exopolysaccharides (EPS), proteins and sometimes DNA [16]. **Exopolysaccharides** often constitute a large part of the matrix and are often necessary for the formation of multilayered biofilms and sometimes also for adhering to surfaces. Several families of **proteins** are also important constituents of biofilms. Pili and fimbriae are thought to help cells adhere to each other and to surfaces, and have in certain bacteria shown to be up-regulated during biofilm formation [20]. MSCRAMMs (microbial surface components recognizing adhesive matrix molecules) are adhesive proteins known to be involved in the formation of biofilms in Gram-positive bacteria, including the Bap proteins first identified in *Staphylococcus aureus* [21] and subsequently found in several species [22]. They appear to be secreted into the medium and to be involved in intercellular interactions. Proteins binding to carbohydrates like lectin and glucan, also seem to contribute to interactions between cells and influence the structure of biofilms in species like *Pseudomonas aeruginosa* [23, 24] and *Streptococcus mutans* [25]. A subgroup of self-associating autotransporters is shown to be involved in biofilm formation in some Gram-negative bacteria by binding cells together [26]. **Extracellular DNA (eDNA)** is additionally found to contribute to the matrix of biofilms in species like *P. aeruginosa* and *B. cereus* [27, 28].

The architecture/structure of biofilms depends on physical conditions as well as biological factors and can be divided in two: **irregular topology** with mushroom-like structures separated by empty cavities and low surface coverage and **flat topology** with compact layers and high surface coverage [16].

1.3 Biofilm formation

Biofilm formation can be defined as "a developmental process in which bacteria undergo a regulated lifestyle switch from a nomadic unicellular state to a sedentary multicellular state where subsequent growth results in structured communities and cellular differentiation" [19]. An illustration of formation and dispersion of biofilms is shown in Figure 1.

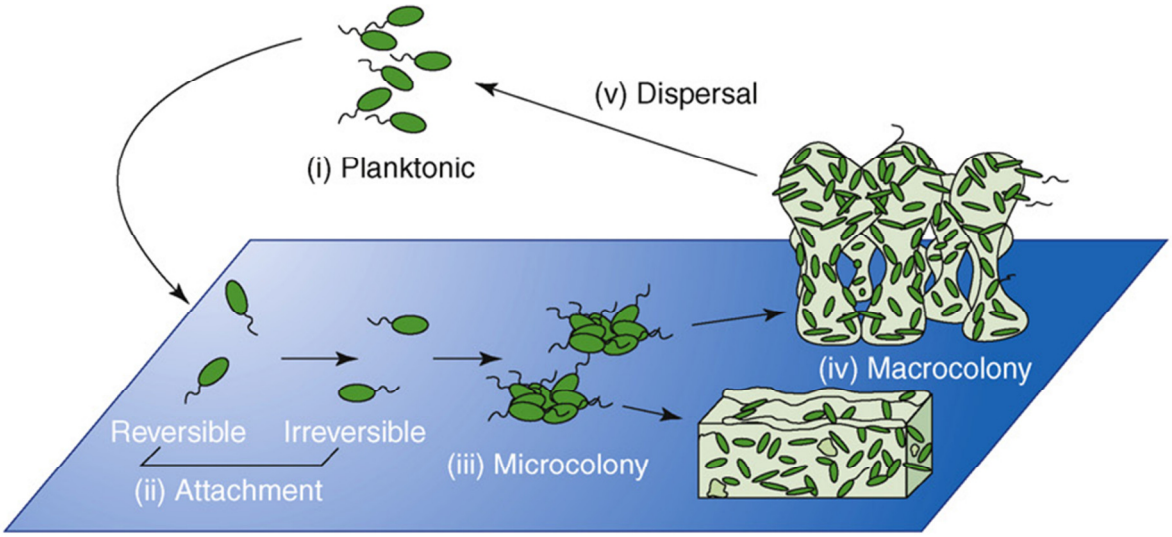

Figure 1: Model for formation and dispersion of biofilms. Bacteria are first transiently attached to a surface and can either reverse or strengthen this weak attachment. If the attachment is strengthened and the bacteria become irreversibly attached, they can form small clusters of cells called microcolonies. These can grow to form macrocolonies exhibiting different types of architecture, where the cells are embedded in an extracellular matrix. Cells can finally be released from the macrocolonies and become planktonic. Figure obtained from Monds *et al*. [29].

General hypothetical models for biofilm development adjusted to fit both non-motile and motile species have been constructed [19]. When environmental conditions favor biofilm formation, non-motile bacteria, like *Staphylococcus* species, may increase their expression of protein and polysaccharide adhesins that facilitate cell-cell adherence as well as adherence to surfaces, and production and secretion of exopolysaccharides is initiated [30, 31]. Motile species, however, can use their flagella to reach a surface when conditions are such that biofilm formation is favorable [32, 33]. They may adhere transiently to this surface by the use

of pili and flagella and initiate production of adhesins (e.g. proteins and polysaccharides) ensuring permanent attachment [16]. Motility may then be down-regulated [34, 35] and production of extracellular matrix is initiated [36]. Biofilms can be divided into two categories; monolayer biofilms, where bacteria are only attached to the surface, and multilayered biofilms consisting of bacteria attached both to the surface and to neighboring bacteria [16]. The monolayer biofilm is favored when the dominating interactions occurs between cell and surface rather than between cells, while the multilayer biofilm is favored when bacteria interacts with surfaces and with other bacteria. A model for studying biofilms in Gram-negative motile species has been made by dividing the formation into five genetically distinct stages [19]:

- Initial surface attachment
- Monolayer formation
- Migration to form multilayered microcolonies
- Production of extracellular matrix
- Biofilm maturation with characteristic three-dimensional architecture

1.4 Regulation of biofilm formation

The signals initiating and the mechanisms used to form and disperse a biofilm are complicated and only partly understood, and may vary greatly between different bacterial species. A general overview of regulation mechanisms common to a broad spectrum of bacteria is given by Karatan *et al.*[16]. Many different types of environmental signals influence formation of biofilms, among them **mechanical** signals. Bacteria must be able to sense surfaces at which they can attach, and flagella seem to be involved in this. Expression of genes encoding flagella and synthesis of components of the biofilm is inversely regulated in species like *P. aeruginosa* [37]. In other species like *Bacillus subtilis*, flagella function is not regulated transcriptionally, but rather by arresting flagellar rotation upon biofilm formation [34]. Bacteria sense availability of **nutrients** and the accessible amounts of specific compounds have great impact on the probability of biofilm formation. Some bacteria join biofilms in response to nutrient limitation while others are more likely to form biofilms in nutrient-rich surroundings. Availability of glucose stimulates biofilm formation in *Staphylococcus epidermis* and *Streptococcus mutans,* among others [38, 39]. **Iron and phosphate** are examples of inorganic molecules that can both activate and repress biofilm formation. Low concentrations of iron reduces biofilm in *P. aeruginosa* [40] while biofilm

formation in *S. epidermis* is enhanced when iron concentrations decreases [41]. **Osmolarity** of the environment can also affect biofilm formation and high osmolarity is shown to reduce biofilm formation in *Pseudomonas fluorescens* [42]. Bacteria can additionally respond to **host derived molecules** and **antimicrobial compounds** by forming a biofilm, probably most often to increase survival. *Vibrio cholerae* increases biofilm formation in response to bile acids, and bacteria within biofilms are shown to be less vulnerable to the toxicity of these acids compared to planktonic cells [43]. *P. aeruginosa* and *Escherichia coli* increase their formation of biofilms when exposed to aminoglycosides [44]. **Quorum-sensing** is an intercellular communication system used by bacteria, making it possible to sense and respond to different cell densities. Small molecules called autoinducers are responsible for this type of signaling and are produced, secreted and recognized by the bacteria. *S. aureus* uses an autoinducer peptide (AIP) for signaling, and activation of the quorum sensing system in this species decreases biofilm formation [45]. **Numerous secondary messenger and protein networks** are also involved in regulation of biofilm formation, including bis-(3'-5')-cyclic dimeric guanosine monophosphate (cyclic di-GMP), two-component systems (TCS) and various transcriptional regulators [16].

Dispersion of biofilms may be initiated if the environment inside the biofilm is affected by lack of nutrients or increase in toxic waste products, or if the external environment changes [16].

1.5 Regulation of biofilm formation in Gram-positive bacteria

B. subtilis is a Gram-positive rod-shaped bacterium that has been used as a model system for studying many fundamental biological processes, including biofilm formation. *B. subtilis* cells are flagellated and motile as individual cells but begin to grow in chains forming parallel bundles upon biofilm development [19]. They form a floating biofilm, or pellicle, at the air-liquid interface when reaching a certain cell density. When the incubation period is prolonged, the pellicle wrinkles and some cells begin to grow as aerial projections called fruiting bodies. The tips of these have proven to be favorable locations for sporulation [19].

1.5.1 SinI/SinR system

The extracellular matrix of *B. subtilis* biofilms consists mainly of EPS and the protein TasA [46]. The transcriptional regulator Spo0A and the sigma factor σ^H regulate the operon *epsA-O* [47, 48], in which genes encode enzymes responsible for EPS synthesis and export. Genes within the operon *tapA-sipW-tasA* encode proteins involved in the formation of other

components of the extracellular matrix: TasA is an essential component for structural integrity of the matrix, and creates a network by organizing itself in thin, long appendages [46]. TapA (previously denoted YqxM) anchors TasA to the cell wall and is involved in controlling the polymerization of TasA. Upon contact with D-tyrosine, TapA is released from the cell wall along with TasA [49]. *sipW* encodes a signal peptidase that converts the pre-proteins TapA and TasA into their mature forms. SipW is recently also shown to have a second role, in inducing the expression of the *tapA-sipW-tasA* and *epsA-O* operons when *B. subtilis* is forming biofilms on solid surfaces [50]. The transcriptional regulator SinR represses transcription of both operons (*epsA-O*, *tapA-sipW-tasA*), thereby inhibiting biofilm formation and promoting motility and cell separation [51]. For this reason, SinR is called the master regulator of the lifestyle switch in *B. subtilis*. Spo0A is involved in inducing the expression of *sinI* [52]. SinI antagonizes the repression of SinR by binding to SinR directly, and favors biofilm formation [53]. Slr is a regulatory protein inducing transcription of the *tapA-sipW-tasA* operon, and the gene encoding this protein is negatively controlled by SinR [54]. YlbF and YmcA are other identified proteins involved in inducing biofilm formation in *B. subtilis* [55]. An overview of some of the factors involved in regulation of biofilm in *B. subtilis* is shown in Figure 2.

1.5.2 Regulation of flagellar motility

Flagella are molecular machines consisting of around 30 proteins. A motor located at the base of the flagellum rotates the extracellular helical filament by using energy derived from the proton motive force [34]. FliG subunits are attached to the flagellar basal body and transduce energy from the MotA-MotB proton channel into rotational energy of the flagellum. In *B. subtilis*, EpsE, encoded within the *epsA-O* operon required for synthesis of EPS, is shown to alter the interaction between FliG and MotA in the same manner as a clutch, disengaging the rotor from its power supply. When biofilm formation is induced and the *epsA-O* operon is expressed, EpsE ensures that the flagella do not rotate and disrupt the biofilm, avoiding the need to regulate flagellar expression at a transcriptional level [34]. In *E. coli*, the flagellum is similarly composed of the proton channel MotA-MotB and the motor protein FliG. The protein YcgR is shown to bind to the flagellar motor and inhibit rotation. It is less clear exactly where and how this interaction occurs, but it is shown that c-di-GMP binds to YgcR. Motility decreases as c-di-GMP increases and YcgR is necessary for this effect [35].

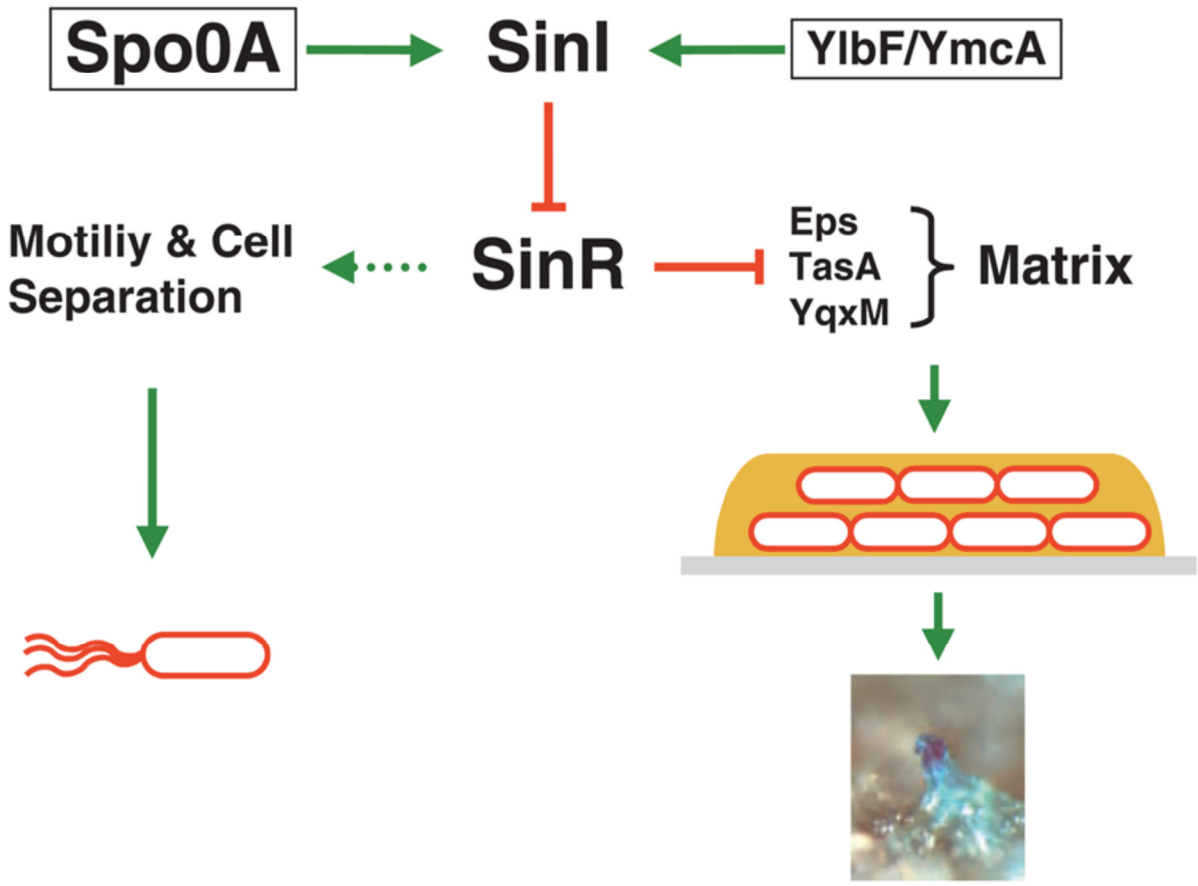

Figure 2: Regulation of biofilm formation in *B. subtilis*. SinR is considered the main regulator of the switch between the planktonic and biofilm associated lifestyles in *B. subtilis*. SinR repress transcription of genes responsible for formation of components of the extracellular matrix of the biofilm and stimulates thereby motility and cell separation. SinI antagonizes SinR activity by direct protein-protein interaction, allowing expression of biofilm associated genes. Spo0A is a transcriptional regulator inducing expression of *sinI*. The proteins YlbF and YmcA are also involved in inducing biofilm formation in *B. subtilis*. Figure obtained from Lemon *et al*. [19]

1.5.3 Regulation of biofilm formation in the *B. cereus* group

The formation of biofilms in the *B. cereus* group has not been studied to the same degree as in *B. subtilis*, but one is beginning to reveal some of the mechanisms involved also in these species. Oosthuizen *et al*. [56] presented in 2002 studies of the proteomes of *B. cereus* cells in biofilms formed on glass wool. Both cells growing in biofilms, and planktonic cells growing in the presence of glass wool, showed up-regulation of the protein YhbH and it was suggested a role of this protein in the switch from the planktonic to the biofilm associated lifestyle in *B. cereus*.

In 2005, Auger *et al*. [57] discovered that the signaling factor autoinducer-2 (AI-2) inhibited formation of biofilms in *B. cereus* strain ATCC 10987 in a concentration dependent matter.

AI-2 was also shown to promote the release of a large proportion of cells from already established biofilms. The bacterium was proven to both synthesize and recognize this factor. In other species, AI-2 controls several cellular processes like production of pathogenicity factors, toxins and formation of biofilm containing mixed species [57].

In a study by Hsueh *et al*. from 2006 [58], it was shown that in *B. cereus* strain ATCC 14579, a deletion mutant of the *plcR* gene encoding a regulator of extracellular virulence factors, significantly enhanced biofilm formation compared to the wild type strain. The mutant also produced increased amounts of a biosurfactant involved in formation of biofilms.

In 2006, Wijman *et al*. [59] were the first to state that *B. cereus* predominantly formed biofilms at the air-liquid interface. They studied biofilm formation in 56 different strains and found that the formation was strongly dependent on incubation time, temperature, medium and type of strain. They also suggested that biofilms were favorable locations for sporulation.

In 2008, Hsueh *et al*. [60] found that a *codY* disruption mutant in *B. cereus* UW101C was deficient in biofilm formation compared to the wild type (fourfold reduction). They suggested that CodY repressed the production of an extracellular protease in response to amino acids and intracellular levels of GTP, and thereby influenced biofilm formation. The CodY protein was further investigated by Lindbäck *et al*. [61] who showed that *B. cereus* CodY repressed expression of the operon *tapA-sipW-tasA* and the *sinR* and *sinI* genes (Chapter 1.5.1), in *B. cereus* and that CodY decreased biofilm formation.

Vilain *et al*. presented in 2009 [28] evidence that DNA acted as an important adhesin during the formation of biofilms. They studied the *B. cereus* ATCC 14579 strain, and found that eDNA was an important constituent of the extracellular matrix. They suggested that this might serve to protect the bacteria against antibiotic substances targeting nucleic acids.

In another study published in 2009, Auger *et al*. [62] compared 102 strains of both pathogenic and non-pathogenic strains of *B. cereus* and *B. thuringiensis*. They found most importantly that strains isolated from soil or infections in the digestive tract produced biofilms more efficiently than strains isolated from other types of infections.

Houry *et al*. published in 2010 [32] research performed using the strain *B. thuringiensis* 407. They constructed a non-flagellated mutant and a flagellated but non-motile mutant, and examined their ability to form biofilms. Deletion of flagella increased the number of bacteria bound to glass surfaces in flow cells, possibly due to flagella in the wild type hindering

interactions between the cell walls of bacteria and the surface. The authors nevertheless also stated that motility was important in the formation of biofilm to other surfaces, and in other growth systems than flow cells, as motility gives access to surfaces, is necessary for recruitment of planktonic cells within the biofilm and is required for spreading of the biofilm to uncolonized surfaces [32].

A recently published article from 2011 by Karunakaran *et al*. [63] described cell surface and extracellular polymeric substances of *B. cereus* ATCC 14579 and ATCC 10987. These features were compared between cells incorporated in a biofilm and cells in a planktonic state. During biofilm formation, the cell surface became more hydrophilic and the cell acquired an anionic polymer layer. The extracellular polymeric substances were also analyzed and found to be dominated by basic amino acids, which would be positively charged at physiological pH. This could indicate that adhesion to surfaces was mediated by electrostatic attractive forces between the negatively charged cell surfaces and the positively charged extracellular polymers through so called polymer bridging [63].

The regulatory system consisting of SinR and SinI (Chapter 1.5.1) is also found in *B. anthracis* and was investigated by Pflughoeft *et al*. [64]. These regulatory proteins seemed to function via the same mechanisms, but the types of genes they controlled differed, as could be expected since *B. anthracis* is non-motile and an inefficient biofilm-former.

To conclude, several factors shown to affect biofilm formation in the *B. cereus* group have been identified. However, less is known about the regulation system used for switching between the motile and sedentary states, than in *B. subtilis*. Intense research on *B. subtilis* has identified a broad spectrum of factors affecting biofilm formation, including the master regulator SinR, and much is also known about how these factors are regulated and how they influence each other. Even though there are indications of similar systems of regulation in the *B. cereus* group, a lot remains to be explored.

1.6 Cyclic di-GMP

C-di-GMP (Figure 3) is a second messenger shown to play a central role in controlling the switch between the planktonic and the biofilm-associated lifestyle of a variety of bacteria and is best studied in Gram-negatives like *P. aeruginosa* and *V. cholera* [65]. It induces formation of biofilms through stimulation of biosynthesis of adhesins and exopolysaccharides, as well as inhibiting motility. Other cellular functions like virulence, cell cycle progression and

antibiotic production are also influenced by c-di-GMP. A second messenger control modules consist of four components; two enzymes degrade and produce, respectively, the second messenger in response to certain signals. The second messenger binds to an effector molecule and allosterically regulates it. The effector molecule then interacts with a target molecule that produces a molecular response [65].

1.6.1 Production and degradation of c-di-GMP

c-di-GMP is synthesized from two molecules of guanosine-5'-triphosphate (GTP) by diguanylate cyclase (DGC) enzymes, and is degraded by phosphodiesterase (PDE) enzymes [65] (Figure 3). The PDEs produce 5'-phosphoguanylyl-(3'-5')-guanosine (5'-pGpG) which is broken down into two molecules of guanosine monophosphate (GMP) [65]. The genomes of most bacteria contain genes encoding several of these proteins, but the number varies greatly between species.

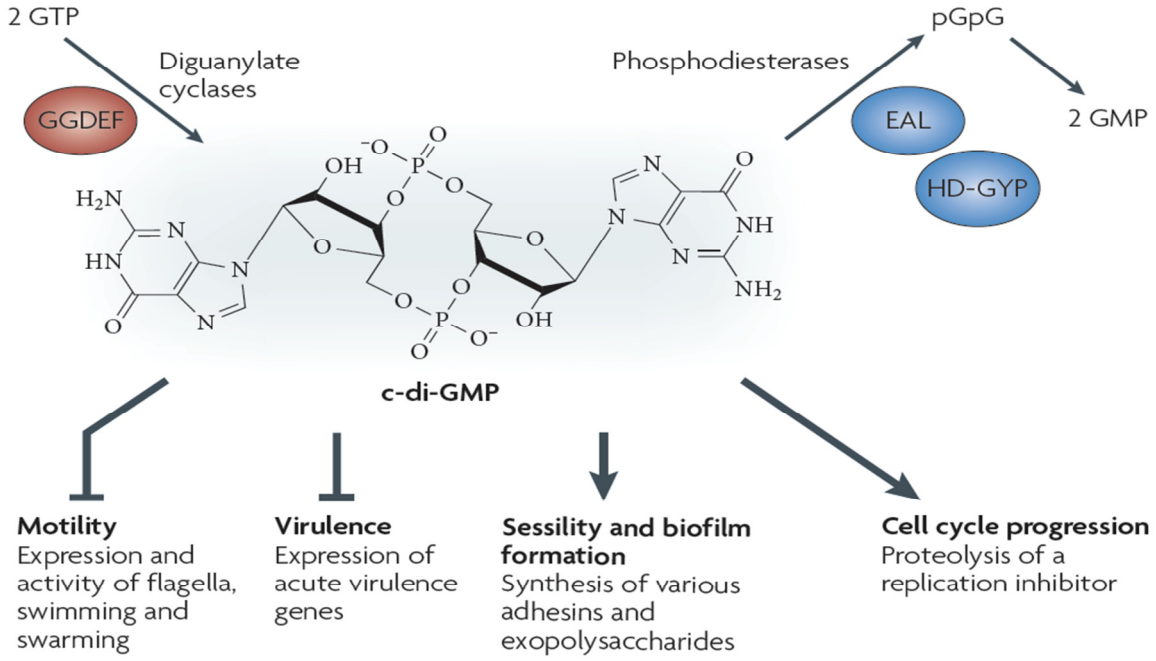

Figure 3: Metabolism and effects of c-di-GMP. c-di-GMP is synthesized from two molecules of guanosine-5'-triphosphate (GTP) by diguanylate cyclase (DGC) enzymes, and is degraded by phosphodiesterase (PDE) enzymes. The PDEs produce 5'-phosphoguanylyl-(3'-5')-guanosine (5'-pGpG) which is then broken down into two molecules of guanosine monophosphate (GMP). The amino acid sequence motif GGDEF of the DGCs are key residues of the active site of the enzyme. The amino acid sequence motifs EAL and HD-GYP are key residues of the active sites of PDEs. c-di-GMP affects several cellular processes, including motility, virulence, biofilm formation and cell cycle progression. Motility and expression of virulence genes is inhibited, while biofilm formation and cell cycle progression is stimulated. Figure obtained from Hengge [65].

The amino acid sequence motif GGDEF of the DGCs is a key residue of the active site of the enzymes and has given name to the GGDEF protein domain required for the activity of the enzyme. The active DGC is a homodimeric protein, in which each subunit binds one molecule of GTP. The active site (A-site) is located at the interface between the two subunits. Certain DGC proteins contain a secondary c-di-GMP binding site containing a RxxD motif, referred to as the I-site. Binding of c-di-GMP to this site may allosterically inhibit DGC acitivity, thereby preventing excessive production of c-di-GMP [65].

The amino acid sequence motifs EAL and HD-GYP are key residues of the active sites of PDEs and have given name to the EAL and HD-GYP domains associated with the activity of the enzyme. These enzymes are monomeric. The active PDE containing an EAL domain or a HD-GYP domain is c-di-GMP-specific and responsible for the conversion of c-di-GMP to 5'-pGpG. Non-specific PDEs are responsible for the further degradation into two GMP molecules [65].

Proteins can contain one single type of these domains, or several, in which case the different domains are covalently attached to each other. However, these combination proteins usually exhibit either DGC or PDE activity [65].

1.6.2 Signal inputs

GGDEF, EAL and HD-GYP domains are often linked to N-terminal sensory input domains in the same protein [65]. A broad range of signals can therefore possibly influence intracellular c-di-GMP levels, including oxygen, light, starvation and extracellular substances like antibiotics and signaling molecules. The domains can also be linked to two-component receiver (REC) domains of two-component signaling pathways [65].

1.6.3 Effector components

C-di-GMP effector molecules are diverse, and both proteins and RNA have been shown to bind c-di-GMP.

C-di-GMP binding proteins found in various Gram-negative bacteria have been shown to be involved in e.g. regulating adhesion, flagellar activity, twitching motility, biofilm formation, virulence gene expression, and EPS synthesis [65, 66]. Proteins containing PilZ domains were the first c-di-GMP binding domains to be identified [67]. Transcriptional regulators are also shown to bind and respond to c-di-GMP [68]. Additionally, proteins containing degenerated GGDEF and EAL domains and which have lost their ability to metabolize c-di-GMP have been shown to function as important regulatory proteins of the cell in response to c-di-GMP,

for example in *Caulobacter crescentus* [69]. A protein encoded by this bacterium, contains an EAL domain involved in degrading c-di-GMP and a GGDEF domain lacking metabolizing activity because of an altered active site motif. The GGDEF domain does, however, activate PDE activity of the associated EAL domain upon binding to GTP. LapD is located in the inner membrane of *P. fluorescens* and contains an enzymatically inactive EAL domain able to bind to c-di-GMP in the cytoplasma and thereby regulating the extracellular adhesin, LapA [70]. PelD is a membrane-bound protein found in *P. aeruginosa* shown to bind c-di-GMP, and to be involved in polysaccharide synthesis. This protein contains an RxxD motif which may function as an I-site [71].

Riboswitches using c-di-GMP as a ligand have also been identified. Riboswitches are mRNA domains that control gene expression, typically located in the 5' untranslated region (5'UTR) of genes [72]. The first c-di-GMP-binding riboswitches to be discovered were the GEMM domains found in *V. cholera*, *Clostridum difficile* and *B. cereus* [73]. These were found to be associated with expression of virulence genes, pilus formation and flagellum biosynthesis. Another riboswitch found to sense c-di-GMP, called "c-di-GMP-II", was presented by Lee *et al*. [74], also identified in the bacterium *C. difficile*. This riboswitch regulated self-splicing of the mRNA by ribozymes.

CHAPTER 2: BACKGROUND AND AIM OF THE THESIS

2.1 Background for the thesis

C-di-GMP has been shown to inversely regulate the planktonic, motile state and the biofilm-associated state in various Gram-negative bacteria, including *E. coli* [75], *Yersinia pestis* [76], *P. aeruginosa* [77] and *V. cholerae* [78]. Less research has so far concerned the role of c-di-GMP in Gram-positive bacteria, although recent publications have shown that c-di-GMP is an important regulator of biofilm and motility in *C. difficile* [79, 80].

B. thuringiensis 407 Cry÷ (Bt407) is commonly used as a model strain for studying genetics of *B. thuringiensis.* The wild type strain (Cry+) was originally isolated from an insect larvae in Brazil by Dr. Sergio Batista Alves and belongs to serotype H1 (*Bacillus thuringiensis* serovar *thuringiensis*; Dr. Didier Lereclus, personal communication). The original strain was cured of the Cry-encoding plasmid by Dr. Olivia Arantes, producing a strain (*B. thuringiensis* 407 Cry÷) which is no longer able to form insecticidal crystals [81]. It is therefore principally undistinguishable from *B. cereus* strains. The genome of Bt407 has been sequenced (NCBI: ACMZ01000000), and Bt407 is an efficient biofilm former and is also easily transformable. It was therefore chosen as a model organism for this study.

By analysis of the Bt407 genome sequence, the strain was shown to carry ten genes predicted to encode proteins containing GGDEF and/or EAL domains, associated with the metabolism of c-di-GMP (Fagerlund & Økstad, unpublished results; Figure 4). In this thesis, these genes will be referred to as *cdgxxx* where xxx denotes a three-digit number. The N-terminal of several of the *cdg* genes is associated with PAS or GAF domains, which are sensing domains able to bind to a variety of small-molecule ligands [82]. Cdg135 has both a GGDEF and an EAL domain (Figure 4), predicted to have DGC or PDE activity, respectively, based on conservation of the active site residues. Cdg113 contains an EAL domain but lacks an active site motif and was therefore predicted probably not to be involved in the degradation of c-di-GMP. Similarly, Cdg141 contains a GGDEF domain but lacks an A-site, and is therefore unlikely to be involved in synthesis of c-di-GMP. However, it contains an I-site characterized by an RxxD motif, suggesting allosteric binding to c-di-GMP and involvement in a negative feedback mechanism.

Preliminary biofilm assay and motility results (Fagerlund & Økstad, unpublished results) had prior to the start of this thesis work indicated that Cdg135, Cdg113 and Cdg141 all exhibited significant effects on both biofilm formation and swimming motility.

2.2 Aim of the thesis

The aim of this study was to functionally characterize proteins encoded by a selection of identified genes in Bt407 predicted to be involved in metabolism and/or sensing of c-di-GMP. The genes *cdg135*, *cdg141* and *cdg113* were chosen on the basis of preliminary results indicating a significant effect on biofilm formation when over-expressed and/or knocked out. Cdg135 in particular was a candidate for being involved in a switch between the motile, planktonic and sedentary, biofilm-associated states of life in Bt407. Cdg113 and Cdg141 were both predicted to lack enzymatic activity and could possibly represent c-di-GMP responsive effector molecules or regulators as they seemed to influence phenotypes expected to be regulated by c-di-GMP. It was also of interest to identify additional downstream effector proteins that might be regulated by c-di-GMP and/or by Cdg113 and Cdg141 as possible regulators.

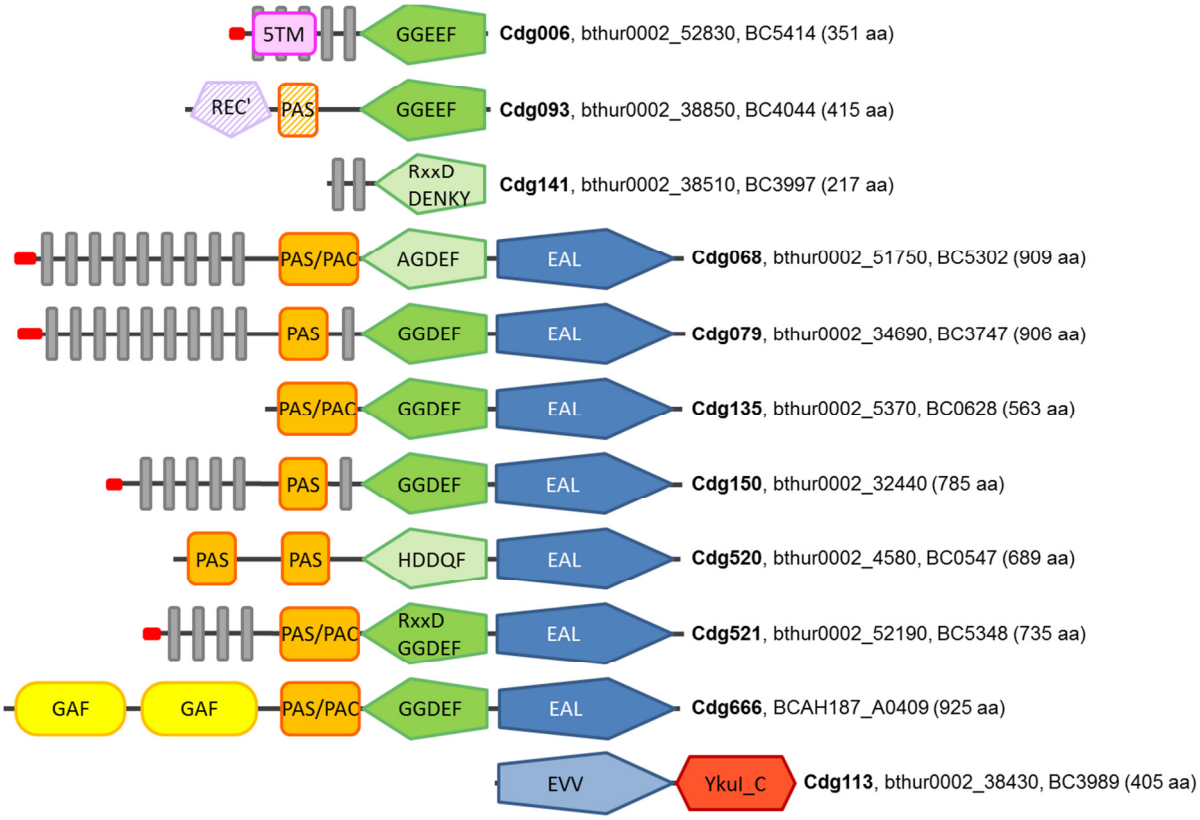

Figure 4: Genes in Bt407 predicted to be involved in metabolism and/or sensing of c-di-GMP. GGDEF domains (green), EAL domains (blue), PAS domains (orange), Ykul_C domain (red), and predicted transmembrane segments (grey) are illustrated. GGDEF domains predicted to show DGC activity and GGDEF domains predicted to be enzymatically inactive are in dark and light green, respectively. Amino acid sequence at the A-site along with RxxD if the I-site is present is indicated in the GGDEF domains. EAL domains predicted to show PDE activity and EAL domains predicted to be enzymatically inactive are dark and light blue respectively. Locus tags from both Bt407 and ATCC 14579 are shown. Figure made by Annette Fagerlund.

CHAPTER 3: MATERIALS

3.1 Bacterial strains

Table 1: List of bacterial strains used in this thesis work (all strains except from wild type made by Annette Fagerlund)	
Strain	**Description**
Bt407 wild type	*Bacillus thuringiensis* 407 (Cry÷) wild type [81] (Chapter 2.1)
Bt407 + pHT304-pXyl-135	Bt407 wild type over-expressing Cdg135
Bt407 + pHT304-pXyl-135mut	Bt407 wild type over-expressing mutated Cdg135. Two amino acids in the GGDEF domain are exchanged, giving GGAAF
Bt407 + pHT304-pXyl-bspA	Bt407 wild type over-expressing BspA
Bt407 + pHT304-pXyl-141	Bt407 wild type over-expressing Cdg141
Bt407 + pHT304-pXyl-141mut	Bt407 wild type over-expressing mutated Cdg141. Two amino acids in the RxxD motif are exchanged, giving AxxA
Bt407 + pHT304-pXyl-113	Bt407 wild type over-expressing Cdg113
Bt407 + pHT304-pXyl-empty vector	Bt407 wild type containing empty vector. Control for over-expression strains
Bt407Δ135	Bt407 wild type with deletion of *cdg135*
Bt407Δ135 + pHT304-pXyl-empty vector	Deletion mutant of *cdg135* containing empty vector
Bt407ΔbspA	Wild type with deletion of *bspA*
Bt407ΔbspA + pHT304-pXyl-empty vector	Deletion mutant of *bspA* containing empty vector
Bt407Δ141	Bt407 wild type with deletion of *cdg141*
Bt407Δ113	Bt407 wild type with deletion of *cdg113*
E. coli XL1-Blue + pHT304-pXyl-135	*E. coli* XL1-Blue containing plasmid carrying *cdg135*
E. coli XL1-Blue + pHT304-pXyl-135mut	*E. coli* XL1-Blue containing plasmid carrying mutated *cdg135*
E. coli XL1-Blue + pHT304-pXyl-113	*E. coli* XL1-Blue containing plasmid carrying *cdg113*
E. coli XL1-Blue + pHT304-pXyl-141	*E. coli* XL1-Blue containing plasmid carrying *cdg141*
E. coli XL1-Blue + pHT304-pXyl-141mut	*E. coli* XL1-Blue containing plasmid carrying mutated *cdg141*
E. coli XL1-Blue + pHT304-pXyl-bspA	*E. coli* XL1-Blue containing plasmid carrying *bspA*
E. coli XL1-Blue + pHT304-pXyl-empty vector	*E. coli* XL1-Blue containing empty vector

3.2 Vectors

pHT304-pXyl is a low-copy number *E. coli*/*Bacillus* shuttle vector with a plasmid copy-number of 4 ± 1 in *B. cereus*, in which *xylR* and the *xylA* promoter from *B. subtilis* has been inserted into the pHT304 cloning site [83], allowing xylose-inducible expression of downstream cloned genes. It contains genes giving resistance to erythromycin and ampicillin.

Erythromycin is used as a resistance marker in *B. thuringiensis* while erythromycin or ampicillin is used in *E. coli.*

3.3 Primers

Table 2: Names and sequences of all oligonucleotides used in this thesis	
Name	**Sequence (5' to 3')**
pHT304pXyl-F2	ggtttgatcagcgatatccac
00113-R	gaaagccttgccttattctcaa
P-BC1060-R	tacggatcctttgcatagttccctcct
S2_pUC19R	taacaatttcacacaggaaacagc
141-R-KpnI	aatggtacctcttcctatcatatatcttcaaatcg
00135-R	gccttttgcaaagcaaactc
Up-02561-F	gtgcaatgtaaaggggttgc
Down-02561-R	gtctaactttcccgccatca
Up-113-F	tgaacaatttccagggcaag
Down-113-R	cagtcgtaattgatggcgaag
141upF	atgcgaattcaagtggaaaa
141downR	ttcttgtttagcagcgttttca
135upF	catcaccatggaggacacaa
135downR	tgcaacactctgggcattta
31070-F	ttagctgaacgatttgtaccg
31070-R	ccacctaaataagcaccaagg
49610-F	ttcactgtattaattatcgcaagg
49610-R	tttatttctggtacgattgcag
31060-F	aagtaatttccaaattcaccatctg
31060-R	tttttgtgttaaacgaggatgg
49600-F	tgtaaagaacaaggtattcaaatgga
49600-R	ccgtgtttctcagcaatctct
31280-F	ttagaccacgaacgtgcatt
31280-R	gccagcaagaatacctgagc
gatB_left	agctggtcgtgaagaccttg
gatB_right	cggcataacagcagtcatca
rpsU_left	aagatcggtttctaaaactggtaca
rpsU_right	tttcttgccgcttcagattt
udp_left	actagagaaacttggaaatgatcg
udp_right	gacgcttaattgcacggaac

3.4 Enzymes

DyNAzyme II DNA polymerase (Finnzymes)

*Eco*RI (Fermentas)

Lysozyme (Sigma-Aldrich)

Proteinase K (Sigma-Aldrich)

RNase A (Sigma Aldrich)

SUPERase·In (Ambion)

Superscript III Reverse Transcriptase (Invitrogen)

Turbo DNase (Ambion)

*Xba*I (Fermentas)

3.5 Molecular weight standards

GeneRuler 1Kb DNA Ladder, Figure 5 (Fermentas)

0.24-9.5 Kb RNA Ladder, Figure 7 (Invitrogen)

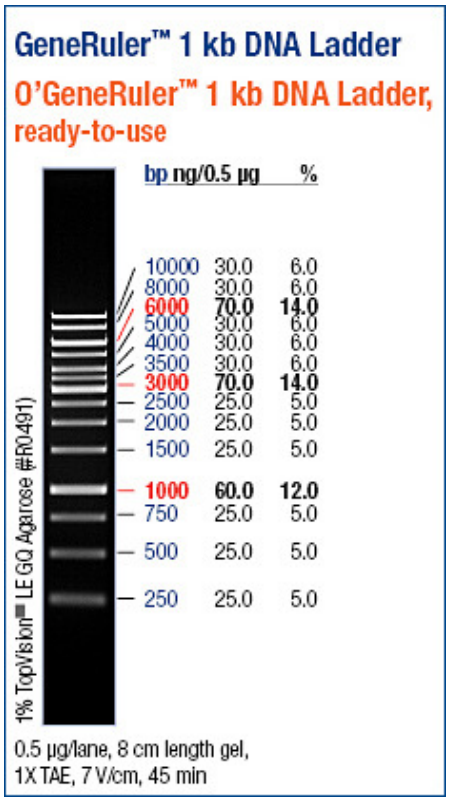

Figure 5: GeneRuler 1Kb DNA Ladder (www.fermentas.com)

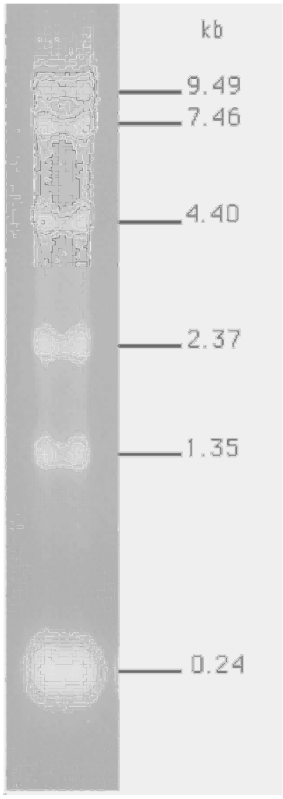

Figure 6: 0.24-9.5 Kb RNA Ladder (Invitrogen product description)

3.6 Reagents and solutions provided

Acetic acid (Merck)

Acetone (VWR)

Agar bacteriological (No. 1) (Oxoid)

Agarose (Sigma-Aldrich)

Ampicillin (Sigma-Aldrich)

β-mercaptoethanol (Sigma-Aldrich)

Bactopeptone (Becton, Dickinson and Company)

Boric acid (H_3BO_3) (Sigma-Aldrich)

Bovine Albumin fraction V Solution (BSA) 7.5% (Gibco)

Chloroform (VWR)

Crystal violet (Sigma-Aldrich)

Cy3 dye (GE Healthcare)

Cy5 dye (GE Healthcare)

dATP (Qiagen)

dCTP (Qiagen)

dGTP (Qiagen)

dTTP (Qiagen)

DEPC-treated water/RNase free water (Ambion)

Di-sodium hydrogen phosphate 2-hydrate ($Na_2HPO_4 \times 2H_2O$) (Merck)

6 × DNA Loading Dye (Fermentas)

Erythromycin (Sigma-Aldrich)

Ethanol (Arcus kjemi)

Ethidium bromide (EtBr) (Sigma-Aldrich)

Ethylenediaminetetraacetic acid (EDTA) (M&B laboratory chemicals)

10 × FastDigest Buffer (Fermentas)

Ficoll 400 (Sigma Aldrich)

5 × First-strand buffer (Invitrogen)

Formamide (Sigma-Aldrich)

Glucose (Merck)

Hydrochloric acid (HCl) (VWR)

Isoamylalcohol (Merck)

Isopropanol (Kemetyl)

Light Cycler 480 SYBR Green I Master (Roche)

Magnesium chloride ($MgCl_2$) (Sigma)

Methanol (Merck)

Monopotassium phosphate (KH_2PO_4) (Merck)

Sodium hydroxide (NaOH) (VWR)

Orange G (Merck)

Potassium chloride (KCl) (Merck)

Random hexamers (Applied Biosystems)

10 × Reaction Buffer (Finnzymes)

20 × Saline-sodium citrate (SSC) buffer (Gibco)

Salmon sperm DNA (1 mg/ml) (Sigma-Aldrich)

Sodium acetate, water free (NaOAc) (Merck)

Sodium acetate (NaOAc) (3 M, pH 5.5) (Ambion)

Sodium chloride (NaCl) (Merck)

Sodium dodecyl sulfate (SDS) (Sigma-Aldrich)

Tris-Base (Sigma-Aldrich)

Tris-HCl (10 mM, pH 8.5) (Elution Buffer, Qiagen)

Tryptone (Oxoid)

10 × Turbo DNase-buffer (Ambion)

Xylose (Sigma-Aldrich)

Yeast extract (Oxoid)

3.7 Solutions prepared at the lab

Ampicillin (100 mg/ml)

2 g ampicillin

Milli Q water (MQ-dH_2O) added to 20 ml

The solution was sterile-filtrated, aliquoted in sterile eppendorf tubes and stored at -20 °C.

Crystal violet solution (0.3% w/v)

0.6 g Crystal violet

MQ-dH_2O added to 200 ml

Dissolved on a magnetic stirrer overnight, sterile-filtrated and stored at room temperature.

dNTP-mix (final concentration 10 mM each)

10 µl dATP (100 mM)

10 µl dGTP (100 mM)

10 µl dTTP (100 mM)

10 µl dCTP (100 mM)

60 µl MQ-dH_2O

The components were mixed and stored at -20 °C.

Erythromycin (100 mg/ml)

2 g erythromycin

Ethanol (96%) added to 20 ml

The solution was aliquoted in sterile eppendorf tubes and stored at -20 °C.

Ethidium bromide (5 mg/ml)

0.5 g of ethidium bromide (EtBr) was added to 100 ml MQ-dH_2O. The container was wrapped in aluminum foil and the mixture was stirred magnetically for several hours to ensure dissolution of the dye. The solution was stored at 4 °C.

Sodium chloride (5 M)

292.2 g Sodium chloride (NaCl)

Distilled water (dH_2O) added to 1 L

The solution was autoclaved and stored at room temperature.

Sodium hydroxide (1 M)

40 g Sodium hydroxide (NaOH)

MQ-dH2O added to 1 L

The solution was stored at room temperature.

Orange mix

10 g Ficoll 400

0.125 g Orange G

2 ml EDTA (0.5 M, pH 8.0)

The components were dissolved in 50 ml MQ-dH_2O and sterile-filtrated. The solution was aliquoted in sterile eppendorf tubes and stored at -20 °C.

Phosphate buffered saline (PBS)

8 g NaCl

0.2 g KCl

0.27 g KH_2PO_4

1.78 g $Na_2HPO_4 \times 2H_2O$

987.5 ml dH_2O

pH was adjusted to 7.4 with HCl and the solution was autoclaved and stored at 4 °C.

20% Sodium Dodecyl Sulphate

200 g Sodium dodecyl sulphate (SDS)

MQ-dH_2O added to 1 L

The components were carefully heated up to help the dissolution process and the solution was stored at room temperature.

SET-buffer

0.438 g NaCl

5 ml EDTA (0.5 M, pH 8.0)

2 ml Tris-HCl (1 M, pH 8.5)

MQ-dH_2O added to 100 ml

The solution was stored at room temperature.

Sodium acetate (NaOAc) (3 M, pH 5.2)

246.09 g NaOAc (3 M)

dH_2O added to 800 ml

~100 ml Acetic acid

dH_2O added to 950 ml

pH was adjusted to 5.2 and the volume was adjusted to 1 L with dH_2O. The solution was autoclaved.

50 × TAE (Tris/acetat/EDTA buffer)

242.0 g Tris-Base

57.1 ml acetic acid (17.5 M)

100 ml EDTA (0.5 M, pH 8.0)

MQ-dH_2O added to 1 L

The solution was stored at room temperature.

10 × TBE (Tris/Borate/EDTA buffer)

108.0 g Tris-Base

55.0 g boric acid

9.3 g EDTA

MQ-dH_2O added to 1 L

The solution was stored at room temperature.

Tris-EDTA (TE)-buffer

10 ml Tris-HCl (1 M, pH 8.0)

2 ml EDTA (0.5 M, pH 8.0)

MQ-dH_2O added to 1 L

The solution was autoclaved and stored at room temperature.

Xylose (1 M)

7.5 g xylose was dissolved in 50 ml MQ-dH_2O and the solution was sterile-filtrated, aliquoted in sterile eppendorf tubes and stored at -20 °C.

3.8 Growth media

Bactopeptone medium

10 g Bactopeptone

5 g Yeast extract

10 g NaCl

The components were dissolved in MQ-dH_2O and the volume was adjusted to 1 L. The solution was autoclaved and stored at 4 °C.

Lysogeny broth (LB)-agar plates

10 g Tryptone

5 g Yeast extract

10 g NaCl

pH was adjusted to 7.0 with 5.8 M HCl. No. 1 bacteriological agar (12.5 g) was added and the volume was adjusted to 1 L with MQ-dH_2O. The solution was autoclaved and then cooled to approximately 45-50 °C before plated out. The plates were stored at 4 °C.

Lysogeny broth (LB)-medium

10 g Tryptone

5 g Yeast extract

10 g NaCl

MQ-dH_2O added to 1 L

pH was adjusted to 7.0 with HCl (5.8 M). The solution was autoclaved and stored at 4 °C.

Super Optimal broth with Catabolite repression (SOC)-medium

20 g Tryptone

5 g Yeast extract

0.5 g NaCl

The components were added to 950 ml MQ-dH_2O and the mixture was shaken until dissolution. KCl (250 mM, 10 ml) was then added and pH was adjusted to 7.0 with HCl (5.8 M). The volume was adjusted to 1 L with MQ-dH_2O and the solution was autoclaved. After allowing the solution to cool down, 5 ml sterile $MgCl_2$ (2 M) and 20 ml sterile glucose (1 M) was added. The solution was stored at -20 °C.

3.9 Commercial kits

RNeasy Mini Kit (Qiagen)

Up to 100 µg of RNA can be isolated. RNA binds to a silica-based membrane and a high-salt buffer system is used. A highly denaturing guanidine-thiocyanate-containing buffer is present to inactivate RNases (RNeasy Mini Handbook, RNAprotect Bacteria Reagent Handbook).

Contents: RNeasy mini spin columns

Buffer RLT

Buffer RW1

Buffer RPE (4 volumes of 96% ethanol was added before use)

E.Z.N.A. Plasmid Miniprep Kit 1 (Omega Bio-Tek)

Alkaline-SDS is used to lyse the bacterial cells. DNA reversibly binds to the HiBind matrix allowing contaminants to be removed (E.Z.N.A. plasmid miniprep kit I- Handbook).

Contents: HiBind Miniprep columns

Solution I

Solution II

Solution III

Buffer HB

Elution Buffer

DNA Wash buffer, concentrate (diluted with ethanol before use)

Fairplay III Microarray Labeling Kit (Agilent)

cDNA is synthesized from RNA, purified, labeled with fluorescent dyes and then repurified (FairPlay III Microarray Labeling Kit Instruction Manual).

Contents: 10 × AffinityScript RT buffer

20 × dNTP mix with amino allyl dUTP

DTT (0.1 M)

RNase block (40 U/µl)

AffinityScript HC Reverse Transcriptase

Glycogen (20 mg/ml)

DMSO (high purity)

2 × Coupling Buffer

DNA-binding solution

Microspin cups

2 ml receptacle tubes

RNase free DNase set (Qiagen)

Purifies RNA bound to a RNeasy spin column by adding DNase I for digestion of DNA contamination (RNeasy Mini Handbook).

Contents: DNase I, RNase-free (lyophilized)

RDD buffer

3.10 Various equipment

Centrifuge, rotor radius=85 mm (Hettich)

Centrifuge, rotor radius=184 mm (Nunc-tubes)/159 mm (plates) (Hettich)

Cuvettes for electroporation: Genepulser Cuvettes 0.2 cm electrode (Bio-Rad)

Cuvettes for measuring OD_{600} (VWR)

Cuvettes for measuring concentration of RNA/DNA: UVette 220-1600 nm (Original Eppendorf)

Electroporator Gene Pulser II (Bio-Rad)

Filtered pipette tips (ART)

Genepix 4000b Microarray Scanner (Axon)

Hybridization chambers

Lidded plastic tubes: 20 ml (Sterilin)

Lifterslips

Microarray slides (Information in Chapter 4.11)

Micron filter device: Amicon Ultra 0.5 ml 30 K Ultracel 30K Membrane Millipore

Nunc-tubes (15 ml, 50 ml) (Corning Incorporated)

PCR machine (Applied Biosystems GeneAmp PCR System 2700)

PCR tubes (Sarstedt)

Photo box for gels: Gel Doc 1000 (Bio-Rad)

Plastic sealing film used in RT-qPCR: EU Opti-Seal (Bioplastics)

Plate scanner used in biofilm assay: HTS 7000 Plus Bio Assay Reader (Perkin Elmer)

Plates used in biofilm assay: Flexible, 96 well PVC microtiter plates, U-bottoms, with lids (Falcon)

Plates used in biofilm assay: Polystyrene microtiter plates, flat bottoms (Falcon)

Plates used in RT-qPCR: EU Semiskirted thin-wall plate 96 × 0.2 ml (Bioplastics)

Precellys machine (Bertin technologies)

Precellys tubes VK01 (Bertin technologies)

RNase away (Sigma)

RT-qPCR machine, Light Cycler 480 Real-Time PCR System (Roche)

UV-spectrophotometer, Biophotometer (Eppendorf)

CHAPTER 4: METHODS

4.1 Growth of bacteria

4.1.1 *B. thuringiensis* 407

Bacteria from frozen stocks stored at -80 °C were streaked on LB-agar containing antibiotics when appropriate and incubated at 30 °C overnight. The plates were placed in closed plastic bags before incubation to prevent the agar from drying out. One colony was inoculated in 5 ml LB-medium and incubated at 30 °C overnight with rotation at 225 rpm in lidded flasks (20 ml). Overnight culture (500 µl) was transferred to 50 ml freshly prepared bactopeptone medium. Erlenmeyer flasks (500 ml) with metal caps and baffles were used. The cultures were incubated at 30 °C and were subject to rotation at 225 rpm. Antibiotics and xylose was added to the growth medium when appropriate. OD_{600} was measured regularly using a UV-spectrophotometer. Samples were taken approximately once every hour or half hour with an increased frequency of measurements during the exponential growth phase. Motility was studied at each sampling point by observing the bacteria in a microscope.

4.1.2 *E. coli* XL1-Blue

Bacteria were streaked on LB-agar containing antibiotics when appropriate. The plates were placed in closed plastic bags and incubated at 37 °C overnight. One colony was inoculated in 5 ml LB-medium and incubated at 37 °C with rotation at 220 rpm. Erlenmeyer flasks with volumes of 100 ml were used and the tops were covered with aluminum foil.

4.2 Genomic DNA (gDNA) preparations

The preparation was performed using a protocol derived from Pospiech & Neumann [84]. Three ml of an overnight culture was aliquoted in two eppendorf tubes and centrifuged at 16 000 × *g* for 2 minutes. The supernatant was discarded. Pellets were resuspended in 0.5 ml SET-buffer containing 0.5 mg lysozyme (Sigma-Aldrich) per 0.5 ml buffer. This mixture was incubated at 37 °C for 10 minutes. SDS (50 µl, 10%) and 6.3 µl proteinase K (20 mg/ml, Sigma-Aldrich) was added and the components were mixed and incubated at 55 °C for 45 minutes. The tube was inverted regularly during this incubation period. NaCl (200 µl, 5 M) and 700 µl chloroform:isoamylalcohol (24:1) was added and the tube was incubated for 10 minutes in room temperature using a rotor wheel to ensure constant inversions. The tube was then centrifuged at 11 500 × *g* for 10 minutes and the aqueous phase was transferred to a fresh eppendorf tube. The DNA was precipitated using an equal volume of isopropanol. The tube was inverted and immediately centrifuged at 16 000 × *g* for 10 minutes. The supernatant

was carefully pipetted off and discarded. The pellet was washed using 1 ml 70% ethanol and the tube was vortexed and centrifuged at 16 000 × *g* for 5 minutes. The supernatant was discarded and the tube was centrifuged once more at 16 000 × *g* for 2 minutes before rests of supernatant were removed. The pellet was then allowed to air dry for approximately 15 minutes. The DNA was dissolved in 100 µl Tris-HCl (10 mM, pH 8.5) containing 0.02 µg/µl RNase A (Sigma-Aldrich). gDNA samples were stored at 4 °C.

4.3 Polymerase chain reaction (PCR)

PCR involves enzymatic amplification of specific nucleic acid sequences. The DNA is first heated up and a denaturation involving separation of the two complementary DNA strands takes place. The temperature is then lowered allowing the primers to anneal to each of the strands. Primers are oligonucleotides complementary to the ends of the sequence to be amplified. The enzyme DNA polymerase binds to the primer/single strand DNA complex and the temperature is raised again so that the enzyme is able to synthesize complementary strands by extending the oligonucleotides. These steps are repeated a number of times, causing an exponential amplification of product. The PCR program also includes a preheating step to ensure initial denaturation, and a final elongation step to complete extension of all single strands [85].

When performing PCR on genes localized in plasmids, it was sufficient to use as template either 50 µl of an overnight culture or a single colony dissolved in 50 µl of MQ-dH_2O. The samples were in these cases first incubated at 99.9 °C for 10 minutes to lyse the bacteria. When the target for the PCR reaction was chromosomal genes from bacteria in the *B.cereus* group, it was necessary to first isolate genomic DNA. The genome preparations were diluted 1:10, 1:100 or 1:1000 in MQ-dH_2O before being used as templates in PCR reactions.

Agarose gel electrophoresis was used to analyze the PCR- products (Chapter 4.7). This was performed alongside one lane containing a molecular weight marker with DNA fragments of known size, enabling estimation of the size of the PCR products by interpolation.

For each PCR reaction, the following components were mixed:
1 µl template
2.5 µl forward primer (10 µM)
2.5 µl reverse primer (10 µM)
1 µl dNTP mix (10 µM each, Chapter 3.7)
1 µl DyNAzyme II polymerase (Finnzymes)

5 µl 10 × Reaction Buffer (Finnzymes)
37 µl MQ-dH_2O

The following cycling conditions were used when performing PCR for confirming deletion of genes:

94 °C: 3 minutes
30 cycles of: 94 °C: 30 seconds, 52 °C: 30 seconds, 72 °C: 2 minutes 10 seconds
72 °C: 7 minutes
4 °C →

The following cycling conditions were used when performing PCR for confirming cloned inserts of plasmids:

94 °C: 3 minutes
30 cycles of: 94 °C: 30 seconds, 52 °C: 30 seconds, 72 °C: 60 seconds
72 °C: 7 minutes
4 °C →

4.4 Preparation of RNA

Generally when handling RNA, it is important to work as quickly as possible, to use RNase-free equipment and solutions only and to change gloves frequently. These cares are taken to avoid contamination with RNases and degradation of RNA. “RNeasy Mini kit” (Qiagen, Chapter 3.9) and “RNase free DNase set” (Qiagen, Chapter 3.9) were used for isolation and purification of RNA.

Samples were first harvested from bacterial cultures grown to desired optical densities. The appropriate volume of culture to be harvested depended on the optical density of the culture. The maximum capacity of the RNeasy mini spin column is 100 µg RNA. A volume of 1 ml culture with OD_{600} of 3 has proven to be suitable by previous experience in the laboratory. To stop growth immediately and fix transcripts, samples were added directly to tubes containing equal volumes of ice cold methanol and centrifuged for 20 minutes at 4 °C and 2800 × *g*. Supernatants were discarded and pellets were stored at -70 °C until use. These were then thawed on ice and any rests of supernatant were removed. RLT (900 µl) containing 10 µl/ml β-mercaptoethanol was used to resuspend the pellets. The suspensions were transferred to Precellys tubes and placed in the Precellys machine for cell lysis. The machine was programmed as follows: 5800 rpm vigorous shaking for 30 seconds in two rounds separated

by a pause of 20 seconds. The tubes were then centrifuged at 16 000 × *g* for 1 minute and the samples were carefully transferred to RNase-free eppendorf tubes to avoid contamination with particles from the Precellys tubes. An equal volume of 70% ethanol was added to each tube and 700 µl was transferred to RNeasy Mini columns and centrifuged at 16 000 × *g* for 20 seconds. The flow through was discarded. This step was repeated until the whole sample had been transferred to the column. RW1 (350 µl) was added and centrifuged in the same manner. DNase I mix (80 µl consisting of 70 µl Buffer RDD and 10 µl DNase I) was added and the columns were incubated at room temperature for 15 minutes. RW1 wash buffer (350 µl) was added and the columns were centrifuged again. The flow through was discarded. 500 µl RPE was added and the columns were centrifuged in the same way. The flow through was discarded. This wash step was repeated once using another 500 µl RPE. The empty columns were centrifuged at 16 000 × *g* for 2 minutes and transferred to RNase-free eppendorf tubes. RNase-free water (50 µl) was added to each column and centrifuged at 16 000 × *g* for 30 seconds. Another 50 µl RNase-free water was added, and the tubes were centrifuged at 16 000 × *g* for 1 minute. The RNA-samples were immediately placed on ice.

The concentration and purity of the RNA samples were measured through spectrophotometry (Chapter 4.8) and the integrity of the RNA molecules was examined by agarose gel electrophoresis (Chapter 4.7).

4.5 Isolation and precipitation of plasmids

The "E.Z.N.A Plasmid Miniprep Kit 1" (Omega Bio-Tek) was used for isolation of plasmids from *E. coli* strains. The reactions were scaled up two-fold compared to the original protocol provided by the kit and two columns were consequently used. Plasmids were precipitated after isolation.

4.5.1 Isolation of plasmids

Overnight culture (10 ml) containing the appropriate antibiotic was incubated for ~12-16 hours at 37 °C and 225 rpm in an Erlenmeyer flask (100 ml). The culture was transferred to a Nunc tube (15 ml) and centrifuged at 2800 × *g* for 10 minutes. The supernatant was discarded. The pellet was resuspended in 500 µl Solution I and vortexed until no clumps of cells were visible. Equal volumes of the suspension were transferred to two fresh eppendorf tubes. Solution II (250 µl) was added to each tube and the tubes were carefully inverted until a clear lysate was obtained. Solution III (350 ml) was then added followed by immediate inversion several times until a white flocculate formed. The tubes were centrifuged at 11 500 × *g* for 10 minutes. Columns were placed in collection tubes and prepared by adding 100 µl

Equilibration Buffer and centrifuging at 11 500 × *g* for 1 minute. The supernatants were carefully transferred to the columns and centrifuged at 11 500 × *g* for 1 minute. Flow-through was discarded and 500 µl Buffer HB was added before the columns were centrifuged as above. Flow-through was discarded and 700 µl DNA Wash Buffer was added. The tubes were centrifuged, the flow through discarded, and this wash step was repeated once. Empty columns were then centrifuged at 11 500 × *g* for 2 minutes and the columns were transferred to fresh eppendorf tubes. Elution Buffer (30 µl) was added to each column and centrifuged at 11 500 × *g* for 1 minute. The eluates were pooled and the concentration and purity of DNA was measured with UV-spectrophotometry (Chapter 4.8).

4.5.2 Ethanol precipitation of DNA

MQ-dH_2O was added to a total volume of 100 µl. Sodium acetate (3 M, pH 5.2, 11.1 µl) was added and the tube was vortexed. Ice cold ethanol (250 µl) was added and the tube was vortexed again and stored at -20 °C overnight. The precipitated DNA was centrifuged at 16 000 × *g* and 4 °C for 20 minutes and the supernatant was discarded. The pellet was washed once with 500 µl ice cold 70% ethanol and centrifuged at 16 000 × *g* and 4 °C for 10 minutes. The supernatant was removed and the pellet was allowed to dry on a heat block at 37 °C for approximately 5 minutes before resuspension in MQ-dH_2O. As the cooling centrifuge was out of order, centrifuging at 4°C was replaced by centrifuging in the cold room.

4.6 Restriction digests

Restriction enzymes were used to confirm the identities of isolated plasmids. The plasmids were treated with *Xba*I (Fermentas) and *Eco*RI (Fermentas) in a double digest reaction. Each reaction required the following components:

1 µl plasmid DNA
1 µl 10 × FastDigest Buffer
0.5 µl *Xba*I
0.5 µl *Eco*RI
7 µl MQ-dH_2O

This mixture was incubated at 37 °C for 1 hour and the fragments were analyzed by agarose gel electrophoresis (Chapter 4.7)

4.7 Agarose gel electrophoresis

Agarose gel electrophoresis is a method for separating DNA or RNA molecules by applying samples on an agarose gel which is exposed to an electric field. The negatively charged molecules will move towards the positive pole and larger molecules will migrate more slowly through the gel compared to smaller molecules because of greater friction. Ethidium bromide binds to the nucleic acids and is used to detect the molecules as it fluoresces in UV-light when bound [86]. A gel-loading buffer is added to the samples before applying them to the gel, providing density and color. Electrophoresis buffer is added to the electrophoresis tank to provide ions and buffer capacity. The appropriate concentration of agarose to be used depends on the expected sizes of DNA or RNA molecules to be analyzed. Appropriate concentrations of agarose for separation of DNA molecules according to Voytas [86] are shown in Table 3.

Table 3: Suitable concentrations of agarose to use for separation of DNA molecules of different sizes [86]

Agarose (%)	Effective range of resolution of linear DNA fragments (kb)
0.5	1 to 30
0.7	0.8 to 12
1.0	0.5 to 10
1.2	0.4 to 7
1.5	0.2 to 3

Agarose gel was made by heating the appropriate amount of agarose in electrophoresis buffer until complete dispersion. Ethidum bromide was added to a final concentration of 10 µg/ml. The warmed gel was poured into a closed gel-casting platform containing a comb forming the desired number of slots for sample application. When the gel had solidified, the platform was transferred to the corresponding electrophoresis tank and electrophoresis buffer was added so that the gel was just covered. The electrophoresis buffers used in DNA and RNA gels were 1 × TBE and 1 × TAE (Chapter 3.7) respectively. An appropriate amount of sample was mixed with gel-loading buffer. For DNA preparations, 1 × DNA Loading Dye was used whereas orange mix (Chapter 3.7) was used for RNA preparations. RNA-samples were incubated at 65°C for 5 minutes before applying them to the gel. The samples with total volumes of ~10 µl were pipetted into the slots of the gel. A molecular weight marker was added to one of the slots for estimation of molecule size. The electrophoresis tank was exposed to voltage (approximately 100 V) for approximately an hour depending on the gel volume and the gel was transferred to a photo box, exposed to UV light and photographed.

4.8 Spectrophotometry

To assess concentrations of preparations of DNA and RNA, absorbance was measured at 260 nm. For single stranded RNA, 1 A_{260} unit indicates a concentration of 40 µg/ml. For double stranded DNA, 1 A_{260} unit indicates a concentration of 50 µg/ml. Absorbance is also measured at 280 nm as proteins have a peak absorption at this wavelength. A_{260}/A_{280} ratios of 1.8-1.9 indicate highly purified DNA whereas ratios of 1.9-2.0 indicate highly purified RNA [87]. When assessing the optical density of a bacterial culture, absorption was measured at 600 nm.

4.9 Transformation

4.9.1 Preparing electrocompetent *B. thuringiensis* cells

Overnight culture of appropriate Bt407 strain was diluted 1:100 in 150 ml LB medium in a 1-litre Erlenmeyer flask. The bacteria were grown at 37 °C with rotation at 220 rpm to an OD_{600} of around 1. The culture was distributed to three Nunc tubes (50 ml) and these were centrifuged at 4000 × *g* at 4 °C for 10 minutes. The tubes were afterwards immediately placed on ice and supernatants were removed. Ice cold MQ-dH_2O (1 ml) was added to each tube and the pellets were gently resuspended. The suspensions were transferred to three cold eppendorf tubes. The tubes were centrifuged at 6000 × *g* at 4 °C for 1 minute and the supernatants were discarded. This wash step was repeated three times. The second time however, the contents of two eppendorf tubes were pooled by adding only 2 ml MQ-dH_2O in total. The third time, contents of the two remaining tubes were pooled and only 1 ml MQ-dH_2O was added in total. The cells were resuspended in the volume of MQ-dH_2O that was left after the final wash step. A small volume of MQ-dH_2O can be added, especially if one are doing several transformations and need a larger volume of cells. The cell suspension was aliquoted in two cold eppendorf tubes (50 µl in each tube) and used immediately. Once the harvested culture had been centrifuged, the whole procedure was performed in the cold room and the cells were kept on ice at all times. As the eppendorf cooling centrifuge was out of order, centrifuging at 4°C was replaced by centrifuging in the cold room.

4.9.2 Electroporation

Purified plasmids (2 µl) were mixed with a 50 µl aliquot of competent cells, kept on ice. The cell-DNA suspension was transferred to a cold 0.2 cm electroporation cuvette, and electroporated in the Gene Pulser II electroporator using settings of 200 Ω, 2.0 kV and 25 µF. Immediately afterwards, 500 µl 37 °C SOC medium was added to the cuvette in two rounds to a total volume of 1 ml and the suspension was transferred to a fresh Nunc tube (15 ml). The

cells were incubated at 37 °C with rotation at 220 rpm for 2 hours and the cells were plated on LB agar (containing appropriate antibiotic) in following dilutions: 10 µl, 200 µl, 300 µl and 490 µl. The plates were incubated at 37 °C and checked for colonies the following day.

4.10 Biofilm screening assay

Bt407 forms biofilm at the liquid-air interface and the biofilm adheres to plastic. Flexible, 96 well U-bottom PVC plastic were used. The microtiter plate assay has been used successfully in biofilm screening of various *B. cereus* strains [57, 59].

On the first day of the assay, bacteria were streaked on LB agar and incubated at 30 °C overnight. On the second day, a single colony was inoculated in 10 ml LB medium and incubated overnight at 30 °C with rotation at 225 rpm. On day three, 100 µl overnight culture was inoculated in 10 ml bactopeptone medium and incubated at 30 °C with rotation at 225 rpm for 2 hours and 15 minutes. The culture was then diluted 1:200 in bactopeptone medium and 125 µl of the dilution was added to each well of a PVC microtiter plate. The medium contained antibiotics and xylose when appropriate. Each strain of bacteria was added to eight wells, i.e. to an entire column of the plate. The first column functioned as a blank by adding bactopeptone medium only.

The plates were closed with corresponding lids and placed in a plastic chamber on top of moistened paper. After positioning the lid of the chamber, the chamber was air tightened by wrapping it in plastic foil. The plates were incubated at 30 °C for the proper number of hours.

When harvesting the plates, the wells were first washed with 150 µl PBS (Chapter 3.7). Crystal violet solution (0.3%, 130 µl, Chapter 3.7) was then added to each well and the plates were incubated at room temperature for 20 minutes. The wells were then washed three times with 180 µl PBS. Acetone:ethanol (1:4, 150 µl) was added to each well, and the plate was gently shaken for 30 seconds. From each well, 75 µl was transferred to the wells of a 96 well polystyrene plate with flat bottoms to which 75 µl aceton:ethanol (1:4) was already added, thereby diluting the samples 1:1. The absorbance was measured at 492 nm with an HTS 7000 Bio Assay Reader.

4.11 Microarray analysis

DNA microarrays allow for mapping of the expression of a large set of genes simultaneously, allowing monitoring the expression of the entire set of genes in one bacterium in a single experiment. A microarray is a slide with probes attached and each probe is an oligonucleotide representative for a gene. The slides are designed especially for the type of bacterium one

wishes to examine. RNA is isolated from the bacterial strains to be compared, for example from a wild type and a mutant. RNA is converted to cDNA and labeled with fluorescent dyes. These molecules are called targets. When the slide is exposed to labeled cDNA, a hybridization process will begin where probes bind to their complementary targets. The slides are then scanned at two different wavelengths (635 nm and 532 nm) and the fluorescence signals are recorded. The signal intensities correspond to the amount of labeled cDNA bound to each probe and therefore gives a measurement of the expression of each particular gene. RNA isolated from wild type and mutant are labeled with different dyes (Cy3 and Cy5) and the signal intensities obtained after scanning at both wavelengths will give information on whether a gene is up-regulated or down-regulated in the mutant relative to wild type [88]. An overview of the main steps in a microarray experiment is shown in Figure 7.

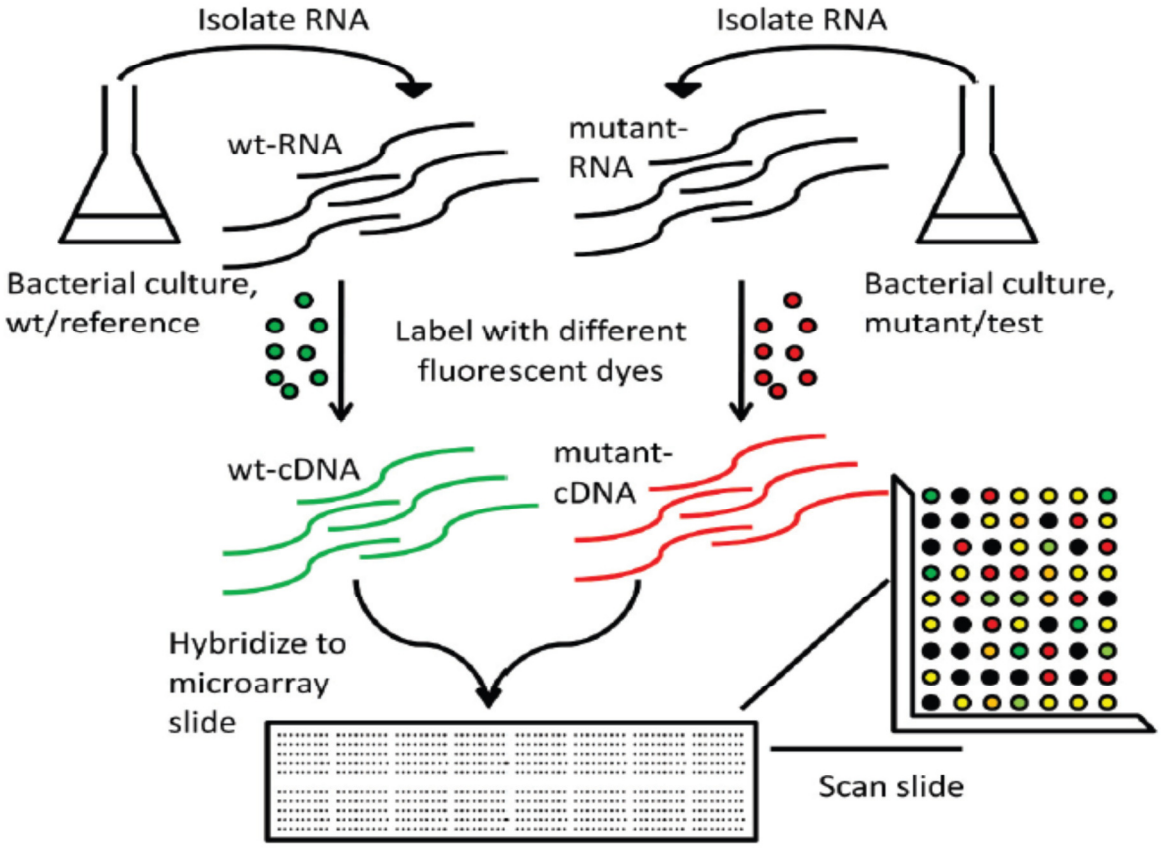

Figure 7: A general overview of the steps involved in a microarray experiment. RNA is first isolated from bacterial cultures of the strains to be compared, e.g. wild type and mutant. RNA is converted to cDNA by reverse transcription and wild type cDNA and mutant cDNA are labeled with different fluorescent dyes. Labeled cDNA from both strains are then hybridized to a microarray slide containing oligonucleotides representing the bacterium's entire set of genes. The slide is scanned at two wavelengths ensuring detection of fluorescence from both dyes. Expression of genes in wild type and mutant can thus be compared. Figure obtained from Karoline Fægri [89].

The “FairPlay III Microarray Labeling Kit” (Agilent, Chapter 3.9) was used for synthesizing, labeling and purifying cDNA. The slides used were spotted arrays, custom printed on aminosilyl-covered glass by Norwegian Microarray consortium, Trondheim. 70-mer oligonucleotides designed for *B. anthracis* Ames with supplementary probes for *B. anthracis* A2012 and *B. cereus* ATCC 14579 were used. Each probe was printed twice on the array and the array was printed twice on the slide. Negative and positive (housekeeping genes) controls were included [89].

4.11.1 Precipitation of RNA

RNA (20 µg) prepared with the RNeasy Mini kit I (Qiagen, Chapter 3.9) was volume adjusted to 100 µl using RNase-free dH_2O. Sodium acetate (3 M, pH 5.5, 11 µl) was added and the components were mixed. Ethanol (96%, 280 µl) was then added and the tube was mixed again. The RNA was precipitated at -80 °C overnight.

4.11.2 cDNA preparation

The precipitated RNA was centrifuged at 16 000 × *g* and 4 °C for 20 minutes. The supernatant was pipetted off and discarded. The pellet was washed once with 500 µl ice cold 70% ethanol and the tube was centrifuged again for 10 minutes. The supernatant was discarded and the pellet allowed to air dry, initially for 5 minutes on a heat block at 37 °C and then for 5 minutes at room temperature. The pellet was then put back on ice and resuspended in 8 µl RNase-free dH_2O. 5 µl random hexamers (Applied Biosystems) were added and the tube was mixed and incubated at 70 °C for 5-10 minutes. The sample was then put directly back on ice. Master mix for synthesis of cDNA was prepared, consisting of the following:

2 µl 10 × AffinityScript reaction buffer
1 µl 20 × dNTP mix (10 mM each, Chapter 3.7)
1.5 µl DTT (0.1 M)
0.5 µl RNase Block (40 U/µl)
2.5 µl AffinityScript HC Reverse Transcriptase (200 U/ml)

Master mix (7.5 µl) was added to the sample and incubated at 42 °C for 60 minutes. 10 µl NaOH (1 M) was added to the mixture and incubated at 70 °C for 10 minutes. The tube was then cooled slowly at room temperature. The tube was briefly spun down and 10 µl HCl (1 M) was added. The cDNA was mixed with 4 µl sodium acetate (3 M, pH 5.2, Chapter 3.7) and 1 µl glycogen (20 mg/ml) and 100 µl ice cold 96% ethanol was added. cDNA was then precipitated at -20 °C overnight. cDNA was recovered by centrifuging at 16 000 × *g* and 4 °C

for 20 minutes. The supernatant was pipetted off and discarded, and the pellet was washed once with 500 µl ice cold 70% ethanol and centrifuged again for 10 minutes. The supernatant was removed completely and the pellet was allowed to air dry for 5 minutes at 37 °C. As the cooling centrifuge was out of order, centrifuging at 4°C was replaced by centrifuging in the cold room.

4.11.3 Resuspension of Cy3 and Cy5

45 µl DMSO was added to each tube containing Cy3 or Cy5 dye in powder form. All steps in the procedure involving handling these dyes were performed with the lights turned off.

4.11.4 NHS-Ester Containing Dye Coupling Reaction

The cDNA pellet was resuspended in 5 µl 2 × Coupling buffer and incubated at 37 °C for 15 minutes. The tube was occasionally vortexed and briefly spun down during this incubation period. Resuspended dye (Cy3 or Cy5 in DMSO, 5µl) was added, mixed carefully with the other components and incubated for 30 minutes at room temperature. The samples were dye-swapped, meaning that wild type cDNA was colored with Cy3 and mutant cDNA with Cy5 in two of the biological replicate, and wild type with Cy5 and mutant with Cy3 in the two remaining biological replicates.

4.11.5 Dye-Coupled cDNA purification

1 × TE Buffer (pH 7.6, 90 µl, Chapter 3.7) and 200µl DNA binding solution:70% ethanol (1:1) was added to each tube and mixed thoroughly. The sample was transferred to a microspin cup placed in a 2 ml receptacle tube and centrifuged at 16 000 × *g* for 30 seconds. Flow-through was discarded and the column was washed once with 200 µl DNA binding solution:70% ethanol (1:1) and twice with 750 µl 75% ethanol. After the final wash, the flow-through was discarded and the empty column was centrifuged for 30 seconds to remove rests of ethanol. The microspin cup was transferred to a fresh eppendorf tube and 50 µl Tris-HCl (10 mM, pH 8.5) was added to eluate the cDNA. This was incubated for 5 minutes at room temperature and centrifuged at 16 000 × *g* for 30 seconds. This elution step was repeated twice by reusing the eluate. Eluates from samples to be applied to the same slide were combined in one eppendorf tube.

4.11.6 Concentration of labeled cDNA

For each combined sample, one micron filter device was washed by adding 500 µl MQ-dH_2O and centrifuging at 13 700 × *g* for 12 minutes at room temperature. Flow-through was discarded. The sample was added to the device and centrifuged for 10 minutes as above. The eluate was then recovered by placing the column upside down in a fresh eppendorf tube and

centrifuging at 1000 × *g* for 2 minutes. The final volume had to be exactly 27 µl. If the volume exceeded this, the eluate was put back in the column and concentrated further. If the volume was less than 27 µl, MQ-dH_2O was added. The samples were kept in the dark at 4 °C until the slides were ready for use.

4.11.7 Prehybridization

For each slide to be prepared, 50 ml prehybridization buffer was made and filled in Nunc tubes (50 ml). This buffer consisted of the following:

12.5 ml 20 × SSC
250 µl SDS (20%, Chapter 3.7)
666 µl BSA (7.5%)
36.6 ml MQ-dH_2O

The buffer was preheated in a water bath at 42 °C for ~15 minutes. One microarray slide was then placed in a tube filled with buffer and incubated in the same water bath for 30 minutes. Each slide was then transferred quickly to a Nunc tube filled with MQ-dH_2O and washed by slowly inverting the tube for 30 seconds. This step was repeated twice with fresh MQ-dH_2O. The slide was then transferred to a tube filled with isopropanol and washed for exactly 30 seconds. The slide was immediately transferred to a tube containing folded lens paper at the bottom and centrifuged at 200 × *g* and 20 °C for 4 minutes. The slide was immediately transferred to an empty tube and allowed to air dry for a few minutes so that rests of isopropanol evaporated. The slide could be stored in this empty tube for a maximum of 1.5 hours.

4.11.8 Hybridization

Hybridization buffer (53 µl) containing the following reagents was prepared for each combined sample/each slide:

24 µl formamide (100%)
20 µl 20 × SSC
1 µl SDS (8%)
8 µl salmon sperm DNA (1 mg/ml)

Hybridization buffer (53 µl) was added to each sample consisting of 27 µl to a total volume of 80 µl. This was incubated at 95 °C for 2 minutes, briefly spun down and incubated at 42 °C for 20 minutes. One lifter slip per slide to be analyzed was washed in 70% ethanol and dried off carefully using lens paper. One slide per each combined sample was placed on a heating

block at 42 °C with the array side pointing upwards. The lifter slip was placed on top of the slide with the protuberant borders facing downwards so that a small space between the lifter slip and the slide was created. The lifter slip had to precisely cover the area containing the printed microarray oligonucleotides. Half of the sample (40 µl) was then pipetted slowly at the edge of the lifter slip so that the sample distributed evenly in the space between the slide and the lifter slip. Each of two small cavities of the hybridization chamber were filled with 5 × SSC (30 µl) and the slide was placed in the middle of the chamber. The lid was attached to the chamber by six screws which were tightened carefully. Holding the chamber horizontally at all times, it was lowered into a water bath at 42 °C and incubated for 17-18 hours. Nunc tubes (50 ml) filled with wash buffer 1 and wash buffer 2 were preheated in a water bath at 42 °C for ~15 minutes.

Composition of wash buffer 1:
12.5 ml 20 × SSC
250 µl SDS (20%)
MQ-dH_2O added to 500 ml

Composition of wash buffer 2:
1.5 ml 20 × SSC
MQ-dH_2O added to 500 ml
Both buffers were sterile-filtrated.

The chamber was removed from the water bath, dried off and opened. The slide with lifter slip attached was transferred to a tube containing wash buffer 1. The lifter slip was carefully removed without disturbing the slide and the slide was washed by slowly inverting the tube for 5 minutes. This washing step was repeated twice using fresh wash buffer 1. The slide was then transferred to a tube containing wash buffer 2 and washed in the same manner. This washing step was repeated once. The slide was transferred to a tube filled with isopropanol and washed for exactly 30 seconds. The slide was then immediately transferred to a tube containing folded lens paper at the bottom and centrifuged at 200 × *g* and 20 °C for 4 minutes. The slide was instantly transferred to an empty tube and allowed to air dry for a few minutes. The slide was scanned using “Genepix 4000b” (Axon), synchronized with the software “GenePix Pro”. Intensities of red (635 nm) and green (532 nm) beams were adjusted so that the ratio between red and green signals intensities from the slide was as close to 1 as possible.

4.11.9 Analysis

The raw image was first analyzed by gridding. This involved positioning a grid consisting of circles corresponding to the position of each probe. Spots of poor quality and "flames" were marked. These markings ensured that the software ignored these particular spots in the further analysis. The boundaries of each spot were determined and intensities of signals from spots and background were calculated for each wavelength. Further analysis was performed using the statistical computing platform R, version 2.13.0 (http://www.r-project.org/) and the package LIMMA (Linear models for microarray data) [90]. Relevant information from the raw image analysis was transferred from GenePix Pro to R. Appropriate cut-off values for red and green signal intensities were decided based on histograms showing intensities for red and green background and spot signals intensities respectively. These cut-off values ensured removal of background signals in the further analysis. Spots of poor quality and spots with weak or saturated signals at both wavelengths were removed. The genes wished to be identified were those differently expressed in the wild type and the mutant corresponding to the spots with different signal intensities when exposed to different wavelengths. Control spots were removed so that they didn't influence the analysis and each normal spot was given a quality weight based on spread of signal intensity within the spot. A small offset was added to stabilize spots with low signal intensities. A normalization step removed systematic bias from the data, i.e. bias arising from variation in the technology. Dye bias was corrected through dye-swap. Technical replicates were averaged and given a quality weight and these averages were compared across multiple slides. $\log_2$ expression ratios and significance were finally estimated [89].

4.12 Reverse transcriptase quantitative PCR (RT-qPCR)

RT-qPCR is a method for quantifying mRNA and thereby analyzing the expression of genes in a highly sensitive manner. Reverse trancriptase is first used to synthesize cDNA which is used as template in the PCR reaction. SYBR Green I fluorescence dye binds to the double stranded PCR-product and the fluorescence intensity will increase following each round of amplification and is proportional to the amount of PCR-product formed. The quantification cycle (Cq) represents the cycle number in which the fluorescence signal exceeds a defined background fluorescence signal. Cq is therefore inversely proportional to the amount of target in the starting material [91]. Reference genes are used for normalization due to differences in the amount of RNA used as starting material and should be stably expressed in the bacterium without being affected by introduction of the particular mutation to be studied. For the *B. cereus* group of bacteria, gatB/Yqey, rpsU and udp have been shown to be suitable reference

genes for RT-qPCR as they are stably expressed throughout their life cycles [92]. These genes will be used as references in this RT-qPCR experiment although it has not been specifically tested whether the introduced mutations affect their expression.

4.12.1 DNase-treatment and cDNA synthesis

RNA (20 µg) isolated with the RNeasy Mini kit (Qiagen, Chapter 3.9) was mixed with RNase-free dH_2O to a total volume of 88 µl. 10 × Turbo DNase-buffer (10 µl) and 2 µl Turbo DNase (Ambion) was added and the tube was incubated at 37 °C for 30 minutes. RLT containing 10 µl/ml β-mercaptoethanol (350 µl) and 250 µl 96% ethanol was added and the components were mixed. This was then transferred to a RNeasy Minispin column and centrifuged at 16 000 × *g* for 20 seconds at room temperature. RPE (500 µl) was added and the column was centrifuged again for 20 seconds. Flow-through was discarded. This wash step was repeated once and the empty column was centrifuged at 16 000 × *g* for 2 minutes. The column was transferred to a fresh eppendorf tube and 30 µl RNase-free dH_2O was added. RNA was eluted by centrifugation at 16 000 × *g* for 20 seconds. This elution step was repeated once with following centrifugation for 1 minute to a total eluate volume of 60 µl. The concentration and purity of RNA was measured by UV-spectrophotometry and the samples were kept on ice at all times. An equivalent amount of each RNA sample was transferred to three PCR-tubes called A, B and C. In this experiment, 3 pairs of samples consisting of wildtype and mutant were used. The volume was adjusted to 8.3 µl by adding RNase-free dH_2O. Random hexamers (0.75 µl, Applied Biosystems) and 0.75 µl dNTP mix (10 mM each, Chapter 3.7) was added to each tube to a total volume of 9.8 µl. The tubes were incubated at 65 °C in a PCR-machine for 5 minutes and then put directly back on ice. To tubes A and B, the following was added:

3 µl 5 × First-strand Buffer
0.75 µl DTT (0.1 M)
0.075 µl SUPERase·In
0.675 µl RNase-free dH_2O
0.75 µl Superscript III Reverse Transcriptase

To tubes C (minus reverse transcriptase control), the following was added:
3 µl 5 × First-strand Buffer
0.75 µl DTT (0.1 M)
0.075 µl SUPERase·In
1.425 µl RNase-free dH_2O

The contents of each tube with a volume of 15.1 µl were mixed gently. The tubes were then incubated at the following program in a PCR machine:

25 °C: 5 minutes

50 °C: 60 minutes

70 °C: 15 minutes

4 °C →

4.12.2 Determination of E and r^2 for the primer pairs

PCR efficiency (E) defines the efficiency of the primer pair by describing the factor by which the amount of PCR-product increases following each cycling round. r^2 (square of Pearson's correlation coefficient) describes the linear relationship between Cq-values and $\log_{10}$ values of concentrations of cDNA starting material. This relationship should be as linear as possible (r^2 close to 1) in the concentration spectrum of relevance so that amount of starting material in the samples can be estimated correctly. In each well of the 96-well qPCR plate, 5 µl Light Cycler 480 SYBR Green I Master, 3 µl primer mix (concentration: 1.7 µM of each primer) and 2 µl cDNA (from samples prepared for the actual RT-qPCR experiment) was added. All primers pairs were used with the following dilutions of cDNA: 0.67 µl, 0.2 µl, 0.067 µl, 0.02 µl, 0.0067 µl and 0.002 µl. Three replicates were fitted on the same plate.

The plate was then sealed with a film and spun down at 700 × *g* for 1 minute immediately before analyzing. The qPCR reactions were performed on a LightCycler 480 Real-Time PCR System (Roche), using the following cycling conditions: 95 °C for 5 minutes, 95-58-72 °C for 10-10-8 seconds for 45 cycles followed by a melting curve analysis and cooling to 40 °C.

The Cq values were determined using the second derivate maximum method using the LightCycler 480 software (Roche) and the melting curves were inspected to ensure that the primers functioned optimally and only one PCR-product had been synthesized (one peak).

The averages of the Cq values were plotted against the $\log_{10}$ values of the amount of cDNA in the Microsoft Excel software. E-values were calculated by the formula $10^{(-1/\text{slope})}$. r^2-values were calculated by the Microsoft Excel software based on the linear relationship between the Cq values and the $\log_{10}$ values of the amount of cDNA.

4.12.3 Negative controls

cDNA in tubes A, B and C were diluted to the suitable concentration in eppendorf tubes. Primer pairs for two reference genes were chosen when checking for the abscense of contaminating genomic DNA in the samples; gatB/Yqey (primers gatB_left and gatB_right) and rpsU (primers rpsU_left and rpsU_right). Again, in each well of the plate, 5 µl Light

Cycler 480 SYBR Green I Master, 3 µl primer mix (concentration: 1.7 µM of each primer) and 2 µl cDNA was added, and the same qPCR conditions as described above (Chapter 4.12.2) were used. All samples were checked using primer pairs for both reference genes and all samples (A, B and C) from all three biological replicates were fitted on the same plate.

4.12.4 Analyzing expression of target genes

When setting up plates with the actual samples, primers specific for three reference genes were used: gatB/Yqey, rpsU and udp (primers udp_left and udp_right). In each well of the plate 5 µl Light Cycler 480 SYBR Green I Master, 3 µl primer mix (concentration: 1.7 µM of each primer) and 2 µl cDNA was added, and the same qPCR conditions as described above (Chapter 4.12.2) were used. One plate was used for each biological replicate, thus ensuring that the qPCR reactions for target and reference genes for each sample were run on the same plate.

Analysis of gene expression data was performed using the delta-delta-Cp method [93] as follows: The Cq values obtained for the two technical replicates (samples A and B) were averaged and transformed into linear scale expression quantities using the formula E^{Cq}. For each sample, the geometric mean of E^{Cq} values obtained for the three reference genes was calculated. Then, the E^{Cq} value obtained for each of the target genes was normalized to the geometric mean of the E^{Cq} obtained for the three reference genes. Then, the expression ratio for each gene between two samples to be compared was calculated. Finally, averages and standard errors were calculated from the expression ratios obtained for each biological replicate.

4.13 Designing primers

Primers thought to distinguish between genes with very similar nucleotide sequences were designed. EMBL-EBI software (http://www.ebi.ac.uk/) was used for pairwise sequence alignments to identify differences in the nucleotide sequences. The software Primer3 (http://primer3.sourceforge.net/) was used for designing compatible oligonucleotides with lengths of 98-102 bp and a melting temperature (Tm) of 60 °C.

CHAPTER 5: RESULTS

5.1 Characterization of the *cdg135* deletion mutant (Bt407Δ135)

The protein encoded by *cdg135*, is a predicted cytoplasmic protein with a putative sensory PAS/PAC domain, a GGDEF domain, and an EAL domain (Figure 4), in which both the GGDEF and EAL domains are predicted to be enzymatically active. Preliminary results had indicated that Cdg135 affected biofilm formation in Bt407 after 24 hours of growth (Fagerlund & Økstad, unpublished results). It was therefore of interest to characterize the *cdg135* deletion mutant by studying its possible effects on motility and whole genome transcriptional activity.

5.1.1 Identification

A Bt407 *cdg135* mutant (Bt407Δ135) had previously been constructed (Fagerlund & Økstad, unpublished results). In order to confirm the identity of the provided strain (Chapter 3.1) prior to performing further experiments for the current thesis, PCR was performed to confirm the absence of the *cdg135* gene for the Bt407Δ135 strain. Genomic DNA isolated as described in Chapter 4.2 was used as template and the PCR was carried out as described in Chapter 4.3 using primers located up- and downstream of *cdg135*, respectively. Expected product size and primers used are shown in Table 4. Agarose gel electrophoresis was used to analyze the PCR product as described in Chapter 4.7. The results are shown in Figure 8 (lane 3). The PCR product matched the expected size and deletion of the gene *cdg135* was thus confirmed.

Table 4: Primers used in PCR analysis for confirming deletion of genes along with expected product sizes

Gene	Forward primer	Reverse primer	Expected product size
cdg135	135upF	135downR	1572 bp
bspA	Up-02561-F	Down-02561-R	1604 bp
cdg141	141upF	141downR	1450 bp
cdg113	Up-113-F	Down-113-R	1716 bp

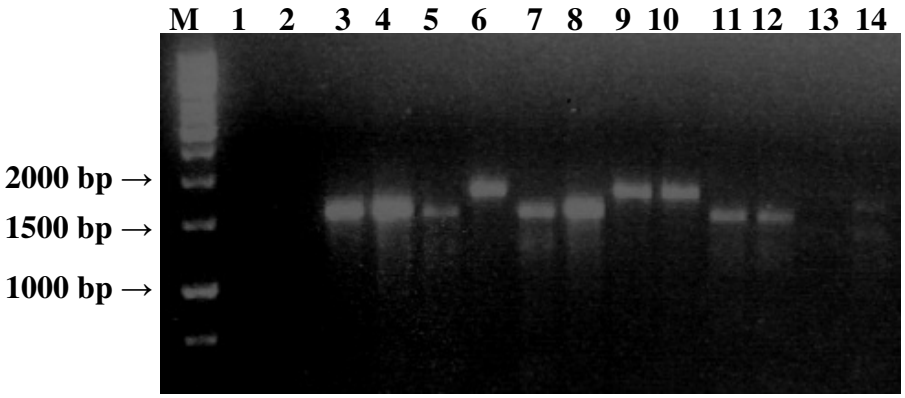

Figure 8: PCR analysis to confirm deletion mutants. Lane M: GeneRuler 1 Kb DNA Ladder: for info on products in lane 1-17, see Tables 14, 20 and 22.

5.1.2 Growth curves with observations for motility

Growth curves comparing Bt407Δ135 and Bt407 wild type were performed three separate times with observations for motility (Chapter 4.1.1). The chosen culture medium was bactopeptone (Chapter 3.8) and the cultures were incubated at 30 °C under rotation at 225 rpm. OD_{600} was measured every half hour and motility was studied by observing the bacteria in a microscope. A representative growth curve is shown in Figure 9. All three growth curve experiments gave similar results except that the duration of the lag-period varied slighty between experiments. The results showed that deletion of *cdg135* did not influence growth in Bt407 under the tested conditions (Figure 9).

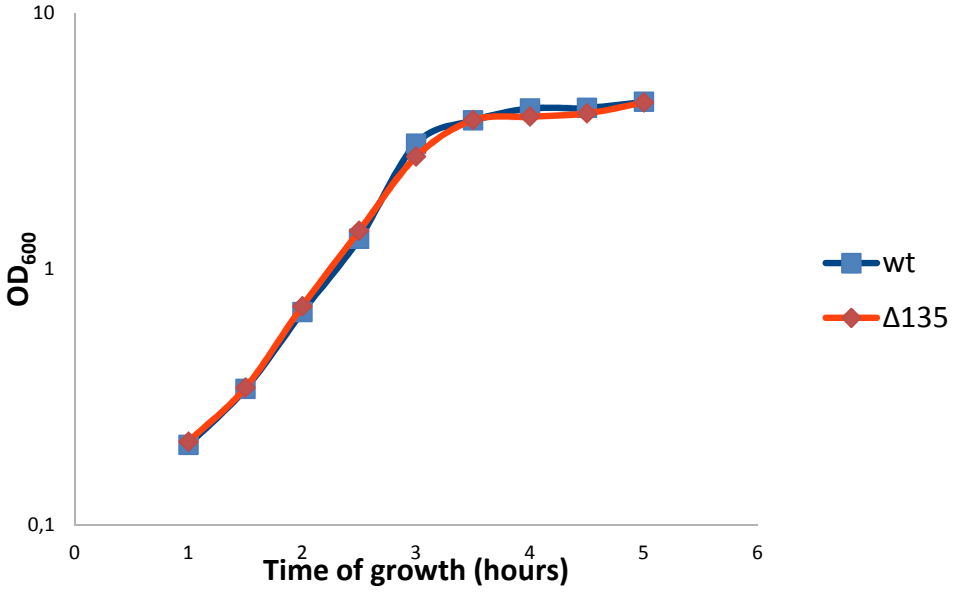

Figure 9: Growth curves comparing growth of Bt407 wild type (wt) and *cdg135* mutant (Δ135). Cells were grown in bactopeptone medium at 30 °C with rotation at 225 rpm. Data shown are representative of three independent experiments.

A significant difference in motility was seen in early exponential phase, about 1.5 hours after initiating incubation of the cultures, by light microscopy. Bt407Δ135 was significantly more motile than the wild type and this observation was reproducible in all three experiments performed. It was hypothesized that this difference could indicate differential expression of genes at this time-point. It was therefore decided to perform a transcriptional analysis of the whole genome using microarrays on samples collected after 1.5 hours of growth. Samples of 12 ml were harvested from four biological replicates of Bt407 and Bt407Δ135 as described in Chapter 4.4. At time of harvest, the bacteria were observed in a microscope and confirmed to show the previously observed difference in motility between the wild type and the Bt407Δ135 strain. OD_{600} was measured upon harvesting and OD_{600} values are shown in Table 5.

Table 5: OD_{600} values of cultures at time of harvest. Four biological replicates (1-4), each consisting of wild type and *cdg135* deletion mutant, were harvested.

Biological replicate	OD_{600} Bt407 wild type	OD_{600} Bt407Δ135
1	0.276	0.236
2	0.252	0.246
3	0.220	0.242
4	0.254	0.232

5.1.3 RNA isolation from Bt407 wild type and *cdg135* deletion mutant

RNA was isolated (Chapter 4.4) and concentration and purity was measured by UV-spectrophotometry (Chapter 4.8). The averages of at least two measurements are shown in Table 6. The RNA concentrations were found to be sufficient and the purity of the RNA samples was acceptable (A_{260}/A_{280} ratio between 1.8 and 2.0).

Table 6: Concentration measurements of RNA isolated from four biological replicates (1-4), each from wild type and the *cdg135* deletion mutant. The ratio of the absorbance at A_{260} and A_{280} was calculated to estimate purity.

Set	RNA concentration Wild type	RNA concentration Δ135	A_{260}/A_{280} Wild type	A_{260}/A_{280} Δ135	A_{260} Wild type	A_{260} Δ135
1	0.2923 µg/µl	0.7763 µg/µl	1.94	1.95	0.07	0.19
2	1.0745 µg/µl	0.9553 µg/µl	1.84	1.94	0.24	0.22
3	2.2589 µg/µl	1.3772 µg/µl	1.87	1.89	0.51	0.31
4	0.9953 µg/µl	1.1878 µg/µl	1.88	1.87	0.23	0.27

The integrity of the isolated RNA was studied through agarose gel electrophoresis as described in Chapter 4.7. Results are shown in Figure 10. The bands separated by the gel were sharp, indicating RNA of good integrity. However, the upper band (23S rRNA) should be more intense than the lower band (16S rRNA) and this was not obvious in these samples. The

slightly blurred bands observed in set 3 and 4 were due to problems with focusing the camera. The quality of RNA was still found to be adequate and the obtained RNA was used in the microarray experiment.

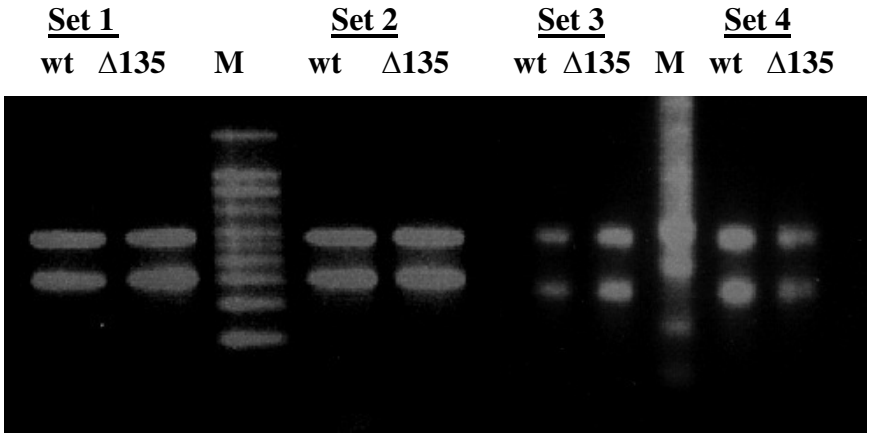

Figure 10: Results from agarose gel electrophoresis used for inspecting the integrity of RNA. Set 1 to 4: RNA isolated from biological replicates 1 to 4. wt: RNA isolated from Bt407 wild type, Δ135: RNA isolated from Bt407Δ135, M: 0.24-9.5 Kb RNA Ladder

5.1.4 Transcriptional analysis using microarrays

The amount of RNA used as starting material for the microarray procedure was 20 µg and the experiment was performed as described in Chapter 4.11. The four biological replicates were dye-swapped meaning that wild type cDNA was labeled with Cy3 and *cdg135* deletion mutant cDNA with Cy5 in RNA sets 1 and 3 and that wild type was labeled with Cy5 and *cdg135* deletion mutant with Cy3 in RNA sets 2 and 4. Set 1 of wild type and mutant was used for hybridizing slide 1, set 2 for slide 2, set 3 for slide 3 and set 4 for slide 4.

The intensities of the scanning beams from each wavelength (635 nm/532 nm) used in scanning the slides had to be adjusted so that the count ratio for each slide was as close to 1 as possible. This ratio describes the ratio of the sum of detected green and the sum of detected red signal intensities. The intensities chosen for the red (635 nm) and the green (532 nm) channel and count ratios obtained for each slide are shown in Table 7.

Table 7: Count ratios for scanned slides 1-4 used in microarray experiment comparing wild type and *cdg135* deletion mutant. Intensities chosen for red (635) and green (532) channel are also shown.

Slide	PTM Gain 635	PTM Gain 532	Count ratio
1	810	670	1.01
2	800	640	1.05
3	730	700	1.05
4	830	610	0.97

All slides were included in the analysis performed as described in Chapter 4.11.9 using the statistical computing platform "R" (http://www.r-project.org/) and the package LIMMA (Linear models for microarray data) [90]. Histograms showing the distribution of intensities from red and green spot signals as well as from red and green background signals are shown in Appendix 1 (Figures 35 to 38). Minimum spot intensities for inclusion in the further analysis were decided based on the aforementioned histograms to ensure removal of background signals. Cut-off values of 270 and 500 for red and green signal intensities respectively were chosen. Results from the analysis are shown in Tables 8 and 9. One gene, encoding a putative collagen adhesion protein orthologous to *B. cereus* ATCC 14579 BC_1060, was found to be significantly down-regulated in the *cdg135* deletion mutant (Table 8). In addition and as expected, the *cdg135* gene itself was found to be down-regulated in the *cdg135* mutant compared to the wild type. Four genes were significantly (False discovery rate (FDR)-corrected P-values<0.5) up-regulated in the *cdg135* mutant (Table 9). These four genes appeared to constitute two homologous operons, each composed of a gene encoding a major facilitator superfamiliy (MFS) transporter and a gene encoding an aldo/keto reductase. Both aldo/keto reductases show 76% identity in amino acid sequence towards the characterized aldo/keto reductase YtbE from *B. subtilis* [94]. A third aldo/keto reductase was additionally found to up-regulated in the deletion mutant, however with an FDR-corrected P-value of 0.12 (Table 9).

Table 8: Results from microarray experiment comparing wild type and *cdg135* deletion mutant: genes down-regulated in the *cdg135* deletion mutant. Locus tag in both Bt407 and ATCC 14579 and predicted function of each protein along with fold change (expression ratio), log_2(fold change), and adjusted P-values values are shown.

Locus tag in Bt407	Locus tag in ATCC 14579	Predicted function	Fold-change#	log_2(fold-change)	adj. P-value
Not annotated	BC1060	Collagen adhesion protein	2.6	1.36	<0.00009
bthur0002_5370	BC0628	Cdg135$^{\Delta}$	1.5	0.59	0.12

Fold change is the ratio of expression in the wild-type divided by the expression in the *cdg135* mutant

$^{\Delta}$ This gene is deleted in the mutant strain

Table 9: Results from microarray experiment comparing wild type and *cdg135* deletion mutant: genes up-regulated in the *cdg135* deletion mutant. Locus tag in both Bt407 and ATCC 14579 and predicted function of each protein along with fold change (expression rati) and log_2(fold change) values are shown. * adj. P-value 0.12. All other genes: adj. P-value <0.05

Locus tag in Bt407	Locus_tag in ATCC 14579	Predicted function	Fold change	log_2(fold change)
bthur0002_31060	BC3392	YtbE (Aldo/keto reductase)	2.6	1.36
bthur0002_49600	BC5057	YtbE (Aldo/keto reductase)	1.6	0.71
bthur0002_49610	BC5058	MFS-type transporter	2.5	1.31
bthur0002_31280	BC3410	Aldo/keto reductase	1.6*	0.67*
bthur0002_31070	BC3393	MFS-type transporter	1.6	0.65

Fold change is the ratio of expression in the *cdg135* mutant divided by the expression in the wild-type

5.1.5 RT-qPCR to confirm up-regulation of genes

The slides used in the microarray experiment contained oligonucleotides designed for *B. anthracis* Ames with supplementary probes for *B. anthracis* A2012 and *B. cereus* ATCC 14579 as described in Chapter 4.11. ATCC 14579 shows high sequence similarity with Bt407, and it was therefore appropriate to use this slide for gene expression analysis in Bt407. However, there was some risk of cross-hybridization due to sequence differences in particular genes between strains. For example, the slide was specifically designed to distinguish between the two very similar aldo/keto reductase genes BC3392 and BC5057 in *B. cereus* ATCC 14579, which show 93,7% identity in nucleotide sequence (Annette Fagerlund, personal communication). However, comparison of the sequences of the microarray oligo probes designed for these two genes and the sequences of their respective orthologs bthur0002_31060 and bthur0002_49600 in Bt407 indicated that cDNA from both Bt407 genes were likely to hybridize to either one of the oligonucleotides on the slide designed to detect BC3392 and BC5057. Similarly, cross-hybridization was likely to occur between the probes designed for the two MFS-transporter genes BC3393 and BC5058 and their respective Bt407 orthologs bthur0002_31070 and bthur0002_49610. Therefore, in order to be able to confirm that both operons encoding a MFS-transporter and an aldo/keto reductase were up-regulated in the *cdg135* mutant, PCR primers able to discriminate between the Bt407 homologs were designed (Chapter 4.13) and used to further analyze expression of all genes listed in Table 9 by RT-qPCR analysis. RNA from the biological replicates 2, 3 and 4 isolated

for use in the microarray experiment (Table 6, Figure 10) was treated with Turbo DNase, purified and utilized in RT-qPCR as described in Chapter 4.12. Concentrations and purity of RNA was measured twice after treatment with Turbo DNase and purification. Averages of these measurements are shown in Table 10. Concentration and purity of the RNA samples was found to be adequate for use in the further analysis.

Table 10: Concentration measurements of RNA isolated from biological replicates 2-4, each from wild type and the *cdg135* deletion mutant, after treatment with Turbo DNase and purification. The ratio of the absorbance at A_{260} and A_{280} was calculated to estimate purity.

Set	RNA concentration Wild type	RNA concentration Δ135	A_{260}/A_{280} Wild type	A_{260}/A_{280} Δ135	A_{260} Wild type	A_{260} Δ135
2	0.2104 µg/µl	0.2300 µg/µl	1.98	2.01	0.10	0.11
3	0.1159 µg/µl	0.1323 µg/µl	2.01	1.96	0.05	0.06
4	0.1865 µg/µl	0.1548 µg/µl	1.96	1.95	0.09	0.07

cDNA synthesis

Before expression of genes was analyzed by qPCR, RNA was converted to cDNA by reverse transcription (Chapter 4.12.1). The maximum volume for the reaction was 8.3 µl. 8.3 µl of the RNA sample with the lowest concentration (Table 10: wild type, set 3) equaled 0.96 µg RNA. Therefore, 0.96 µg RNA was used in the experiment, for all samples. Each RNA sample from wild type and *cdg135* mutant from biological replicates 2, 3, and 4 was aliquoted in three tubes (A, B and C). cDNA was synthesized from samples A and B as described in Chapter 4.12.1 while samples C were negative control reactions without added reverse transcriptase. These contained consequently no cDNA and functioned as controls for contamination of genomic DNA in the samples. After withdrawal of a small amount of synthesized cDNA from samples A and B for use in determination of E and r^2 for the new primer pairs (see below), all samples A, B and C were diluted 1:20 in RNase-free dH_2O for use in the subsequent qPCR experiments.

Primers used in qPCR and determination of their E and r^2 values

Primer pairs specific for each of the five target genes (Table 9) to be analyzed were designed (Chapter 4.13), and PCR effeciencies (E) and r^2 for each primer pair was estimated as described in Chapter 4.12.2 and by Pfaffl, 2011 [93] from qPCR reactions run as described in Chapter 4.12.2 on a dilution series of pooled cDNA. The PCR efficiency of each primers pair describes the factor by which the amount of PCR-product increases following each cycling round. r^2 describes the linear relationship between quantification cycle (Cq)-values,

determined using the LightCycler 480 software (Roche) and $\log_{10}$ values of concentrations of cDNA starting material. This relationship should be as linear as possible (r^2 close to 1) in the concentration spectrum of relevance so that amount of starting material in samples can be estimated correctly. Calculated values of E and r^2 of the primer pairs used in this RT-qPCR experiment are shown in Table 11.

The three genes gatB/Yqey, rpsU and udp, shown to be stably expressed throughout the *B. cereus* life cycle [92], were chosen for use as reference genes. Primer pairs and previously determined E and r^2 values for the reference gene primers are shown in Table 11. Sequences of all qPCR primers used are listed in Table 2.

Table 11: Primer pairs used in RT-qPCR experiment analyzing expression of target genes bthur0002_31070, bthur0002_31060, bthur0002_49610, bthur0002_49600 and bthur0002_31280 along with E and r^2 values.

Name of gene	Forward primer	Reverse primer	E	r^2
gatB/Yqey (bthur0002_41620)	gatB_left	gatB_right	1.93	0.9968
rpsU (bthur0002_41630)	rpsU_left	rpsU_right	1.87	0.9957
udp (bthur0002_50610)	udp_left	udp_right	1.85	0.9992
bthur0002_31070	31070-F	31070-R	2.06	0.9970
bthur0002_31060	31060-F	31060-R	2.06	0.9981
bthur0002_49610	49610-F	49610-R	1.95	0.9980
bthur0002_49600	49600-F	49600-R	1.95	0.9978
bthur0002_31280	31280-F	31280-R	2.09	0.9985

E, PCR efficiency. r^2, square of Pearson's correlation coefficient from serial dilutions.
The E and r^2 values for the reference genes used: gatB/Yqey, rpsU and udp were previously determined by Annette Fagerlund.

Negative controls

Contaminating DNA can act as potential templates in the RT-qPCR experiment and give false positive results. To examine whether any contaminating gDNA was present in the samples, qPCR reactions using samples A, B and C were run using primer pairs for reference genes gatB/Yqey and rpsU. Differences in Cq values obtained with the negative controls (samples C) relative to the corresponding samples for which reverse transcriptase was included in the cDNA synthesis reaction (samples A and B), were all somewhere between 16 and 24. Since the amplification factor of each round is maximum 2, a difference of 16 means that samples A and B contained 2^{16} = ~65 000 more DNA than samples C. This indicated very little contamination of gDNA which would not influence the analysis.

Transcriptional analysis of target genes in wild type and *cdg135* mutant samples

cDNA samples A and B were used for analyzing expression of target genes giving two technical replicates for each biological replicate. Primer pairs specific for target and reference genes (Table 11) were used in the qPCR experiment. Analysis of data was performed using the mathematical model described by Pfaffl [93] which normalizes the data using values obtained from the reference genes taking into account the estimated E and r^2 values, as described in Chapter 4.12.4. The results shown in Table 12 are averages of the *cdg135* deletion mutant/wild type expression ratios. Results are also shown graphically in Figure 11.

Table 12: Results from RT-qPCR experiment analyzing expression of genes bthur0002_31070, bthur0002_31060, bthur0002_49610, bthur0002_49600 and bthur0002_31280 in wild type and *cdg135* deletion mutant based on three biological replicates, each including two technical replicates. Fold change (expression ratio) and log_2(fold change) values based on average mutant/wild type ratios and standard errors are shown

Locus tag in Bt407	Fold change	Standard error	log_2(fold change)
bthur0002_31070	7.1	1.6	2.8
bthur0002_31060	7.4	1.5	2.9
bthur0002_49610	7.6	0.5	2.9
bthur0002_49600	7.2	1.3	2.9
bthur0002_31280	19.5	2.1	4.3

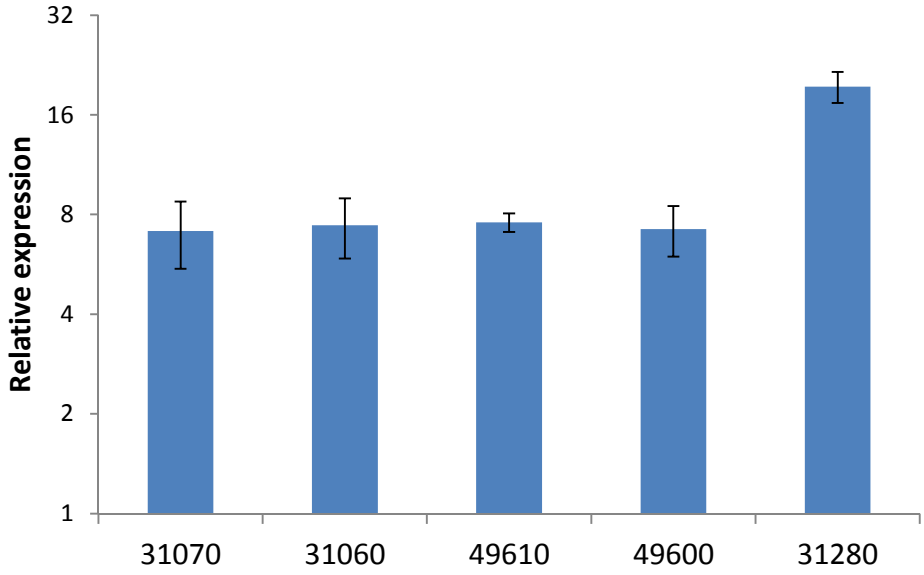

Figure 11: Relative expression of genes bthur0002_31070, bthur0002_31060, bthur0002_49610, bthur0002_49600 and bthur0002_31280 (bthur0002 omitted for clarity below each column) in Bt407Δ135 compared to Bt407 wild type. The results shown are averages and standard errors of three biological replicates, each based on two technical replicates. Note that the y-axis is on log_2 format.

These results confirmed the up-regulation of the five examined genes in the *cdg135* mutant compared to the wild type strain, as originally identified in the microarray experiment (Table 9). However, the methods gave different results with respect to degree of up-regulation as shown in Table 13.

Table 13: Comparisons of results from microarray analysis and RT-qPCR experiment analyzing expression of genes found to be up-regulated in *cdg135* mutant compared to wild type (wildtype/mutant expression ratio).

Locus tag in Bt407	Microarrays: fold change	RT-qPCR: fold change
bthur0002_31070	1.6	7.1
bthur0002_31060	2.6	7.4
bthur0002_49610	2.5	7.6
bthur0002_49600	1.6	7.2
bthur0002_31280	1.6	19.5

5.2 Characterization of interaction between BspA and Cdg135

The microarray experiment indicated that an ortholog to the gene with locus tag BC_1060 in *B. cereus* ATCC 14579 was down-regulated in the *cdg135* deletion mutant (Table 8). This gene encodes a putative collagen adhesion protein (GenBank protein ID AAP08047), showing the typical features of Gram-positive cell wall-anchored surface proteins, including a LPXTG sortase substrate motif in the C-terminal end (Figure 12B) [95]. This gene had not been annotated in the currently available draft genome sequence of Bt407, and will be referred to as *bspA* (*Bacillus* surface protein A) in the current thesis. Preliminary results from work performed in the Økstad group had indicated that both knockout mutants of *bspA* and *cdg135* in Bt407 were deficient in biofilm formation compared to wild type (Fagerlund & Økstad, unpublished results). It has also been shown that *bspA* is located downstream of a riboswitch called Bc2 that binds c-di-GMP and thereby induces expression of downstream genes [73]. *bspA* and the Bc2 riboswitch are illustrated in Figure 12A. As *cdg135* is possibly involved in the metabolism of c-di-GMP and as *bspA* is located downstream of a c-di-GMP sensitive riboswitch, it was of interest to study the possible connection between the proteins BspA and Cdg135.

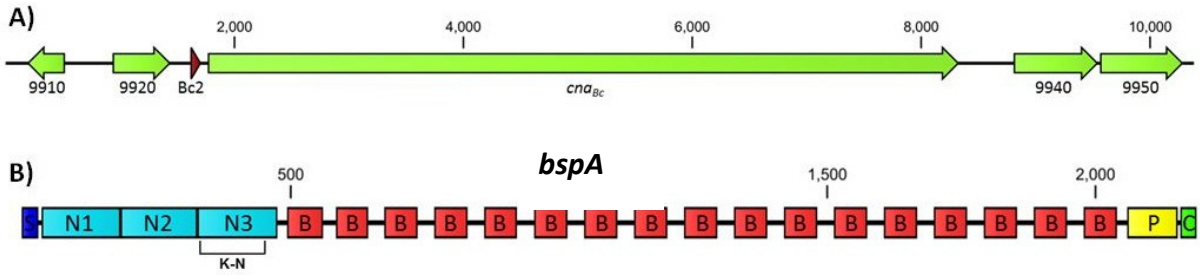

Figure 12: A) Organization of the gene *bspA* and its flanking region. The c-di-GMP sensitive riboswitch Bc2 is indicated in red. B) Domain organization of BspA showing the signal peptide sequence (S), the predicted subdomains of the A-region (N1, N2, N3), the domain repeats of the B-region (B), the proline-rich repeat region and the cell wall sorting signal containing the LPXTG sortase substrate motif. Figure made by Annette Fagerlund.

To study possible interactions between the proteins BspA and Cdg135, it was of interest to examine the effect of over-expression of BspA in a *cdg135* mutant, and conversely, the over-expression of Cdg135 in a *bspA* mutant, on growth, motility and biofilm formation. As controls, wild type strains over-expressing Cdg135 or BspA were included, in addition to wild type and mutant strains containing the pHT304-pXyl empty vector construct. The corresponding strains without plasmids were also included in the analysis. Finally, control strains over-expressing a mutated variant of Cdg135 (Cdg135mut) was included. In the Cdg135mut variant, two substitutions had been introduced in the signature GGDEF motif sequence known to be required for DGC activity in GGDEF domain proteins. Thus, the strains shown in Table 14 were to be tested for growth effects, motility and ability to form biofilms.

5.2.1 Preparation and/or confirmation of strains to be tested for growth, motility and biofilm formation

Table 14: List of all strains to be tested for growth, motility and biofilm formation. Strains marked with asterisk were constructed in the current thesis. Lanes used for identification of inserted plasmids and deletion mutants in PCR analysis are also shown.

Strain	Description	Lane in PCR confirming:	
		Presence of plasmids (Figure 15)	Deletion of gene (Figure 8)
Bt407	Wild type		
Bt407 + pHT304-pXyl-135	Wild type over-expressing Cdg135	1	
Bt407 + pHT304-pXyl-135mut	Wild type over-expressing mutated Cdg135. Two amino acids in the GGDEF motif are exchanged, giving GGAAF	7	
Bt407 + pHT304-pXyl-bspA	Wild type over-expressing BspA	4	

Table 14: continued			
Bt407 + pHT304-pXyl-empty vector	Wild type containing empty vector. Control for over-expression strains	3	
Bt407Δ135	Wild type with deletion of *cdg135*		3
Bt407Δ135 + pHT304-pXyl-bspA *	Deletion mutant of *cdg135* over-expressing BspA	11	8
Bt407Δ135 + pHT304-pXyl-empty vector	Deletion mutant of *cdg135* containing empty vector	6	4
Bt407ΔbspA	Wild type with deletion of *bspA*		1
Bt407ΔbspA + pHT304-pXyl-135*	Deletion mutant of *bspA* over-expressing Cdg135	16	13
Bt407ΔbspA + pHT304-pXyl-135mut*	Deletion mutant of *bspA* over-expressing mutated Cdg135	17	14
Bt407ΔbspA + pHT304-pXyl-empty vector	Deletion mutant of *bspA* containing empty vector	5	2

Recombinant strains that were not available at the start of the present study (labeled by asterisk in Table 14) were prepared by transformations. Plasmid constructs were isolated from *E. coli* as described in Chapter 4.5 after growing the bacteria in LB-medium containing 100 µg/ml ampicillin (Chapter 4.2.1).

Restriction analysis was performed after isolation of plasmids (Chapter 4.6) to confirm their identities. The plasmids were subject to double digests using *Xba*I and *Eco*RI. Expected fragment sizes after restriction digests are shown in Table 15 and results are shown in Figures 13 and 14.

Table 15: Expected sizes of fragments in restriction analysis using *Eco*RI and *Xba*I in a double digest reaction			
	pHT304-pXyl-135	**pHT304-pXyl-135mut**	**pHT304-pXyl-bspA**
*Xba*I+*Eco*RI	1785, 7936 bp	1785, 7936 bp	470, 6286, 7936 bp

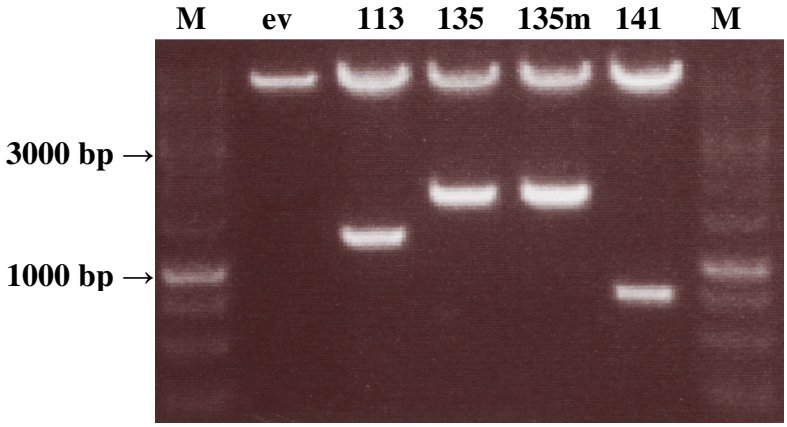

Figure 13: Restriction analysis of isolated plasmids. All plasmids were digested with *Xba*I and *Eco*RI and run on a 1% agarose gel. Lanes M: GeneRuler 1 Kb DNA Ladder, lane ev: pHT304-pXyl-empty vector, lane 113: pHT304-pXyl-113, lane 135: pHT304-135, lane 135m: pHT304-pXyl-135mut, lane 141: pHT304-pXyl-141

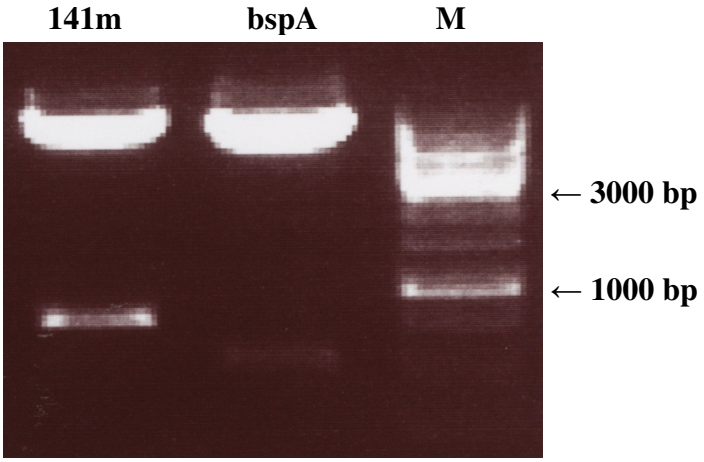

Figure 14: Restriction analysis of isolated plasmids. All plasmids were digested with *Xba*I and *Eco*RI and run on a 1% agarose gel. Lane M: GeneRuler 1 Kb DNA Ladder, lane bspA: pHT304-pXyl-bspA, lane 141m: pHT304-pXyl-141mut

As restriction digests of all constructs gave bands of the expected sizes, they were successfully confirmed to be correct. Plasmid constructs were transformed into the correct Bt407 strain and grown on LB containing 10 µg/ml erythromycin to select for tranformants (Chapter 4.9). As none of the transformations were successful after three attempts, isolation of plasmids and transformations were finally performed by Annette Fagerlund. The reason the experiment did not work previously was probably that transformations had to be performed in a cold room (4 °C) as described in Chapter 4.9.

PCR (Chapter 4.3) and agarose gel electrophoresis (Chapter 4.7) was used to identity strains already prepared and strains prepared through transformations in this study. The primers used for identifying deletion mutants were located up- and downstream of the deleted gene respectively. When confirming insertion of plasmid in over-expression strains, one primer was located in the vector while the other was located within the inserted gene. Primer pairs used in the PCR reactions for confirming insertion of plasmids and deletion of genes along with expected product sizes are shown in Table 16 and Table 4, respectively.

Table 16: Primers used in PCR analysis for confirming insertion of plasmids along with expected product sizes

Plasmid	Forward primer	Reverse primer	Expected product size
pHT304-pXyl-135	pHT304pXyl-F2	00135-R	1288 bp
pHT304-pXyl-135mut	pHT304pXyl-F2	00135-R	1288 bp
pHT304-pXyl-bspA	pHT304pXyl-F2	P-BC1060-R	299 bp
pHT304-pXyl-141	pHT304pXyl-F2	141-R-KpnI	993 bp
pHT304-pXyl-141mut	pHT304pXyl-F2	141-R-KpnI	993 bp
pHT304-pXyl-113	pHT304pXyl-F2	00113-R	1390 bp
pHT304-pXyl-empty vector	pHT304pXyl-F2	S2_pUC19R	343 bp

The results for confirming insertion of the plasmids are shown in Figure 15. Insertion of plasmids in all strains in Table 14 was thus confirmed except in strains Bt407Δ135 + pHT304-pXyl-bspA, Bt407ΔbspA + pHT304-pXyl-135 and Bt407ΔbspA + pHT304-pXyl-135mut. The PCR-products of these strains were therefore analyzed with another agarose gel electrophoresis. The results are shown in Figure 16. The strain Bt407ΔbspA + pHT304-pXyl-135 was identified by the second agarose gel electrophoresis, but Bt407Δ135 + pHT304-pXyl-bspA and Bt407ΔbspA + 135mut remained to be identified (did not give a PCR-product, possibly due to low purity DNA). These strains will studied further by the Økstad group.

The results for identification of the deletion mutants are shown in Figure 8. All deletion mutants described in Table 14 were identified except for the *bspA* mutant strains, but which was confirmed by the same PCR test by Ewa Jaroszewicz after completion of the practical lab work for this thesis (personal communication).

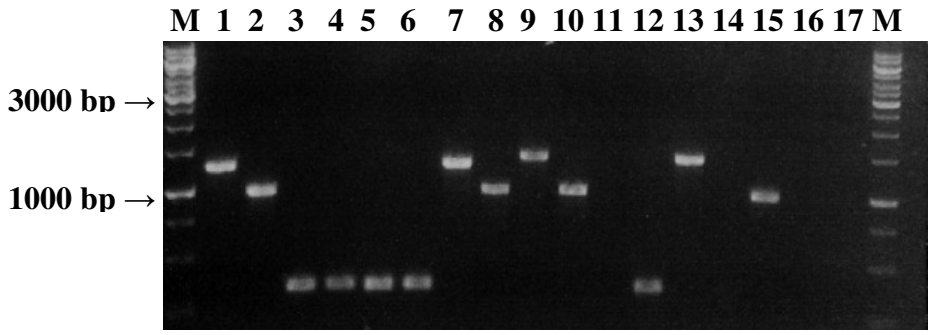

Figure 15: Results from PCR for confirming insertion of plasmids. Lanes M: GeneRuler 1 Kb DNA Ladder; for info on products in lane 1-17, see Tables 14, 20 and 22.

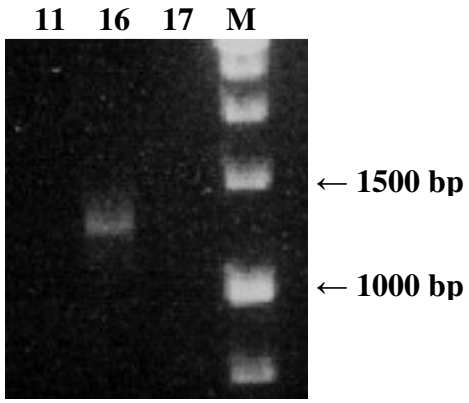

Figure 16: Results from PCR for identifying insertion of plasmids. Lane M: GeneRuler 1 Kb DNA Ladder, lane 11: Bt407 Δ135 + pHT304-pXyl-bspA, lane 16: Bt407 ΔbspA + 135, lane 17: Bt407 ΔbspA + 135mut

5.2.2 Growth curves with observations for motility

Growth curves were performed for all strains listed in Table 14 in three biological replicates. The strains were grown in bactopeptone medium at 30 °C and with rotation at 225 rpm. OD_{600} was measured at least once every hour. Motility was observed in the microscope by visual inspection. Erythromycin (10 µg/ml) and xylose (1 mM) was added to the medium when growing pHT304-pXyl constructs. A representative set of growth curves is shown in Figure 17. Most strains were non-affected in growth, except for Bt407Δ135 + pHT304-pXyl-bspA and Bt407ΔbspA + pHT304-pXyl-135mut that both showed an increased lag period. The presence of plasmids in these two strains was not successfully identified by PCR (Figure 16) and, this growth defect could indicate lack of plasmids.

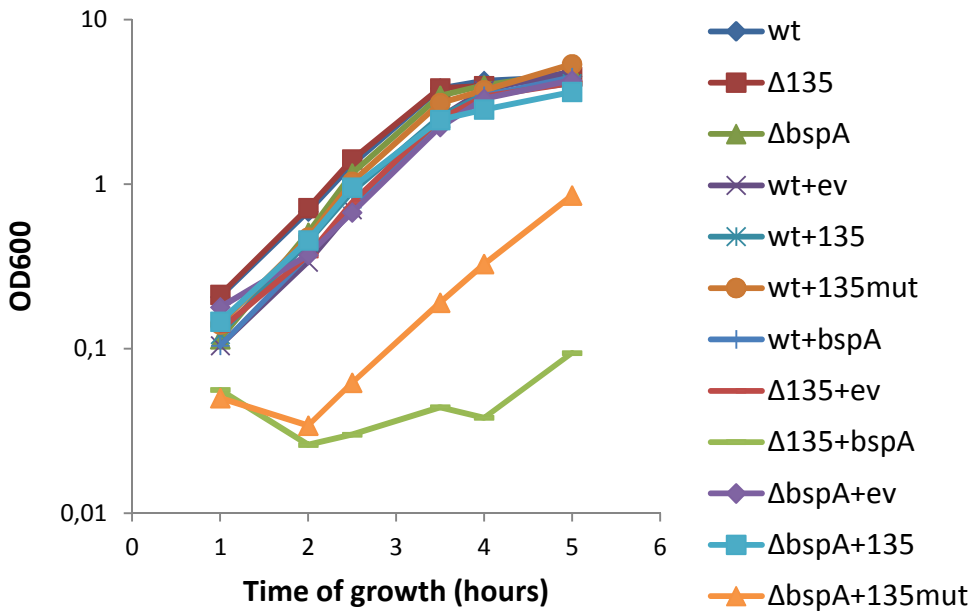

Figure 17: Growth curves comparing growth of all strains described in Table 14; wt: Bt407 wild type, Δ135: Bt407Δ135, ΔbspA: Bt407ΔbspA, wt+ev: Bt407 + pHT304-pXyl-empty vector, wt+135: Bt407 + pHT304-pXyl-135, wt+135mut: Bt407 + pHT304-pXyl-135mut, wt+bspA: Bt407 + pHT304-pXyl-bspA, Δ135+ev: Bt407Δ135 + pHT304-pXyl-empty vector, Δ135+bspA: Bt407Δ135 + pHT304-pXyl-bspA, ΔbspA+ev: Bt407ΔbspA + pHT304-pXyl-empty vector, ΔbspA+135: Bt407ΔbspA + pHT304-pXyl-135, ΔbspA+135mut: Bt407ΔbspA + pHT304-pXyl-135mut. Cells were grown in bactopeptone medium, containing 1 mM xylose and 10 µg/ml erythromycin for the strains containing pHT304-pXyl plasmids at 30 °C with rotation at 225 rpm. Data shown are representative of three independent experiments.

All strains with deletion of *cdg135* showed increased motility compared to wild type after approximately 1.5 hours of growth.

5.2.3 Biofilm formation

A biofilm screening assay including all strains in Table 14 was performed. Biofilm formation was analyzed after 24, 48 and 72 hours in a microtiter plate assay as described in Chapter 4.10. Erythromycin (10 µg/ml) and xylose (1 mM) was added to the medium when growing pHT304-pXyl constructs. Results are shown in Figures 18-21 and are based on averages of three biological replicates (each with eight technical replicates).

Deletion mutants of *cdg135* and *bspA* were both deficient in biofilm formation compared to wild type after 24, 48 and 72 hours of growth (Figure 18). This effect was, however, more evident in the *cdg135* mutant compared to in the *bspA* mutant. Over-expression of Cdg135 seemed to significantly stimulate the formation of biofilms whereas the strain over-expressing

mutated Cdg135 produced less biofilm than wild type (Figure 19). Over-expression of BspA produced biofilm at the same level as wild type carrying empty vector (Figure 19). The *cdg135* deletion mutant produced very little biofilm at 24, 48 and 72 hours and over-expression of BspA did not to seem compensate for this (Figure 20). This is however one of the two recombinant strains where PCR screening (Figure 16) and growth curve experiments (Figure 17) could indicate that the strain did not contain the correct plasmid, and requires further investigation. While the *bspA* deletion mutant was deficient in biofilm formation, the *bspA* mutant over-expressing Cdg135 was an efficient biofilm producer and Cdg135 can thus compensate for the loss of BspA expression (Figure 21). The *bspA* deletion mutant over-expressing mutated Cdg135 seemed to be deficient in biofilm formation, however, this is the second strain where PCR-screening (Figure 16) and growth curve experiments (Figure 17) could indicate that the strain did not contain the correct plasmid, and requires further investigation.

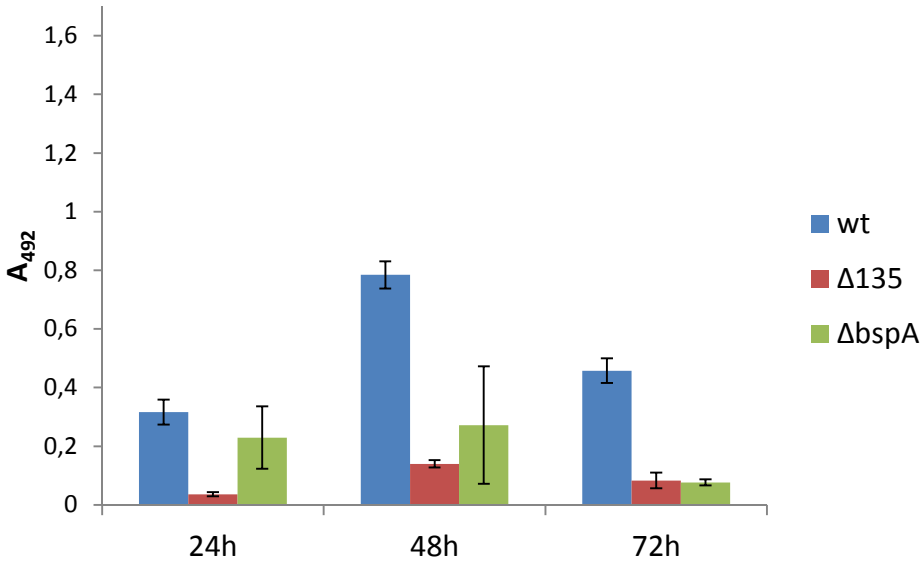

Figure 18: Biofilm formation assayed using a microtiterplate crystal violet staining assay. Cells were grown in bactopeptone medium and at 30 °C. Comparison of wild type (wt), the *cdg135* deletion mutant (Δ135) and the *bspA* deletion mutant ΔbspA. The results shown are averages and standard errors of three biological replicates, each based on eight technical replicates.

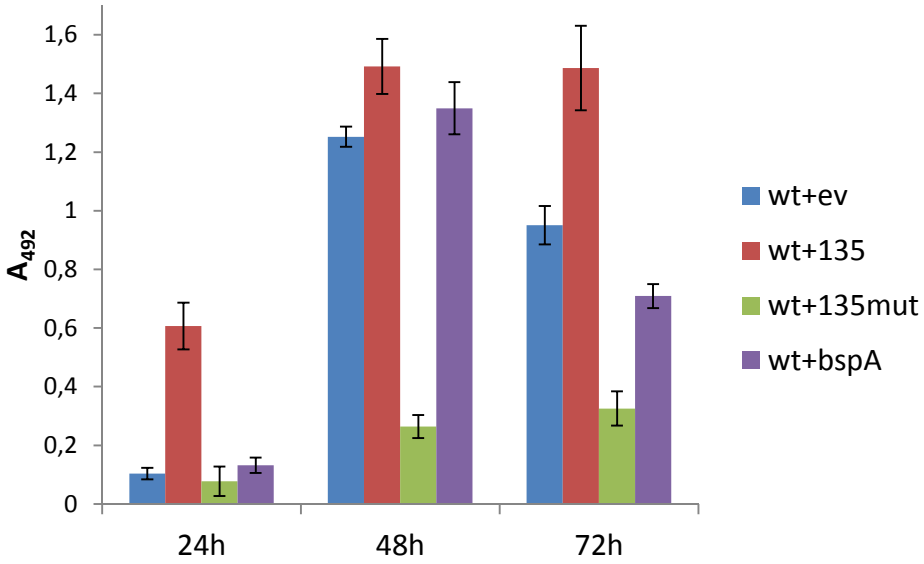

Figure 19: Biofilm formation assayed using a microtiterplate crystal violet staining assay. Cells were grown in bactopeptone medium and at 30 °C containing 1 mM xylose and 10 µg/ml erythromycin. Comparison of wild type carrying empty vector (wt+ev) and wild type over-expressing Cdg135 (wt+135), mutated Cdg135 (wt+135mut) and BspA (wt+bspA) respectively. The results shown are averages and standard errors of three biological replicates, each based on eight technical replicates.

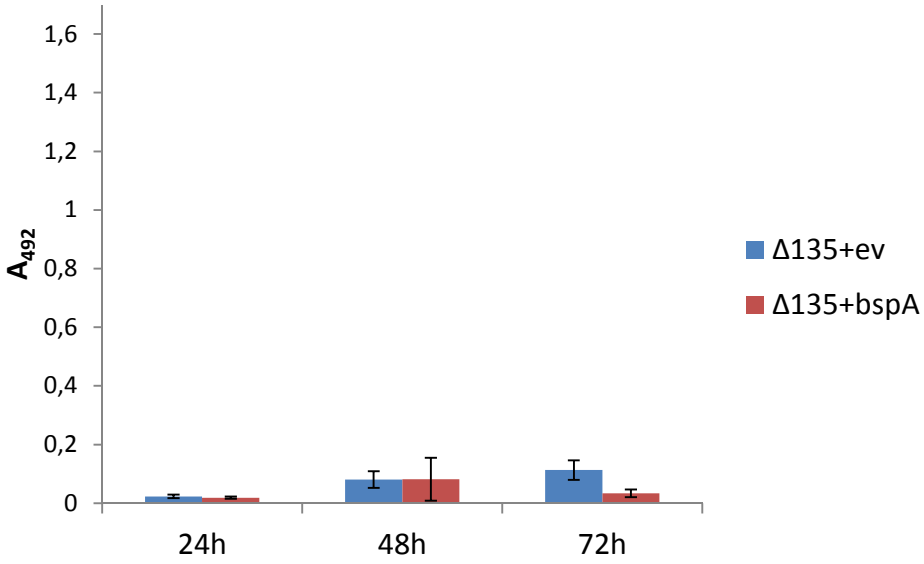

Figure 20: Biofilm formation assayed using a microtiterplate crystal violet staining assay. Cells were grown in bactopeptone medium and at 30 °C containing 1 mM xylose and 10 µg/ml erythromycin. Comparison of the *cdg135* deletion mutant carrying empty vector (Δ135+ev) and over-expressing BspA (Δ135+bspA) respectively. The results shown are averages and standard errors of three biological replicates, each based on eight technical replicates.

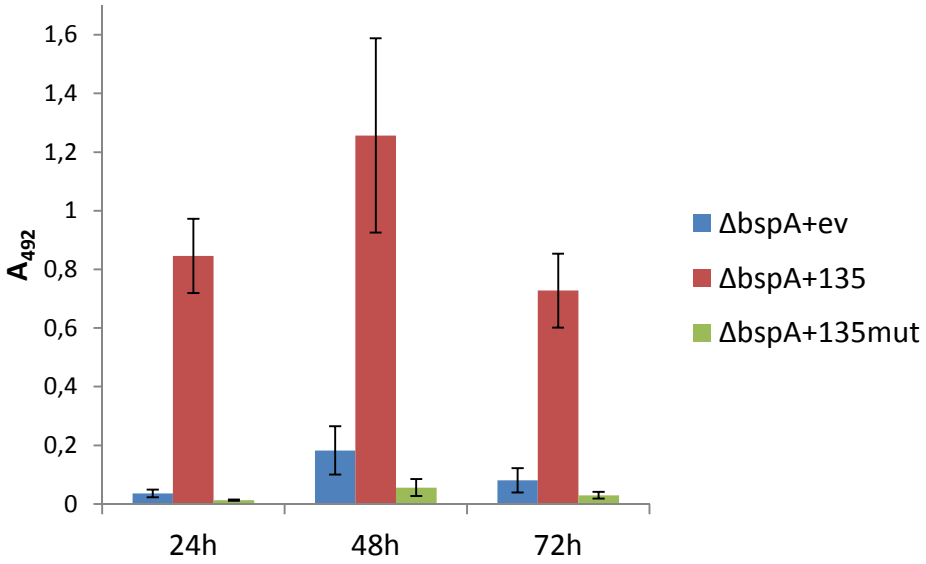

Figure 21: Biofilm formation assayed using a microtiterplate crystal violet staining assay. Cells were grown in bactopeptone medium and at 30 °C containing 1 mM xylose and 10 µg/ml erythromycin. Comparison of the *bspA* deletion mutant carrying empty vector (ΔbspA+ev) and over-expressing Cdg135 (ΔbspA+135) and mutated Cdg135 (ΔbspA+135mut) respectively. The results shown are averages and standard errors of three biological replicates, each based on eight technical replicates.

5.3 Characterization of the *cdg141* deletion mutant (Bt407Δ141)

Cdg141 contains a GGDEF domain which lacks the active site motif and is therefore predicted to be enzymatically inactive. It contains, however, a RxxD motif which may potentially function as an I-site involved in allosteric binding to c-di-GMP. Preliminary results indicated that Cdg141 affected biofilm formation after 24 hours of growth (Fagerlund & Økstad, unpublished results), and it was decided to characterize the *cdg141* gene further. The deletion mutant was first analyzed with respect to growth, motility and whole-genome transcription activity.

5.3.1 Identification

PCR was used to confirm the identity of the *cdg141* deletion mutant (Bt407Δ141), previously constructed by A. Fagerlund, prior to performing further experiments for the current thesis. PCR (Chapter 4.3) was performed with primers located up and downstream of *cdg141* respectively. The PCR-product was analyzed with agarose gel electrophoresis (Chapter 4.7) and the results are shown in Figure 8 (lane 5). Primers used in the PCR analysis and expected

product size are shown in Table 4. As the PCR-product matched the expected size, deletion of *cdg141* was successfully identified.

5.3.2 Growth curves with observations for motility

Growth curves comparing Bt407Δ141 and Bt407 wild type were performed three separate times with observations for motility (Chapter 4.1.1). Chosen culturing medium was bactopeptone (Chapter 3.8) and the cultures were incubated at 30 °C and were subject to rotation at 225 rpm. OD_{600} was measured every half hour and motility was studied by observing the bacteria in a microscope. A representative growth curve is shown in Figure 22. All three growth curve experiments gave similar results except that the duration of the lag-period varied slighty between experiments. The results showed that deletion of *cdg141* did not influence growth under the tested conditions.

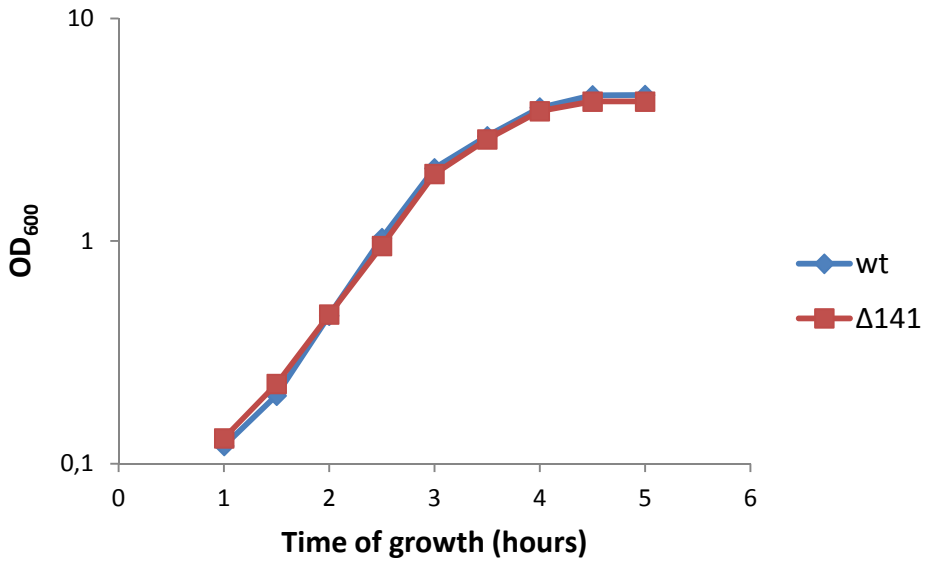

Figure 22: Growth curves comparing growth of wild type (wt) and *cdg141* deletion mutant (Δ141). Cells were grown in bactopeptone medium at 30 °C with rotation at 225 rpm. Data shown are representative of three independent experiments.

No significant difference in motility was observed.

It was desirable to perform a transcriptional analysis of the whole genome using microarrays comparing Bt407 wild type and Bt407Δ141. It was decided to harvest samples after 3.5 hours of growth for use in the microarray analysis, since an increase in expression of *cdg141* upon transition to stationary phase had previously been observed (Fagerlund & Økstad, unpublished results). Samples of 1.5 ml were harvested from four biological replicates of

Bt407 and Bt407Δ141 as described in Chapter 4.4. OD_{600} was measured upon harvesting and the OD_{600} values are shown in Table 17.

Table 17: OD_{600} values of cultures at time of harvest. Four biological replicates (1-4), each consisting of wild type and *cdg141* deletion mutant, were harvested

Set	OD_{600} Bt407 wild type	OD_{600} Bt407 Δ141
1	3.82	3.62
2	3.88	3.90
3	3.74	3.73
4	3.90	3.97

5.3.3 RNA isolation from Bt407 wild type and *cdg141* deletion mutant

RNA was isolated as described in Chapter 4.4 and the concentrations were measured through UV-spectrophotometry (Chapter 4.8). The averages of at least two measurements are shown in Table 18. A_{260}/A_{280} ratios of the samples marked with asterisk in Table 18 could indicate contamination with proteins. Purity and concentrations of RNA were still found to be adequate.

Table 18: Concentration measurements of RNA isolated from four biological replicates (1-4), each from wild type and the *cdg141* deletion mutant. The ratio of the absorbance at A_{260} and A_{280} was calculated to estimate purity.

Set	RNA concentration Wild type	RNA concentration Δ141	A_{260}/A_{280} Wild type	A_{260}/A_{280} Δ141	A_{260} Wild type	A_{260} Δ141
1	0.8915 µg/µl	0.8094 µg/µl	2.41*	2.38*	0.17	0.15
2	1.0515 µg/µl	0.8234 µg/µl	1.88	2.44*	0.24	0.16
3	0.9945 µg/µl	1.2919 µg/µl	1.88	1.88	0.23	0.30
4	1.1952 µg/µl	1.1248 µg/µl	1.85	1.85	0.28	0.26

The integrity of the RNA molecules was studied through agarose gel electrophoresis (Chapter 4.7). The results are shown in Figure 23. The bands separated by the gel were sharp, indicating RNA of good integrity. However, the upper band (23S rRNA) should be more intense than the lower band (16S rRNA) and this was not obvious in these samples. The quality of RNA was still found to be adequate and the obtained RNA was used in the microarray experiment.

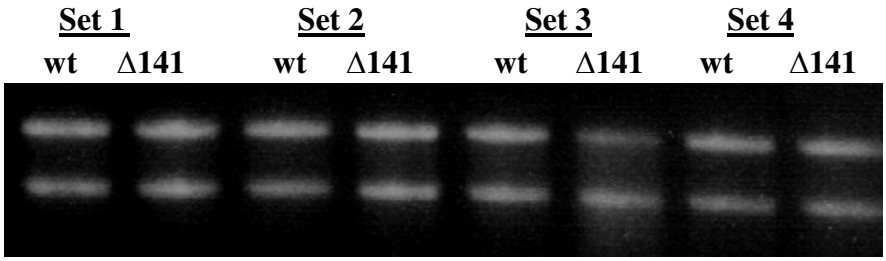

Figure 23: Results from agarose gel electrophoresis used for inspecting the integrity of RNA. Set 1 to 4: RNA isolated from biological replicates 1 to 4. wt: RNA isolated from Bt407 wild type, Δ141: RNA isolated from Bt407Δ141

5.3.4 Transcriptional analysis using microarrays

20 µg of RNA was used as starting material for the microarray procedure and the experiment was performed as described in Chapter 4.11. The four biological replicates were dye-swapped meaning that wild type cDNA was dyed with Cy3 and *cdg141* deletion mutant cDNA with Cy5 in RNA sets 1 and 3 and that wild type was dyed with Cy5 and *cdg141* deletion mutant with Cy3 in RNA sets 2 and 4. Set 1 of wild type and mutant was used for hybridizing slide 1, set 2 for slide 2, set 3 for slide 3 and set 4 for slide 4.

The intensities of the scanning beams from each wavelength (635 nm/532 nm) used when scanning the slides had to be adjusted so that the count ratio for each slide was as close to 1 as possible. This ratio describes the ratio of the sum of detected green and the sum of detected red signal intensities. The intensities chosen for the red (635 nm) and green (532 nm) channel and count ratios obtained for each slide are shown in Table 19 (slide 1 and 2 were affected by "red flames" (high uneven red background) on parts of the lower halves and count ratios of the upper halves of these slides were therefore noted).

Table 19: Count ratios for slides 1-4 along with intensities chosen for red (635) and green (532) channel. The count ratios of the upper halves of slide 1 and 2 are also shown as these slides had red flames on the lower halves.

Slide	PTM Gain 635	PTM Gain 532	Count ratio whole slide	Count ratio upper half
1	750	610	1.55	0.97
2	730	620	1.52	1.03
3	630	710	0.95	
4	750	630	1.04	

Slides 1, 2 and 4 were included in the analysis. Slide 3 was weak and the background signal intensities were too high compared to the spot signal intensities when scanned. The analysis was performed as described in Chapter 4.11.9 using the statistical computing platform "R" (http://www.r-project.org/) and the package LIMMA (Linear models for microarray data)

[90]. Histograms showing the distribution of intensity for red and green spot signals as well as red and green background signals are shown in Appendix 2 (Figures 39-42). Minimum spot intensities for inclusion in the further analysis were decided based on the aforementioned histograms to ensure removal of background signals. Cut-off values of 300 and 250 for red and green signal intensities, respectively, were chosen.

No genes were found to be significantly up- or down-regulated, possibly indicating that deletion of Cdg141 had little effect on transcription of genes in Bt407 at this point of growth and with the tested conditions.

5.4 Characterization of Cdg141

To characterize Cdg141 further, it was of interest to study the effects of over-expressing Cdg141 and deleting *cdg141* in the wild type, on growth, motility and biofilm formation. As controls, wild type and wild type containing pHT304-pXyl-empty vector were included, as well as the complemented *cdg141* deletion strain, and *cdg141* deletion mutant containing pHT304-pXyl-empty vector. Additionally, control strains over-expressing a mutated variant of Cdg141 (Cdg141mut), were to be tested. In the Cdg141mut variant, two substitutions had been introduced in the RxxD motif (I-site), giving AxxA. Thus, the strains shown in Table 20 were to be tested for growth effects, motility and ability to form biofilms.

Table 20: List of all strains to be tested for growth, motility and biofilm formation. Strains marked with asterisk were constructed in this thesis work. Lanes used for identification of inserted plasmids and deletion mutants in PCR analysis are also shown

Strain	Description	Lane in PCR confirming	
		Presence of plasmids (Figure 15)	Deletion of gene (Figure 8)
Bt407	Wild type		
Bt407 + pHT304-pXyl-141	Wild type over-expressing Cdg141	2	
Bt407 + pHT304-pXyl-141mut	Wild type over-expressing mutated Cdg141. Two amino acids in the RxxD motif are exchanged, giving AxxA	8	
Bt407 + pHT304-pXyl-empty vector	Wild type containing empty vector. Control for over-expression strains	3	
Bt407Δ141	Wild type with deletion of *cdg141*		5
Bt407Δ141 + pHT304-pXyl-141*	Complemented deletion mutant of *cdg141*	15	12
Bt407Δ141 + pHT304-pXyl-141mut*	Deletion mutant of *cdg141* over-expressing mutated Cdg141	10	7

Table 20: continued			
Bt407Δ141 + pHT304-pXyl-empty vector*	Deletion mutant of *cdg141* containing empty vector	14	11

5.4.1 Preparation and/or confirmation of strains to be tested for growth, motility and biofilm formation

Recombinant strains that were not available at the start of the present study (labeled by asterisk in Table 20) were prepared by transformations. Plasmid constructs were isolated from *E. coli* as described in Chapter 4.5 after growing the bacteria in LB-medium containing 100 µg/ml ampicillin (Chapter 4.1.2).

Restriction analysis (Chapter 4.6) was performed after isolation of plasmids to confirm their identities. The plasmids were subject to double digests using *Xba*I and *Eco*RI. Expected fragment sizes after restriction digests are shown in Table 21 and results are shown in Figures 13 and 14. As restriction digests of all constructs gave bands of the expected sizes, they were successfully confirmed to be correct.

Table 21: Expected sizes of fragments in restriction analysis using *Eco*RI and *Xba*I in a double digest reaction			
	pHT304-pXyl-141	**pHT304-pXyl-141mut**	**pHT304-pXyl-empty vector**
*Xba*I+*Eco*RI	725, 7936 bp	725, 7936 bp	7936 bp, 27 bp

Plasmid constructs were transformed into the correct Bt407 strain and grown on LB agar containing 10 µg/ml erythromycin to select for tranformants (Chapter 4.9). As none of the transformations were successful after three attempts, isolation of plasmids and transformations were finally performed by Annette Fagerlund. The reason the experiment did not work initially, was that the transformations had to be performed in the cold room as described in Chapter 4.9.

PCR (Chapter 4.3) and agarose gel electrophoresis (Chapter 4.7) was used to identify strains already prepared and strains prepared through transformations. The primers used for confirming deletion of genes were located up and downstream of the deleted gene, respectively. When confirming insertion of plasmid in the over-expression strains, one primer was located in the vector while the other was located within the inserted gene. Primer pairs used for confirming insertion of plasmids and deletion of genes are shown in Table 16 and Table 4, respectively, along with expected product sizes.

The results from the PCR analysis for conformation of insertion of plasmids are shown in Figure 15. Insertion of plasmids in all strains described in Table 20 was confirmed, except from Bt407Δ141+ pHT304-pXyl-empty vector. The PCR-product was therefore tested by another agarose gel electrophoresis. The results are shown in Figure 24. The PCR product matched the expected size (weak band) and insertion of plasmid Bt407Δ141+ pHT304-pXyl-empty vector was thus confirmed.

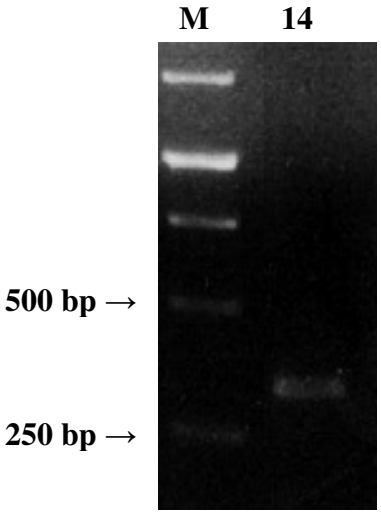

Figure 24: Results from PCR for identifying insertion of plasmids. Lane M: GeneRuler 1 Kb DNA Ladder, lane 14: Bt407Δ141 + pHT304-pXyl-empty vector

The results for identification of the deletion mutants are shown in Figure 8. All deletion mutants described in Table 20 were successfully confirmed.

5.4.2 Growth curves with observations for motility

Growth curves were performed for all strains showed in Table 20 in three biological replicates with observations for motility (Chapter 4.1.1). The strains were grown in bactopeptone medium at 30 °C and with rotation at 225 rpm. OD_{600} was measured at least once every hour. Motility was observed in a microscope by visual inspection. Erythromycin (10 µg/ml) and xylose (1 mM) was added to the medium when growing strains containing pHT304-pXyl constructs. A representative set of growth curves are shown in Figure 25. Most strains were non-affected in growth, except for Bt407 + pHT304-pXyl-141 and Bt407Δ141 + pHT304-pXyl-141, which both showed an increased lag period (Figures 26 and 27). Thus, both tested strains carrying this Cdg141 over-expression construct showed a growth defect, while the two strains over-expressing the mutated Cdg141, in which the I-site RxxD motif had been substituted for an AxxA sequence, displayed normal growth.

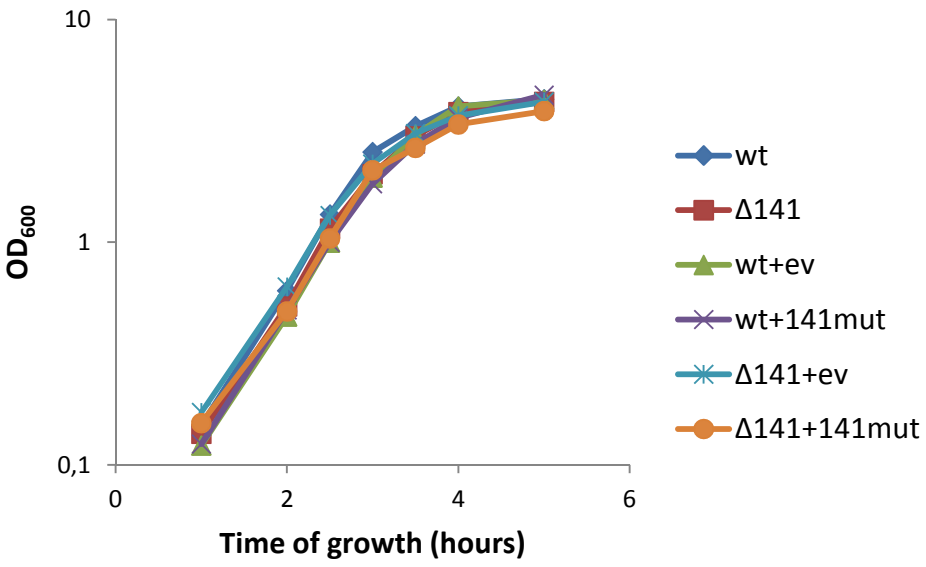

Figure 25: Growth curves comparing growth of all strains described in Table 20 except for Bt407 + pHT304-pXyl-141 and Bt407Δ141 + pHT304-pXyl-141: wt: Bt407 wild type, Δ141: Bt407Δ141, wt+ev: Bt407 + pHT304-pXyl-empty vector, wt+141mut: Bt407 + pHT304-pXyl-141mut, Δ141+ev: Bt407Δ141 + pHT304-pXyl-empty vector, Δ141+141mut: Bt407Δ141 + pHT304-pXyl-141mut. Cells were grown in bactopeptone medium, containing 1 mM xylose and 10 µg/ml erythromycin for the strains containing pHT304-pXyl-plasmids, at 30 °C with rotation at 225 rpm. Data shown are representative of three independent experiments.

No significant differences in motility were observed.

To investigate the influence of xylose concentration, inducing expression of *cdg141* from the plasmid-borne *xylA* promoter, on growth of Bt407 over-expressing Cdg141, growth curves with xylose titrations were performed for this strain. The following concentrations covering a broad spectrum were chosen for the first experiment: 0 mM, 0.001 mM, 0.01 mM, 0.1 mM and 1 mM. This experiment was performed in cooperation with Veronika Smith in the research group and results are shown in Figure 26.

The curves in Figure 26 seemed to separate in two clusters, which could have indicated that a threshold concentration of xylose somewhere between 0.1 mM and 1 mM was necessary for expression of Cdg141 from the *xylA* promoter on the pHT304-pXyl plasmid and for the extended lag phase phenotype to occur. To explore this hypothesis, the experiment was repeated using the following concentrations: 0.1 mM, 0.25 mM, 0.5 mM, 0.75 mM and 1 mM. This experiment was also performed in cooperation with Veronika Smith. The results are shown in Figure 27.

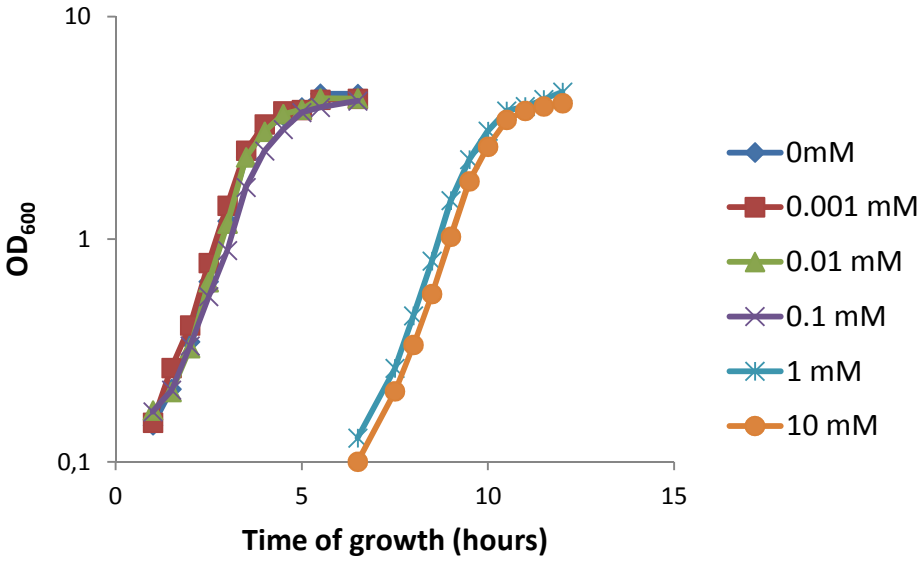

Figure 26: Growth curves comparing growth of wild type over-expressing Cdg141 with different concentrations of xylose. Cells were grown in bactopeptone medium containing 10 µg/ml erythromycin at 30 °C with rotation at 225 rpm.

The lag-phases of the growth curves in Figure 27 seemed to be depending on concentration of xylose in the medium. These results did not support the hypothesis of a threshold concentration necessary for expression of Cdg141 from the xylose-inducible *xylA* promoter on the pHT304-pXyl plasmid.

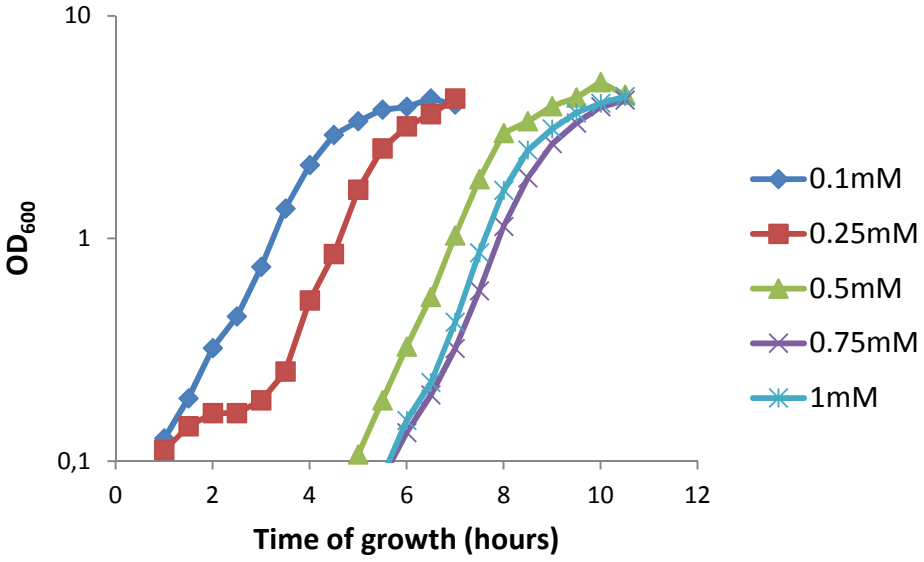

Figure 27: Growth curves comparing growth of wild type over-expressing Cdg141 with different concentrations of xylose. Cells were grown in bactopeptone-medium containing 10 µg/ml erythromycin at 30 °C with rotation at 225 rpm.

5.4.3 Biofilm assays

Biofilm screening assay including all strains in Table 20 was performed. Biofilm formation was analyzed after 24, 48 and 72 hours of growth in a microtiter plate assay as described in Chapter 4.10. Erythromycin (10 µg/ml) and xylose (1 mM) was added to the medium when growing pHT304-pXyl constructs. Results are shown in Figures 28-30 and are based on averages of three biological replicates (each with eight technical replicates).

Deletion of *cdg141* did not seem to affect biofilm formation in Bt407 (Figure 28). Wild type over-expressing Cdg141 produced almost no biofilm, not even after 72 hours (Figure 29). This was most probably due to lack of growth, since this strain was shown to have a growth defect in the presence of the concentration of xylose used in this experiment (Figure 26). Wild type over-expressing mutated Cdg141, however, appeared to produce more biofilm than the wild type containing empty vector (Figure 29). As expected, the complemented deletion mutant of *cdg141* formed almost no biofilm (Figure 30), most probably due to affected growth, as over-expression of Cdg141 was shown to induce a prolonged lag phase (Figure 26). The deletion mutant over-expressing mutated Cdg141 and empty vector, respectively, seemed to be equally efficient biofilm formers (Figure 30).

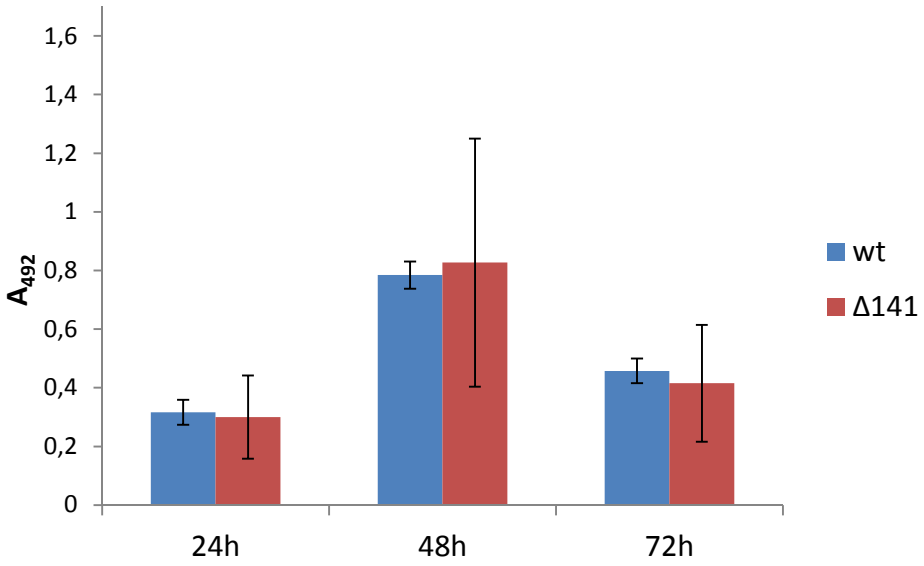

Figure 28: Biofilm formation assayed using a microtiterplate crystal violet staining assay. Cells were grown in bactopeptone medium and at 30 °C. Comparison of wild type (wt) and *cdg141* deletion mutant (Δ141). The results shown are averages and standard errors of three biological replicates, each based on eight technical replicates.

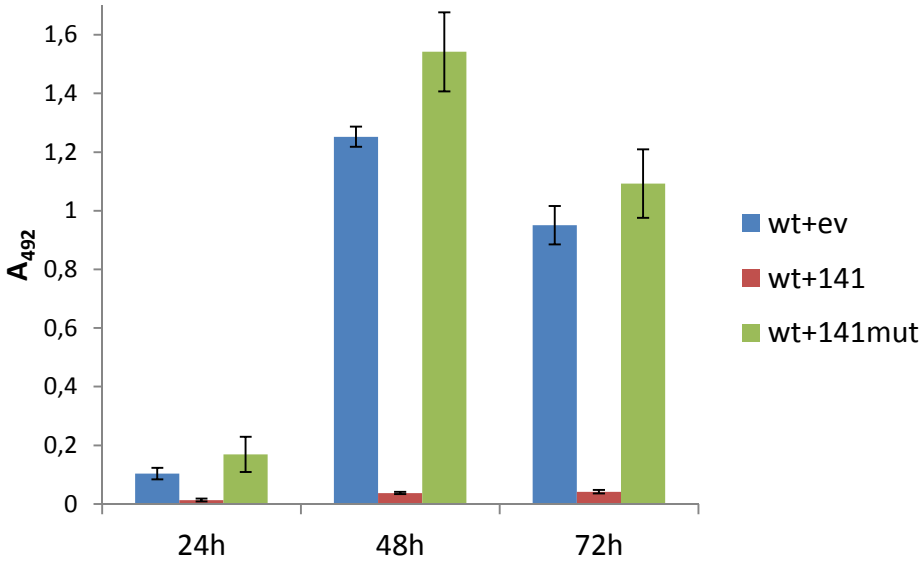

Figure 29: Biofilm formation assayed using a microtiterplate crystal violet staining assay. Cells were grown in bactopeptone medium and at 30 °C containing 1 mM xylose and 10 µg/ml erythromycin. Comparison of wild type carrying empty vector (wt+ev) and over-expressing Cdg141 (wt+141) and mutated Cdg141 (wt+141mut) respectively. The results shown are averages and standard errors of three biological replicates, each based on eight technical replicates.

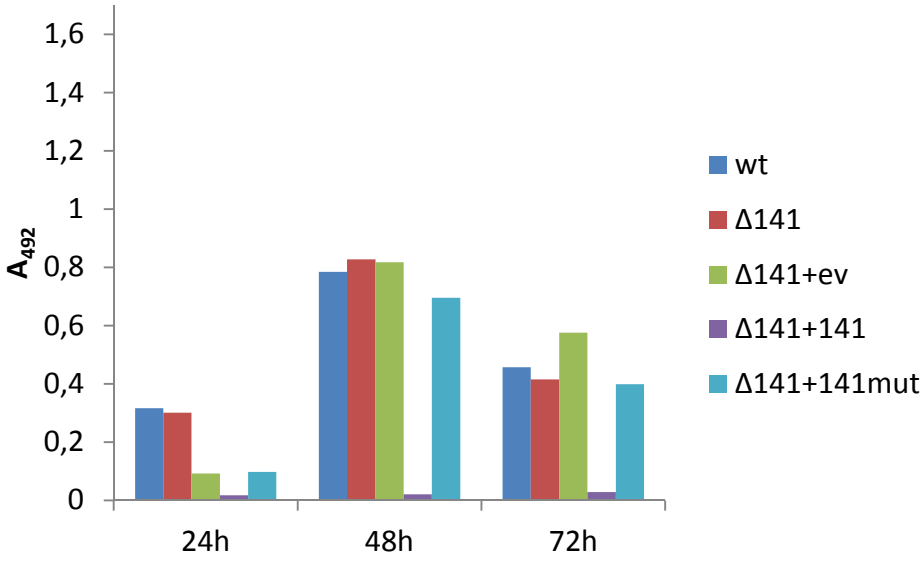

Figure 30: Biofilm formation assayed using a microtiterplate crystal violet staining assay. Cells were grown in bactopeptone medium and at 30 °C containing 1 mM xylose and 10 µg/ml erythromycin. Comparison of the *cdg141* deletion mutant carrying empty vector (Δ141+ev) and over-expressing Cdg141 (Δ141+141) and mutated Cdg141 (Δ141+141mut) respectively. Wild type (wt) and *cdg141* deletion mutant (Δ141) without carrying plasmids are also shown. The results shown are averages and standard errors of three biological replicates, each based on eight technical replicates.

5.5 Characterization of Cdg113

Cdg113 contains an EAL domain lacking the motif necessary for enzymatic activity and is therefore probably not involved in the degradation of c-di-GMP. Preliminary results indicated that Cdg113 affected biofilm formation after 24 hours of growth, suggesting a possible role as an effector molecule upon binding c-di-GMP. Cdg113 was therefore studied further by means of effects on growth, motility and biofilm formation.

To characterize Cdg113 further, it was of interest to study the effects of over-expressing Cdg113 and deleting *cdg113* in the wild type, on growth, motility and biofilm formation. As controls, wild type and wild type containing pHT304-pXyl-empty vector were included, as well as the complemented *cdg113* deletion strain, and *cdg113* deletion mutant containing pHT304-pXyl-empty vector. Thus, the strains shown in Table 22 were to be tested for growth effects, motility and ability to form biofilms.

Table 22: List of all strains to be tested for growth, motility and biofilm formation. Strains marked with asterisk were constructed in the present study. Lanes used for identification of inserted plasmids and deletion mutants in PCR analysis are also shown.

Strain	Description	Lane in PCR confirming	
		Presence of plasmids (Figure 15)	Deletion of gene (Figure 8)
Bt407	Wild type		
Bt407 + pHT304-pXyl-113	Wild type over-expressing Cdg113	9	
Bt407 + pHT304-pXyl-empty vector	Wild type containing empty vector. Control for over-expression strains	3	
Bt407Δ113	Wild type with deletion of *cdg113*		6
Bt407Δ113 + pHT304-pXyl-113*	Complemented deletion mutant of *cdg113*	13	10
Bt407Δ113 + pHT304-pXyl-empty vector*	Deletion mutant of *cdg113* containing empty vector	12	9

5.5.1 Preparation and/or confirmation of strains to be tested for growth, motility and biofilm formation

Recombinant strains that were not available at the start of the present study (labeled by asterisk in Table 22) were prepared through transformations. Plasmid constructs were isolated from *E. coli* as described in Chapter 4.5 after growing the bacteria in LB-medium containing 100 µg/ml ampicillin (Chapter 4.1.2).

Restriction analysis as described in Chapter 4.6 was performed after isolation of plasmids to confirm their identities. The plasmids were subject to double digests using *Xba*I and *Eco*RI. Expected fragment sizes after restriction digests are shown in Table 23 and results are shown in Figure 13. As restriction digests of all constructs gave bands of the expected sizes, they were successfully confirmed to be correct.

Table 23: Expected sizes of fragments in restriction analysis using *Eco*RI and *Xba*I in a double digest reaction

	pHT304-pXyl-113	pHT304-pXyl-empty vector
*Xba*I+*Eco*RI	1255, 7935 bp	7936 bp, 27 bp

Plasmid constructs were transformed into the correct Bt407 strain and grown on LB containing 10 µg/ml erythromycin to select for tranformants (Chapter 4.9). As none of the transformations were successful after three attempts, isolation of plasmids and transformations were finally performed by Annette Fagerlund. The reason the experiment did not work previously was, as again, probably that transformations had to be performed in the cold room as described in Chapter 4.9.

PCR (Chapter 4.3) and agarose gel electrophoresis (Chapter 4.7) was used to identity strains already prepared and strains prepared through transformations. The primers used for identifying deletion mutants were located up and downstream of the deleted gene respectively. When confirming insertion of plasmid in the over-expression strains, one primer was located in the vector while the other was located within the inserted gene. Primers used for confirming insertion of plasmids and deletion of genes are shown in Table 16 and Table 4, respectively, along with expected product sizes. The results for confirming insertion of plasmids are shown in Figure 15. The results for identification of the deletion mutants are shown in Figure 8. All PCR-products matched the expected sizes and the deletion mutants and plasmids of all strains described in Table 22 were thus confirmed.

5.5.2 Growth curves with observations for motility

Growth curves were performed for all strains showed in Table 22 in three biological replicates with observations for motility (Chapter 4.1.1). The strains were grown in bactopeptone medium at 30 °C and with rotation at 225 rpm. OD_{600} was measured at least once every hour. Motility was observed in the microscope by visual inspection. Erythromycin (10 µg/ml) and xylose (1 mM) was added to the medium when growing pHT304-pXyl constructs. A representative set of growth curves are shown in Figure 31. All strains were non-affected in growth.

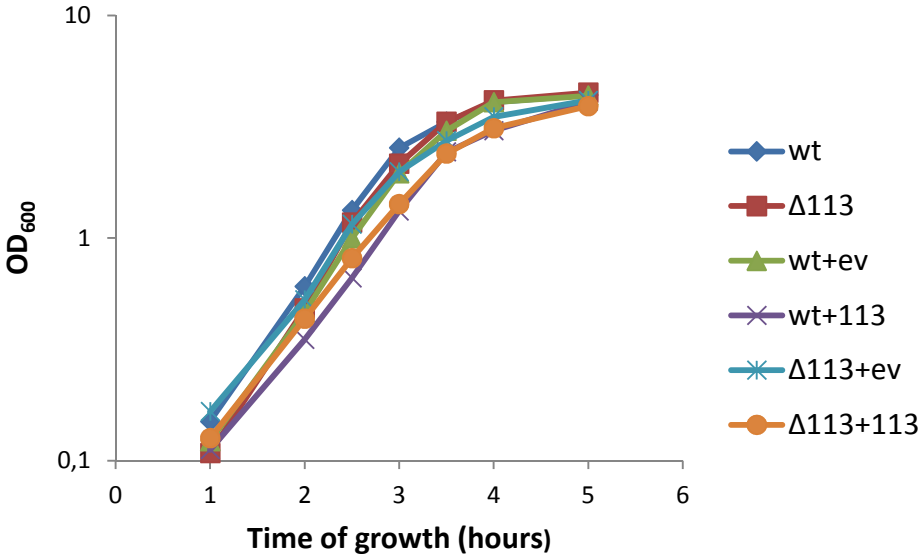

Figure 31: Growth curves comparing growth of all strains described in Table 22. wt: Bt407 wild type, Δ113: Bt407Δ113, wt+ev: Bt407 + pHT304-pXyl-empty vector, wt+113: Bt407 + pHT304-pXyl-113, Δ113+ev: Bt407Δ113 + pHT304-pXyl-empty vector, Δ113+113: Bt407 + pHT304-pXyl-113. Cells were grown in bactopeptone medium, containing 1 mM xylose and 10 µg/ml erythromycin for strains containing pHT304-pXyl plasmids, at 30 °C with rotation at 225 rpm. Data shown are representative of three independent experiments.

No significant differences in motility were observed between strains.

5.5.3 Biofilm assays

Biofilm screening assay including all strains in Table 22 was performed. Biofilm formation was analyzed after 24, 48 and 72 hours of growth in a microtiter plate assay as described in Chapter 4.10. Erythromycin (10 µg/ml) and xylose (1 mM) was added to the medium when growing pHT304-pXyl constructs. Results are shown in Figures 32-34 and are based on averages of three biological replicates (each with eight technical replicates).

The deletion mutant of *cdg113* formed biofilm at the same level as wild type (Figure 32). The over-expression strain of Cdg113 was superior to wild type with respect to biofilm formation, especially after 72 hours (Figure 33). The complemented deletion mutant compensated for the deletion of *cdg113* (Figure 34).

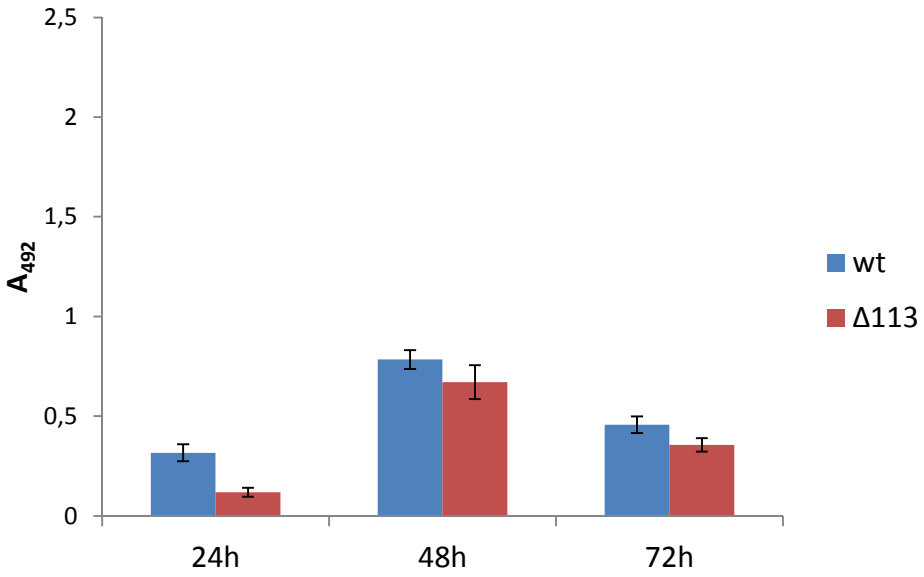

Figure 32: Biofilm formation assayed using a microtiterplate crystal violet staining assay. Cells were grown in bactopeptone medium at 30 °C. Comparison of wild type (wt) and *cdg113* deletion mutant (Δ113). The results shown are averages and standard errors of three biological replicates, each based on eight technical replicates.

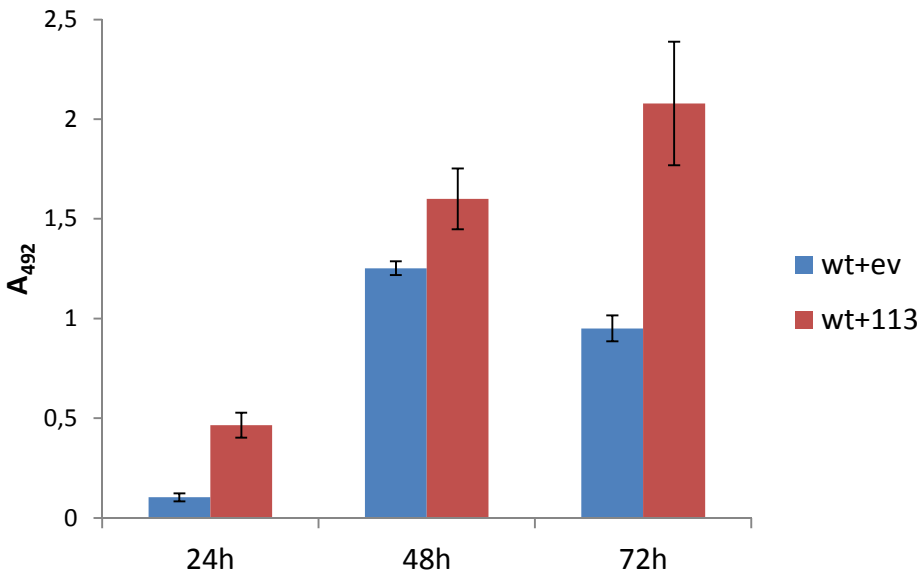

Figure 33: Biofilm formation assayed using a microtiterplate crystal violet staining assay. Cells were grown in bactopeptone medium at 30 °C containing 1 mM xylose and 10 µg/ml erythromycin. Comparison of wild type carrying empty vector (wt+ev) and over-expressing Cdg113 (wt+113), respectively. The results shown are averages and standard errors of three biological replicates, each based on eight technical replicates.

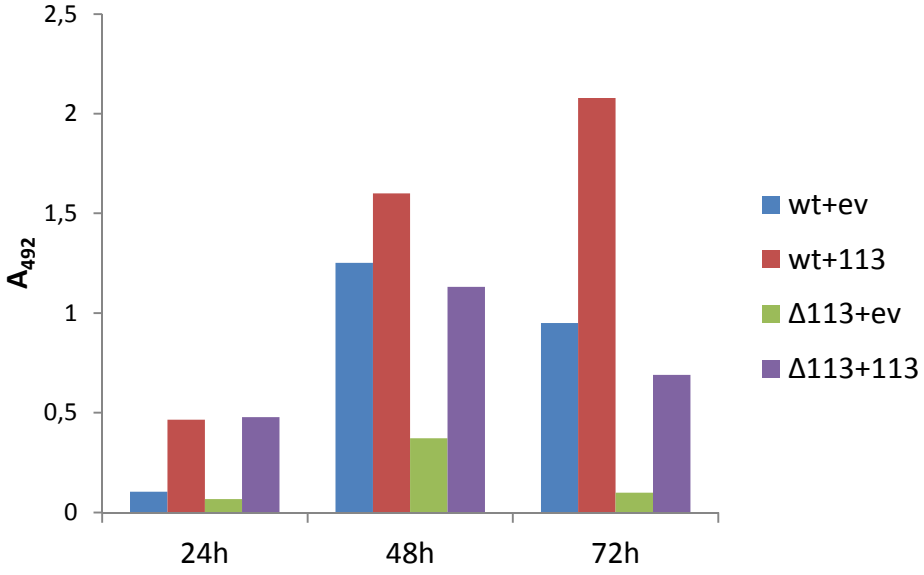

Figure 34: Biofilm formation assayed using a microtiterplate crystal violet staining assay. Cells were grown in bactopeptone medium at 30 °C containing 1 mM xylose and 10 µg/ml erythromycin.Comparison of deletion mutant of *cdg113* carrying empty vector (Δ113+ev) and deletion mutant over-expressing Cdg113 (Δ113+113). Wild type carrying empty vector (wt+ev) and wild type over-expressing Cdg113 (wt+113) are also shown. The results shown are averages and standard errors of three biological replicates, each based on eight technical replicates.

CHAPTER 6: DISCUSSION

6.1 Role of Cdg135 in biofilm formation in Bt407

6.1.1 Function in biofilm formation and motility

The second messenger c-di-GMP is known to inversely regulate the planktonic and biofilm associated lifestyles in Gram-negative bacteria like *V. cholera* [96] and *P. aeruginosa* [97]. Recently, there have, however, been indications that c-di-GMP also plays an important role in regulation of biofilm formation in certain Gram-positive bacteria [80]. C-di-GMP is known to influence several processes in the cell, including stimulation of biofilm formation and inhibition of motility. Diguanylate cyclase (DGC) enzymes containing GGDEF domains synthesize c-di-GMP, while phosphodiesterase (PDE) enzymes with EAL domains are responsible for its degradation. Cdg135 contains a GGDEF and an EAL domain, both with conserved active site residues. Biofilm assays performed in this thesis showed that the *cdg135* deletion mutant was an inefficient biofilm producer compared to wild type after 24, 48 and 72 hours of growth (Figure 18). Furthermore, the over-expression strain produced more biofilm than wild type carrying empty vector, and this difference was most evident at 24 hours (Figure 19). Curiously, the wild type with empty vector produced more biofilm than wild type without empty vector after 48 and 72 hours of incubation (Figure 18). This may be due to stress responses from carrying a plasmid and growing in the presence of antibiotics. Stress responses can stimulate formation of biofilm in certain bacteria [98].

The *cdg135* deletion mutant showed increased motility compared to wild type in early exponential phase growth in liquid culture medium, as observed by visual inspection in a microscope. The same was observed also for derivate strains of Bt407Δ135 (Bt407Δ135 + pHT304-pXyl-empty vector and Bt407Δ135 + pHT304-pXyl-bspA). In a motility assay performed as a follow-up study by Veronika Smith in the group, in which the swimming ability was determined by measuring the diameter of swim zones of bacteria growing on soft agar plates (0.3% agar), no difference in motility was observed between the wild type and the *cdg135* deletion mutant (Fagerlund & Økstad, unpublished results). It may, however, not be surprising that the motility assays on agar plates did not capture any difference in motility comparing these strains, as the difference observed in this thesis during growth in liquid culture was only evident in early exponential phase, and the soft agar plate motility assays show the overall movement of the bacteria only after a certain number of hours. The soft agar motility assays performed by Veronica Smith did, however, detect a significant reduction in swimming motility in the strain over-expressing Cdg135 (Fagerlund & Økstad, unpublished

results), indicating that the assay was sufficiently sensitive for observing an altered motility phenotype upon protein over-expression. This difference in motility was not detectable in experiments performed in the current thesis, where bacteria were grown in liquid medium and relative motility was inspected by light microscopy.

Given the effects of Cdg135 on biofilm formation and motility, including the fact that over-expression of Cdg135 with a mutated GGDEF domain did not give increased biofilm formation (Figure 19), it seems likely that the GGDEF domain within this gene encodes an active DGC leading to synthesis of c-di-GMP. In line with this, preliminary results by Veronika Smith, employing c-di-GMP measurements by LC-MS using a modified version of the method described by Spangler and co-workers [99], have indicated that the strain over-expressing Cdg135 synthesizes high levels of c-di-GMP (Veronika Smith, unpublished). These results suggest that Cdg135 is of importance in controlling biofilm formation and motility in Bt407. It is possible that Cdg135 has DGC activity given the observed effects of Cdg135 on biofilm formation and motility, and the predicted enzymatically active GGDEF domain. Results from the biofilm assays additionally showed that wild type strain over-expressing Cdg135 containing a mutated GGDEF motif produced less biofilm than wild type carrying empty vector (Figure 19), indicating that Cdg135 may also have PDE activity.

To conclude, both biofilm formation and motility are influenced by DGC/PDE enzymes and seem to be inversely regulated in Bt407, potentially as a response to c-di-GMP. This could indicate that c-di-GMP is an important mediator of biofilm formation in the *B. cereus* group. Levels of c-di-GMP must, however, be quantified in all deletion and over-expressing strains in order to test this hypothesis, and this work is already started.

6.1.2 Identification of genes differentially expressed in a *cdg135* deletion mutant

A microarray experiment comparing Bt407 wild type and the isogenic *cdg135* knockout mutant was carried out with harvested samples from early exponential phase, where a difference in motility was observed. Five genes were found to be significantly up- or down-regulated with FDR-corrected P-values<0.05 (Tables 8 and 9). The expression of the gene encoding a putative collagen adhesion protein referred to as BspA in this thesis was found to be reduced by 60% in the *cdg135* mutant compared to wild type (i.e. 2.6 fold higher expression in wild type compared to the *cdg135* mutant). Given the location of *bspA* downstream of a c-di-GMP responsive "on-riboswitch" (Chapter 6.2.1), these results give a further indication of possible DGC activity of Cdg135.

No differential expression of genes affecting motility was however observed contrary to what one would maybe expect after witnessing the distinct difference in motility in the two strains at the time point of analyses. However, the observed increase in motility in the *cdg135* deletion mutant may not be regulated at the transcriptional level. As mentioned in Chapter 1.5.2, *epsE* is part of the *epsA-O* operon in *B. subtilis* and encodes EpsE. When biofilm formation is induced in this species, the *eps* genes are transcribed and EpsE alters the interaction between the flagellar basal body and the proton channel driving flagellar rotation. The flagellum is thereby disengaged from its "power supply" and stops rotating [34]. The same type of regulation is seen in *E. coli* via the protein YcgR which is additionally shown to interact with c-di-GMP [35]. It cannot be excluded that similar mechanisms for regulation exist in Bt407, possibly allowing the regulation of motility at a post-transcriptional level. No locus encoding EPS involved in biofilm formation has yet been identified in the *B. cereus* group, and it is therefore not possible to comment on the organization of these genes in *B. thuringiensis*.

In microarray experiments, after labeling, purifying and up-concentrating cDNA, the samples should be brightly colored. However, in the samples used in the experiments in this thesis, only a weak color could be seen. This could be due to lack of a cooling centrifuge in the lab when synthesizing cDNA from RNA resulting in low concentrations or potentially adverse dye-coupling reactions. The weakly colored samples resulted in low-intensity fluorescent signals upon scanning of the slides, making it necessary to increase the intensity of the scanning beams to an above-optimal level and resulting in a high signal to background noise ratio. This made the analysis of the raw images and the statistical analysis more difficult, as signals form the weakly expressed genes were at a level comparable to the background signal. Only five genes were found to significantly up- or down-regulated and it cannot be excluded that more genes would have been found to be significantly differentially expressed in the *cdg135* deletion strain, if the fluorescent signal from the slides had been of normal intensity.

The oligonucleotides printed on the microarray used in the present study were designed for use in *B. cereus* ATCC 14579, which shows high sequence similarity and a close evolutionary relationship with Bt407. However, small differences between strains in the nucleotide sequence of particular genes and potential resulting cross-hybridization nevertheless posed a problem that had to be taken into account in this experiment. The aldo/keto reductases and MFS-transporters identified in the microarray experiment were in particular subject for such

cross-hybridizations and the expression of all genes found to be up-regulated in the mutant was therefore studied also through RT-qPCR (Table 12, Figure 11).

The degree of up-regulation was generally shown to be much higher in the RT-qPCR experiment than in the microarray experiment (Table 13). Additionally, in RT-qPCR, the gene bthur0002_31280 was up-regulated to a much greater extent than the other genes, but this was not seen in the microarrays. These differences can be partly explained by different sensitivity between the methods. In microarrays, the expression of an exceptional large number of genes is screened simultaneously and the results are based on intensities of signals deriving from amount of dye-coupled cDNA binding to the probes. The analysis gives statistically significant information for genes that are up- or down-regulated, but the relative differential expression in several genes cannot be estimated to the same accuracy as with RT-qPCR. RT-qPCR, on the other hand, uses specific primers for each gene one wishes to examine, and by the use of reference genes, quantitative information on the expression of particular genes is obtained. Additionally, the hybridized slides used in the microarray experiment were of low fluorescent intensity and this may also have affected the accuracy of the results. Finally, the array was not designed for Bt407 and potential cross-hybridizations may also have affected expression ratios for the aldo/keto reductases. The low intensities of fluorescent signals in the experiment may also explain the low expression ratio for the *cdg135* gene in the wild type relative to the *cdg135* mutant. Alternatively, the transcriptional level of *cdg135* is low at this point, and if so, the effect of Cdg135 on expression of downstream genes such as bspA and the aldo/keto reductases requires only low cellular levels of *cdg135* mRNA transcript.

6.2 Role of BspA in biofilm formation in Bt407

6.2.1 BspA

Microarray analysis showed that the gene encoding BspA was down-regulated in the *cdg135* mutant compared to the wild type strain (Table 8). BspA (Figure 12) has the characteristic domain structure of an MSCRAMM (microbial surface components recognizing adhesive matrix molecules) adhesion protein [95, 100], including a non-repetitive N-terminal A-region, a B-repeat region and a proline-rich repeat region (Figure 12B). Proteins within this family have in species like *S. aureus* been shown to be involved in adhesion to surfaces and cell-cell interactions during biofilm formation [30]. BC_1060 in *B. cereus* ATCC 14579 lies downstream of Bc2, a c-di-GMP-responsive “on-riboswitch” [73]. Bt407 was found to have a corresponding riboswitch lying upstream of *bspA*. Eirik Rustan found, in his master thesis [101], indications of decreased biofilm formation when deleting *bspA*. Here, I conclusively

show that the *bspA* deletion mutant is an inefficient biofilm former compared to wild type at 24, 48 and 72 hours (Figure 18). This indicates that BspA is involved in biofilm formation in Bt407. The over-expression strain was however not found to significantly increase biofilm formation (Figure 19). As excessive amounts of the protein do not seem to provide any significant benefit for the bacterium in its ability to form biofilms, the protein may already be present in the cell in saturated concentrations.

6.2.2 Interaction between Cdg135 and BspA

As the expression of the *bspA* gene was down-regulated in the *cdg135* deletion mutant, Cdg135 consequently positively affects the expression of BspA, directly or indirectly. As Cdg135 is predicted to be involved in the synthesis of c-di-GMP, and as the gene encoding BspA is found downstream of a c-di-GMP-sensitive "on-riboswitch", this may be a likely route of direct signaling. It was of interest to investigate whether *bspA* could fully account for the effects observed on biofilm formation when deleting *cdg135*. Over-expression of Cdg135, however, restored biofilm formation in the *bspA* deletion mutant (Figure 21), indicating that Cdg135 controls several factors leading to biofilm formation in addition to BspA, and that over-expression of Cdg135 can compensate for the deletion of *bspA*. Several pathways of signaling are probably controlled by Cdg135 and several of these may be involved, and important, in the formation of biofilms in Bt407. On the other hand, over-expression of BspA did not seem to compensate for the *cdg135* deletion with respect to deficiency in biofilm formation (Figure 20). If the *bspA* construct hosted by this strain encodes functional BspA protein (will be shown by future sequencing of the clone), this could indicate that BspA expression is not enough to restore biofilm formation when the Cdg135 function is lost. The presence of the correct plasmid in this strain does however need to be confirmed before a firm conclusion is drawn, since this strain was not shown to contain the correct plasmid in the PCR-screening (Figure 16), and the strain showed aberrant growth on erythromycin (Figure 17).

6.3 Role of aldo/keto reductases and MFS transporters

Surprisingly, three aldo/keto reductases and two MFS transporters were found to be up-regulated in the *cgd135* deletion mutant (Tables 9 and 12). MFS transporters represent a large group of secondary carriers. Aldo/keto reductases are enzymes involved in a broad spectrum of cellular processes in microbes [102] by catalyzing NADPH-dependent reduction of various substrates [94]. YvgN and YtbE found in *B. subtilis* are proposed to be involved in detoxification of aldehydes derived from bacterial stress [103] and two of the aldo/keto

reductases found to be up-regulated show high amino acid sequence similarity to YtbE. Possibly, deletion of Cdg135 may have caused stress in the bacteria, leading to up-regulation of genes involved in handling the consequences of this stress response. However, no general stress-response genes were found to be differentially expressed.

6.4 Role of Cdg141 in biofilm formation in Bt407

Cdg141 contains a GGDEF domain that apparently lacks the A-site necessary for synthesis of c-di-GMP. It does, however, contain an RxxD motif predicted to function as an I-site involved in allosteric binding to c-di-GMP and possible feedback mechanisms. The over-expression strain as well, as the complemented deletion mutant, had a highly prolonged lag-phase when grown in liquid medium (Figures 26 and 27). The reason why over-expression of Cdg141 interferes with normal growth is not understood. However, it seems to be connected with the RxxD motif, as the over-expression strains with this motif mutated grow normally (Figure 25) and produced biofilm at the same level as wild type (Figures 29 and 30). The fact that both strains began to grow normally after a few hours is curious. One possibility is that the xylose present in the culture medium, inducing expression of Cdg141 from the pHT-pXyl-141 plasmid, may eventually be used up (if Bt407 can use xylose as a carbon source) so that the gene on the plasmid is no longer expressed. As the bacteria are grown in a nutrient rich medium and for a relatively short period of time, this seems unlikely. Another possibility is that the antibiotics present in the medium may be used up, with the consequence that the bacteria lose their plasmids due to lack of selection. However, this is not probable considering the time perspective. Finally, the bacterium may acquire a mutation, e.g. in the plasmid-borne *cdg141* gene or promoter region, potentially leaving the *cdg141* gene non-functional or not expressed. As the plasmid contains a xylose inducible promoter, xylose titrations were performed (Figures 26 and 27). The variability in lag time seemed to be dependent on the amount of xylose added to the culture medium (in the concentration interval 0.1 mM to 1 mM, Figure 27). This could be a result of the xylose-dependent promoter being gradually induced in tes xylose concentration interval. Veronika Smith in the group performed a follow-up experiment by reinoculating the Cdg141 over-expression strain after growth adaption, and studying the growth curve again, under the same conditions. The lag-phase delay was then lost, and this indicates that growth adaption is due to an acquired mutation, either in the plasmid-borne *cdg141* gene or the promoter region of the vector, or as a compensating/suppressing mutation in the bacterial chromosome. Over-expression of Cdg141 is thus incompatible with normal growth in Bt407 and Bt407Δ141.

The microarray experiment comparing Bt407 wild type and *cdg141* deletion mutant showed no statistically significant up- or down-regulated genes with adjusted P-values<0.05. Again, the dye-coupled cDNA samples were color-weak and the hybridizations were probably affected by this, possibly camouflaging genes that in reality may have been significantly differentially regulated. On the other hand, deletion of *cdg141* may have none or only subtle effect on transcription of genes at this particular point of growth under the tested conditions.

Biofilm assays performed in this thesis showed that Bt407 wild type and *cdg141* deletion mutant were equally efficient biofilm formers (Figure 28). Over-expression of Cdg141, however, reduced biofilm formation to a minimum (Figure 29), but this effect was most probably due to strongly reduced growth of the over-expression strain. Thus, there are no results to indicate that Cdg141 is involved in regulating the formation of biofilms in Bt407. However, the effects in the deletion strain may only be very subtle and not detected in the assays used, and any potential effects in the over-expression strain may be masked by the growth defect of the strain.

6.5 Role of Cdg113 in biofilm formation in Bt407

Cdg113 contains an EAL domain lacking the active site motif necessary for PDE activity and is therefore probably not involved in the breakdown of c-di-GMP. Cdg113 is 55% identical to the protein YkuI in *B. subtilis* in terms of amino acid sequence [104]. YkuI contains a non-active EAL domain and has been shown unable to degenerate c-di-GMP molecules. The YkuI_C domain is located at the C-terminal of Cdg113 and contains a possible ligand binding site similar to those found in PAS and GAF domains [104].

Biofilm assays performed in this thesis showed that the *cdg113* deletion mutant produced biofilm at approximately the same level as the Bt407 wild type (Figure 32). The over-expression strain, however, showed increased biofilm formation compared to wild type, especially when allowed to grow for 72 hours (Figure 33). This effect was also seen when complementing the deletion mutant (Figure 34). These results indicate that Cdg113 is somehow able to positively affect the formation of biofilms in Bt407. As this protein contains an EAL domain, but probably lacks enzymatic activity and therefore cannot metabolize c-di-GMP, it may play a role as an effector molecule. YkuI was shown to be able to bind to c-di-GMP [104], and possibly, so is Cdg113. Cdg113 may therefore function as a regulator of biofilm formation in Bt407 upon binding to c-di-GMP.

6.6 Conclusions

Results from the current thesis indicate that Cdg135 probably is involved in controlling biofilm formation and motility in Bt407, possibly by exhibiting DGC activity and catalyzing the synthesis c-di-GMP. Cdg135 was shown to positively affect the expression of the gene *bspA* which is located downstream of a c-di-GMP-sensitive "on-riboswitch" and the protein encoded by *bspA* appears to stimulate biofilm formation in Bt407. The effects of BspA are, however, not essential for the ability of Bt407 to form biofilms, as Cdg135 over-expression could compensate for its loss. Cdg141 does not seem to influence biofilm formation in Bt407, but excessive amounts of Cdg141 probably has toxic effects, as the over-expression strain showed a growth defect. Results from biofilm assays indicated that Cdg113 positively effects biofilm formation in Bt407. As Cdg113 probably lacks enzymatic activity, it could function as an effector molecule, regulating biofilm formation upon binding c-di-GMP.

6.7 Future perspectives

It will be of great interest to study all genes in Bt407 predicted to be involved in metabolism and sensing of c-di-GMP in the future. The functional characterization of Cdg135, Cdg141 and Cdg113 should also be continued. The down-regulation of *bspA* in the *cdg135* mutant compared with the wild type strain, as shown by microarray analysis, should be confirmed through RT-qPCR and the whole microarray experiment could advantageously be repeated. As the effect of Cdg135 on biofilm formation does not seem to be dependent on BspA alone, it would be of interest to find other signaling pathways that are controlled by Cdg135 and that may be involved in biofilm formation in Bt407. Additionally, the three aldo/keto reductase and two MFS transporter genes found to be up-regulated in the *cdg135* mutant should be examined more closely as their role in Bt407 is poorly understood.

The lack of growth observed when over-expressing Cdg141 could be due to toxic effects of Cdg141 or due to functions possibly regulated by Cdg141, and to investigate this further would be appropriate. Plasmids can additionally be isolated from strains of over-expression Cdg141 after growth adaption and sequenced to look for accumulating mutations in *cdg141* or elsewhere on the plasmid or genome. This could potentially contribute to identifying functional parts of Cdg141. It would also be relevant to study the gene *cdg141* further with respect to possible involvement in feedback mechanisms through binding to c-di-GMP via the I-site. Additional microarray experiments are also relevant for studying the effects of Cdg141 further.

Cdg113 was predicted to lack enzymatic activity, but over-expression of the gene enhances biofilm formation. Cdg113 was in this thesis proposed to function as an effector molecule and it would be interesting to perform a whole-genome transcriptional analysis using microarrays to identify possible target molecules potentially regulated by Cdg113.

Additionally, studies of deletion- and over-expression strains of the *cdg* genes in Bt407 with the aim of quantifying levels of c-di-GMP at different time-points in the growth curve are initiated. These studies will provide important information about the influence of the Cdg proteins on c-di-GMP concentration, give indications of enzymatic activity and help to explain observed effects on biofilm formation. Finally, it would be highly interesting to identify what types of signals induce expression of the genes encoding the c-di-GMP metabolizing and/or -sensing proteins.

APPENDICES

Appendix 1: Analysis of microarray experiment comparing *cdg135* deletion mutant and wild type

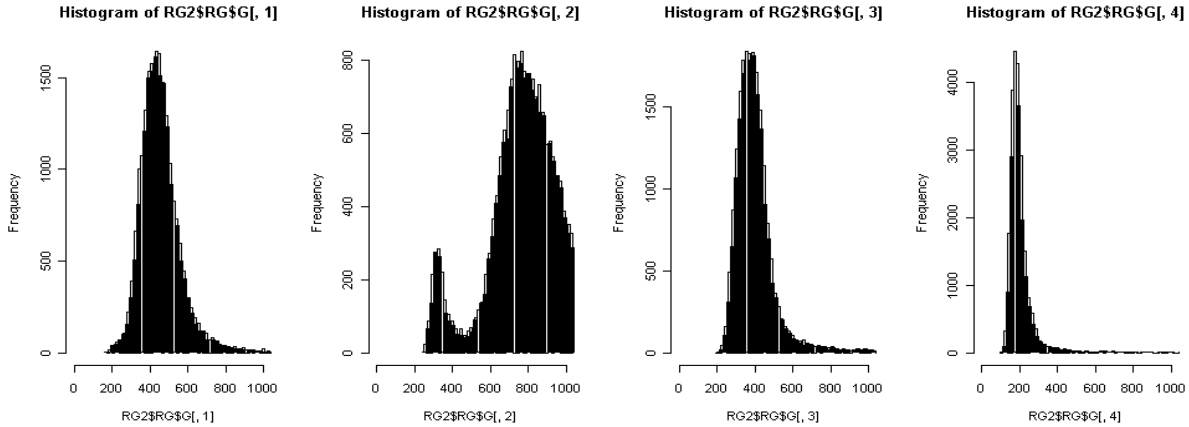

Figure 35: Histograms from analysis of microarray experiment comparing wild type and *cdg135* deletion mutant showing distribution of green spot signal intensities. Histogram 1 to 4 represent slide 1 to 4 respectively.

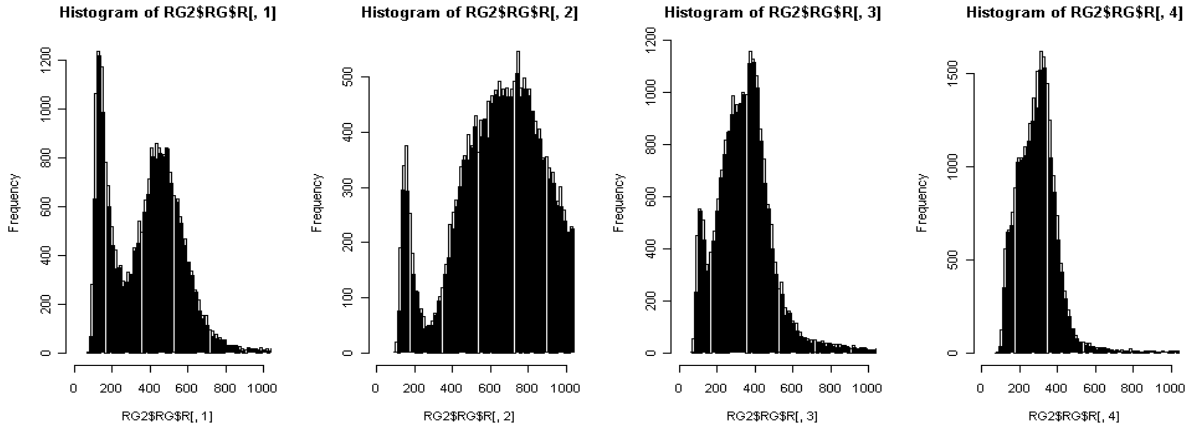

Figure 36: Histograms from analysis of microarray experiment comparing wild type and *cdg135* deletion mutant showing distribution of red spot signal intensities. Histogram 1 to 4 represent slide 1 to 4 respectively.

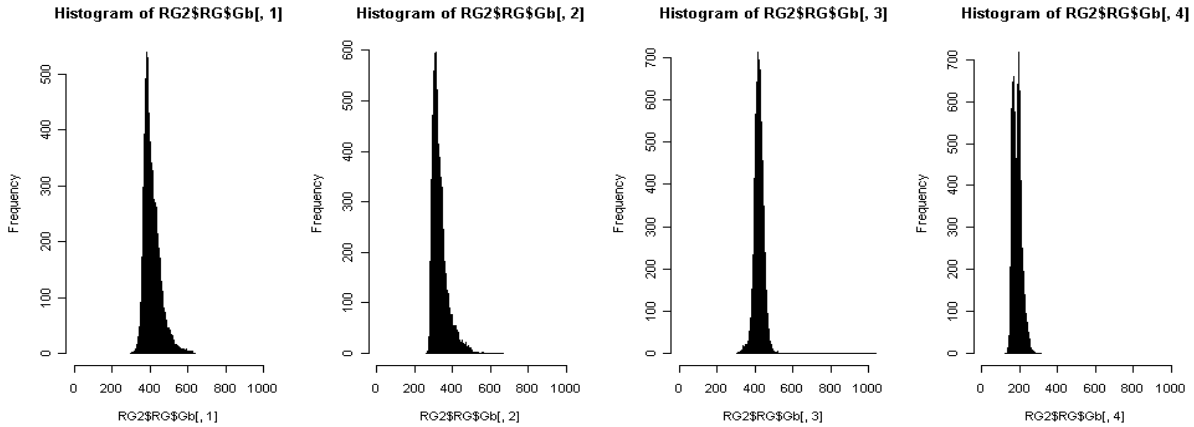

Figure 37: Histograms from analysis of microarray experiment comparing wild type and *cdg135* deletion mutant showing distribution of green background signal intensities. Histogram 1 to 4 represent slide 1 to 4 respectively.

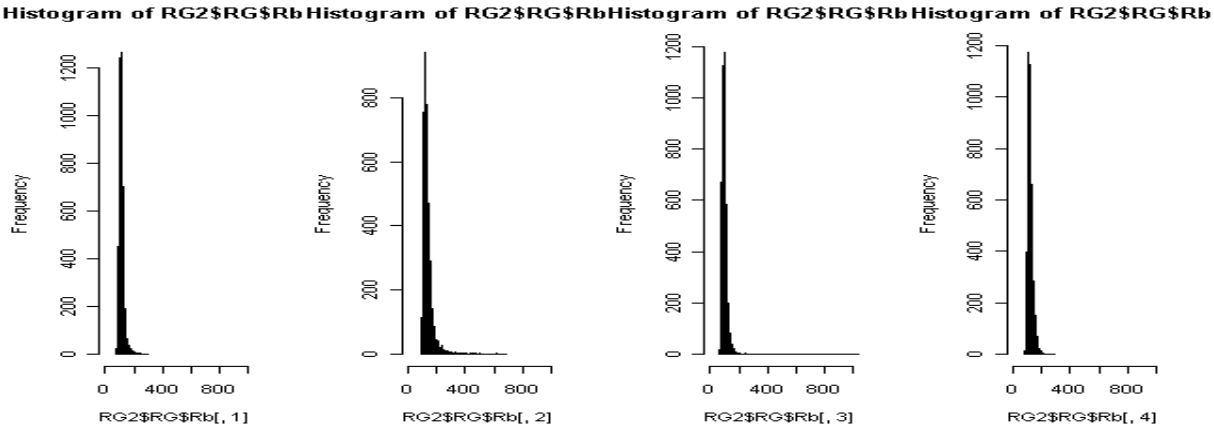

Figure 38: Histograms from analysis of microarray experiment comparing wild type and *cdg135* deletion mutant showing distribution of red background signal intensities. Histogram 1 to 4 represent slide 1 to 4 respectively.

Appendix 2: Analysis of microarray experiment comparing *cdg141* deletion mutant and wild type

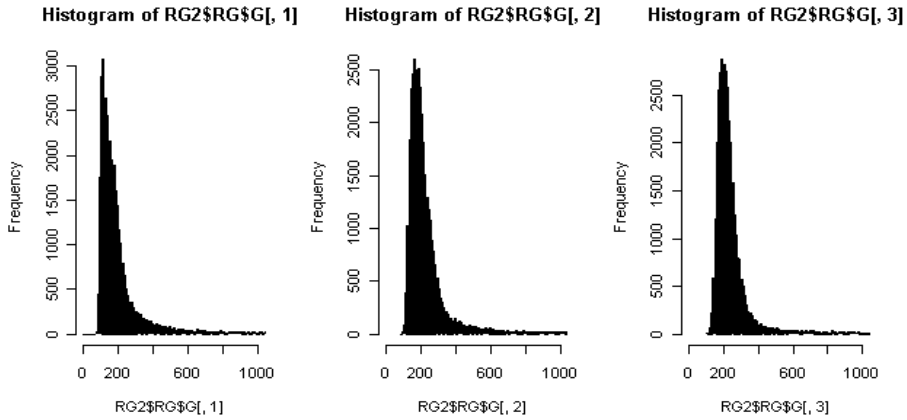

Figure 39: Histograms from analysis of microarray experiment comparing wild type and *cdg141* deletion mutant showing distribution of green spot signal intensities. Histogram 1 to 3 represent slide 1 to 3 respectively.

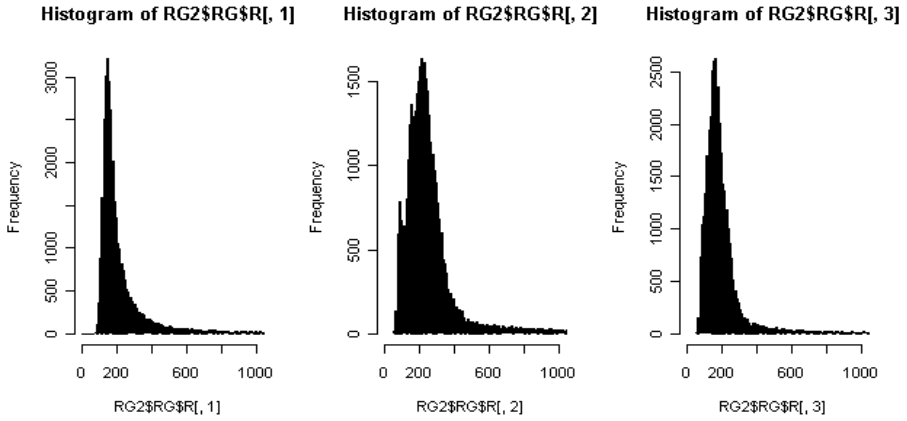

Figure 40: Histograms from analysis of microarray experiment comparing wild type and *cdg141* deletion mutant showing distribution of red spot signal intensities. Histogram 1 to 3 represent slide 1 to 3 respectively.

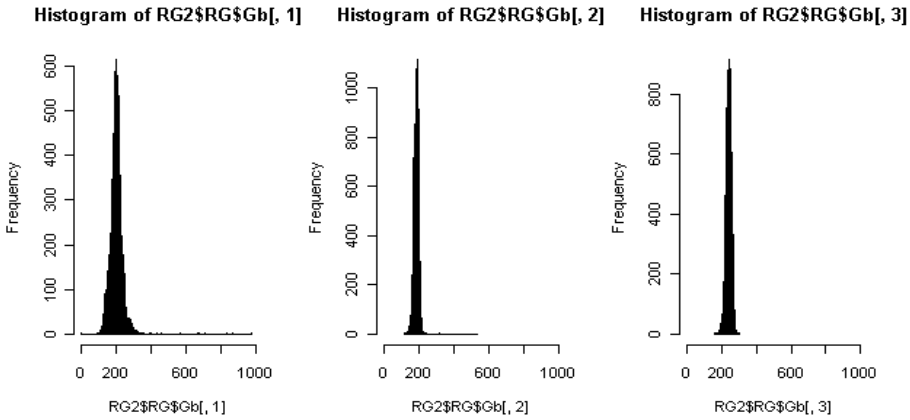

Figure 41: Histograms from analysis of microarray experiment comparing wild type and *cdg141* deletion mutant showing distribution of green background signal intensities. Histogram 1 to 3 represent slide 1 to 3 respectively.

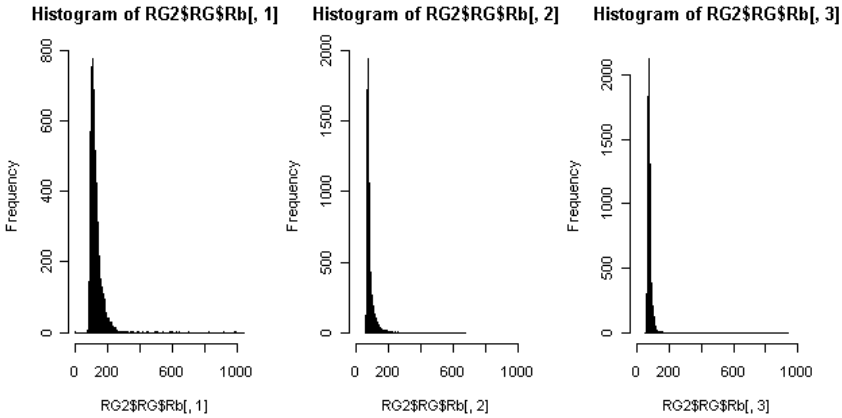

Figure 42: Histograms from analysis of microarray experiment comparing wild type and *cdg141* deletion mutant showing distribution of red background signal intensities. Histogram 1 to 3 represent slide 1 to 3 respectively.

REFERENCES

1. Rasko, D.A., et al., *Genomics of the Bacillus cereus group of organisms.* FEMS Microbiol Rev, 2005. **29**(2): p. 303-29.
2. Drobniewski, F.A., *Bacillus cereus and related species.* Clin Microbiol Rev, 1993. **6**(4): p. 324-38.
3. Guinebretiere, M.H., et al., *Bacillus cytotoxicus sp. nov. is a new thermotolerant species of the Bacillus cereus group occasionally associated with food poisoning.* Int J Syst Evol Microbiol, 2012.
4. Helgason, E., et al., *Bacillus anthracis, Bacillus cereus, and Bacillus thuringiensis--one species on the basis of genetic evidence.* Appl Environ Microbiol, 2000. **66**(6): p. 2627-30.
5. Mock, M. and A. Fouet, *Anthrax.* Annu Rev Microbiol, 2001. **55**: p. 647-71.
6. Okinaka, R., et al., *Sequence, assembly and analysis of pX01 and pX02.* J Appl Microbiol, 1999. **87**(2): p. 261-2.
7. Okinaka, R.T., et al., *Sequence and organization of pXO1, the large Bacillus anthracis plasmid harboring the anthrax toxin genes.* J Bacteriol, 1999. **181**(20): p. 6509-15.
8. Kolsto, A.B., N.J. Tourasse, and O.A. Okstad, *What sets Bacillus anthracis apart from other Bacillus species?* Annu Rev Microbiol, 2009. **63**: p. 451-76.
9. Bottone, E.J., *Bacillus cereus, a volatile human pathogen.* Clin Microbiol Rev, 2010. **23**(2): p. 382-98.
10. Paredes-Sabja, D., P. Setlow, and M.R. Sarker, *Germination of spores of Bacillales and Clostridiales species: mechanisms and proteins involved.* Trends Microbiol, 2011. **19**(2): p. 85-94.
11. Ehling-Schulz, M., et al., *Cereulide synthetase gene cluster from emetic Bacillus cereus: structure and location on a mega virulence plasmid related to Bacillus anthracis toxin plasmid pXO1.* BMC Microbiol, 2006. **6**: p. 20.
12. Shiota, M., et al., *Rapid detoxification of cereulide in Bacillus cereus food poisoning.* Pediatrics, 2010. **125**(4): p. e951-5.
13. Dierick, K., et al., *Fatal family outbreak of Bacillus cereus-associated food poisoning.* J Clin Microbiol, 2005. **43**(8): p. 4277-9.
14. Jensen, G.B., et al., *The hidden lifestyles of Bacillus cereus and relatives.* Environ Microbiol, 2003. **5**(8): p. 631-40.
15. O'Toole, G., H.B. Kaplan, and R. Kolter, *Biofilm formation as microbial development.* Annu Rev Microbiol, 2000. **54**: p. 49-79.
16. Karatan, E. and P. Watnick, *Signals, regulatory networks, and materials that build and break bacterial biofilms.* Microbiol Mol Biol Rev, 2009. **73**(2): p. 310-47.
17. Davey, M.E. and A. O'Toole G, *Microbial biofilms: from ecology to molecular genetics.* Microbiol Mol Biol Rev, 2000. **64**(4): p. 847-67.
18. Schlegelova, J. and S. Karpiskova, *[Microbial biofilms in the food industry].* Epidemiol Mikrobiol Imunol, 2007. **56**(1): p. 14-9.
19. Lemon, K.P., et al., *Biofilm development with an emphasis on Bacillus subtilis.* Curr Top Microbiol Immunol, 2008. **322**: p. 1-16.
20. Domka, J., et al., *Temporal gene-expression in Escherichia coli K-12 biofilms.* Environ Microbiol, 2007. **9**(2): p. 332-46.
21. Cucarella, C., et al., *Bap, a Staphylococcus aureus surface protein involved in biofilm formation.* J Bacteriol, 2001. **183**(9): p. 2888-96.
22. Lasa, I. and J.R. Penades, *Bap: a family of surface proteins involved in biofilm formation.* Res Microbiol, 2006. **157**(2): p. 99-107.
23. Diggle, S.P., et al., *The galactophilic lectin, LecA, contributes to biofilm development in Pseudomonas aeruginosa.* Environ Microbiol, 2006. **8**(6): p. 1095-104.
24. Tielker, D., et al., *Pseudomonas aeruginosa lectin LecB is located in the outer membrane and is involved in biofilm formation.* Microbiology, 2005. **151**(Pt 5): p. 1313-23.

25. Lynch, D.J., et al., *Glucan-binding proteins are essential for shaping Streptococcus mutans biofilm architecture.* FEMS Microbiol Lett, 2007. **268**(2): p. 158-65.
26. Klemm, P., R.M. Vejborg, and O. Sherlock, *Self-associating autotransporters, SAATs: functional and structural similarities.* Int J Med Microbiol, 2006. **296**(4-5): p. 187-95.
27. Matsukawa, M. and E.P. Greenberg, *Putative exopolysaccharide synthesis genes influence Pseudomonas aeruginosa biofilm development.* J Bacteriol, 2004. **186**(14): p. 4449-56.
28. Vilain, S., et al., *DNA as an adhesin: Bacillus cereus requires extracellular DNA to form biofilms.* Appl Environ Microbiol, 2009. **75**(9): p. 2861-8.
29. Monds, R.D. and G.A. O'Toole, *The developmental model of microbial biofilms: ten years of a paradigm up for review.* Trends Microbiol, 2009. **17**(2): p. 73-87.
30. Heilmann, C., *Adhesion mechanisms of staphylococci.* Adv Exp Med Biol, 2011. **715**: p. 105-23.
31. O'Gara, J.P., *ica and beyond: biofilm mechanisms and regulation in Staphylococcus epidermidis and Staphylococcus aureus.* FEMS Microbiol Lett, 2007. **270**(2): p. 179-88.
32. Houry, A., et al., *Involvement of motility and flagella in Bacillus cereus biofilm formation.* Microbiology, 2010. **156**(Pt 4): p. 1009-18.
33. Lemon, K.P., D.E. Higgins, and R. Kolter, *Flagellar motility is critical for Listeria monocytogenes biofilm formation.* J Bacteriol, 2007. **189**(12): p. 4418-24.
34. Blair, K.M., et al., *A molecular clutch disables flagella in the Bacillus subtilis biofilm.* Science, 2008. **320**(5883): p. 1636-8.
35. Armitage, J.P. and R.M. Berry, *Time for bacteria to slow down.* Cell, 2010. **141**(1): p. 24-6.
36. Marvasi, M., P.T. Visscher, and L. Casillas Martinez, *Exopolymeric substances (EPS) from Bacillus subtilis: polymers and genes encoding their synthesis.* FEMS Microbiol Lett, 2010. **313**(1): p. 1-9.
37. Garrett, E.S., D. Perlegas, and D.J. Wozniak, *Negative control of flagellum synthesis in Pseudomonas aeruginosa is modulated by the alternative sigma factor AlgT (AlgU).* J Bacteriol, 1999. **181**(23): p. 7401-4.
38. Dobinsky, S., et al., *Glucose-related dissociation between icaADBC transcription and biofilm expression by Staphylococcus epidermidis: evidence for an additional factor required for polysaccharide intercellular adhesin synthesis.* J Bacteriol, 2003. **185**(9): p. 2879-86.
39. Shemesh, M., A. Tam, and D. Steinberg, *Expression of biofilm-associated genes of Streptococcus mutans in response to glucose and sucrose.* J Med Microbiol, 2007. **56**(Pt 11): p. 1528-35.
40. Singh, P.K., et al., *A component of innate immunity prevents bacterial biofilm development.* Nature, 2002. **417**(6888): p. 552-5.
41. Deighton, M. and R. Borland, *Regulation of slime production in Staphylococcus epidermidis by iron limitation.* Infect Immun, 1993. **61**(10): p. 4473-9.
42. O'Toole, G.A. and R. Kolter, *Initiation of biofilm formation in Pseudomonas fluorescens WCS365 proceeds via multiple, convergent signalling pathways: a genetic analysis.* Mol Microbiol, 1998. **28**(3): p. 449-61.
43. Hung, D.T., et al., *Bile acids stimulate biofilm formation in Vibrio cholerae.* Mol Microbiol, 2006. **59**(1): p. 193-201.
44. Hoffman, L.R., et al., *Aminoglycoside antibiotics induce bacterial biofilm formation.* Nature, 2005. **436**(7054): p. 1171-5.
45. Vuong, C., et al., *Impact of the agr quorum-sensing system on adherence to polystyrene in Staphylococcus aureus.* J Infect Dis, 2000. **182**(6): p. 1688-93.
46. Branda, S.S., et al., *A major protein component of the Bacillus subtilis biofilm matrix.* Mol Microbiol, 2006. **59**(4): p. 1229-38.
47. Branda, S.S., et al., *Fruiting body formation by Bacillus subtilis.* Proc Natl Acad Sci U S A, 2001. **98**(20): p. 11621-6.
48. Hamon, M.A. and B.A. Lazazzera, *The sporulation transcription factor Spo0A is required for biofilm development in Bacillus subtilis.* Mol Microbiol, 2001. **42**(5): p. 1199-209.

49. Romero, D., et al., *An accessory protein required for anchoring and assembly of amyloid fibres in B. subtilis biofilms.* Mol Microbiol, 2011. **80**(5): p. 1155-68.
50. Terra, R., et al., *Identification of Bacillus subtilis SipW as a Bifunctional Signal Peptidase that Controls Surface-Adhered Biofilm Formation.* J Bacteriol, 2012.
51. Kearns, D.B., et al., *A master regulator for biofilm formation by Bacillus subtilis.* Mol Microbiol, 2005. **55**(3): p. 739-49.
52. Shafikhani, S.H., et al., *Postexponential regulation of sin operon expression in Bacillus subtilis.* J Bacteriol, 2002. **184**(2): p. 564-71.
53. Bai, U., I. Mandic-Mulec, and I. Smith, *SinI modulates the activity of SinR, a developmental switch protein of Bacillus subtilis, by protein-protein interaction.* Genes Dev, 1993. **7**(1): p. 139-48.
54. Chu, F., et al., *A novel regulatory protein governing biofilm formation in Bacillus subtilis.* Mol Microbiol, 2008. **68**(5): p. 1117-27.
55. Branda, S.S., et al., *Genes involved in formation of structured multicellular communities by Bacillus subtilis.* J Bacteriol, 2004. **186**(12): p. 3970-9.
56. Oosthuizen, M.C., et al., *Proteomic analysis reveals differential protein expression by Bacillus cereus during biofilm formation.* Appl Environ Microbiol, 2002. **68**(6): p. 2770-80.
57. Auger, S., et al., *Autoinducer 2 affects biofilm formation by Bacillus cereus.* Appl Environ Microbiol, 2006. **72**(1): p. 937-41.
58. Hsueh, Y.H., et al., *Biofilm formation by Bacillus cereus is influenced by PlcR, a pleiotropic regulator.* Appl Environ Microbiol, 2006. **72**(7): p. 5089-92.
59. Wijman, J.G., et al., *Air-liquid interface biofilms of Bacillus cereus: formation, sporulation, and dispersion.* Appl Environ Microbiol, 2007. **73**(5): p. 1481-8.
60. Hsueh, Y.H., E.B. Somers, and A.C. Wong, *Characterization of the codY gene and its influence on biofilm formation in Bacillus cereus.* Arch Microbiol, 2008. **189**(6): p. 557-68.
61. Lindback, T., et al., *CodY, a pleiotropic regulator, influences multicellular behaviour and efficient production of virulence factors in Bacillus cereus.* Environ Microbiol, 2012.
62. Auger, S., et al., *Biofilm formation and cell surface properties among pathogenic and nonpathogenic strains of the Bacillus cereus group.* Appl Environ Microbiol, 2009. **75**(20): p. 6616-8.
63. Karunakaran, E. and C.A. Biggs, *Mechanisms of Bacillus cereus biofilm formation: an investigation of the physicochemical characteristics of cell surfaces and extracellular proteins.* Appl Microbiol Biotechnol, 2011. **89**(4): p. 1161-75.
64. Pflughoeft, K.J., P. Sumby, and T.M. Koehler, *Bacillus anthracis sin locus and regulation of secreted proteases.* J Bacteriol, 2011. **193**(3): p. 631-9.
65. Hengge, R., *Principles of c-di-GMP signalling in bacteria.* Nat Rev Microbiol, 2009. **7**(4): p. 263-73.
66. Ryan, R.P., T. Tolker-Nielsen, and J.M. Dow, *When the PilZ don't work: effectors for cyclic di-GMP action in bacteria.* Trends Microbiol, 2012.
67. Amikam, D. and M.Y. Galperin, *PilZ domain is part of the bacterial c-di-GMP binding protein.* Bioinformatics, 2006. **22**(1): p. 3-6.
68. Hickman, J.W. and C.S. Harwood, *Identification of FleQ from Pseudomonas aeruginosa as a c-di-GMP-responsive transcription factor.* Mol Microbiol, 2008. **69**(2): p. 376-89.
69. Christen, M., et al., *Identification and characterization of a cyclic di-GMP-specific phosphodiesterase and its allosteric control by GTP.* J Biol Chem, 2005. **280**(35): p. 30829-37.
70. Newell, P.D., R.D. Monds, and G.A. O'Toole, *LapD is a bis-(3',5')-cyclic dimeric GMP-binding protein that regulates surface attachment by Pseudomonas fluorescens Pf0-1.* Proc Natl Acad Sci U S A, 2009. **106**(9): p. 3461-6.
71. Lee, V.T., et al., *A cyclic-di-GMP receptor required for bacterial exopolysaccharide production.* Mol Microbiol, 2007. **65**(6): p. 1474-84.
72. Tucker, B.J. and R.R. Breaker, *Riboswitches as versatile gene control elements.* Curr Opin Struct Biol, 2005. **15**(3): p. 342-8.

73. Sudarsan, N., et al., *Riboswitches in eubacteria sense the second messenger cyclic di-GMP.* Science, 2008. **321**(5887): p. 411-3.
74. Lee, E.R., et al., *An allosteric self-splicing ribozyme triggered by a bacterial second messenger.* Science, 2010. **329**(5993): p. 845-8.
75. Povolotsky, T.L. and R. Hengge, *'Life-style' control networks in Escherichia coli: Signaling by the second messenger c-di-GMP.* J Biotechnol, 2011.
76. Bobrov, A.G., et al., *Systematic analysis of cyclic di-GMP signalling enzymes and their role in biofilm formation and virulence in Yersinia pestis.* Mol Microbiol, 2011. **79**(2): p. 533-51.
77. Merritt, J.H., et al., *Specific control of Pseudomonas aeruginosa surface-associated behaviors by two c-di-GMP diguanylate cyclases.* MBio, 2010. **1**(4).
78. Lim, B., et al., *Cyclic-diGMP signal transduction systems in Vibrio cholerae: modulation of rugosity and biofilm formation.* Mol Microbiol, 2006. **60**(2): p. 331-48.
79. Bordeleau, E., et al., *c-di-GMP turn-over in Clostridium difficile is controlled by a plethora of diguanylate cyclases and phosphodiesterases.* PLoS Genet, 2011. **7**(3): p. e1002039.
80. Purcell, E.B., et al., *Cyclic diguanylate inversely regulates motility and aggregation in Clostridium difficile.* J Bacteriol, 2012.
81. Lereclus, D., et al., *Transformation and expression of a cloned delta-endotoxin gene in Bacillus thuringiensis.* FEMS Microbiol Lett, 1989. **51**(1): p. 211-7.
82. Galperin, M.Y., *Bacterial signal transduction network in a genomic perspective.* Environ Microbiol, 2004. **6**(6): p. 552-67.
83. Arantes, O. and D. Lereclus, *Construction of cloning vectors for Bacillus thuringiensis.* Gene, 1991. **108**(1): p. 115-9.
84. Pospiech, A. and B. Neumann, *A versatile quick-prep of genomic DNA from gram-positive bacteria.* Trends Genet, 1995. **11**(6): p. 217-8.
85. Gibbs, R.A., *DNA amplification by the polymerase chain reaction.* Anal Chem, 1990. **62**(13): p. 1202-14.
86. Voytas, D., *Agarose gel electrophoresis.* Curr Protoc Immunol, 2001. **Chapter 10**: p. Unit 10 4.
87. Gallagher, S., *Quantitation of nucleic acids with absorption spectroscopy.* Curr Protoc Protein Sci, 2001. **Appendix 4**: p. Appendix 4K.
88. Ehrenreich, A., *DNA microarray technology for the microbiologist: an overview.* Appl Microbiol Biotechnol, 2006. **73**(2): p. 255-73.
89. Fægri, K., *Adaptive responses in Bacillus cereus group bacteria– microarray comparisons and follow-up studies*, in *Department of Pharmaceutical Biosciences*2010, University of Oslo.
90. Smyth, G.K., J. Michaud, and H.S. Scott, *Use of within-array replicate spots for assessing differential expression in microarray experiments.* Bioinformatics, 2005. **21**(9): p. 2067-75.
91. Nolan, T., R.E. Hands, and S.A. Bustin, *Quantification of mRNA using real-time RT-PCR.* Nat Protoc, 2006. **1**(3): p. 1559-82.
92. Reiter, L., A.B. Kolsto, and A.P. Piehler, *Reference genes for quantitative, reverse-transcription PCR in Bacillus cereus group strains throughout the bacterial life cycle.* J Microbiol Methods, 2011. **86**(2): p. 210-7.
93. Pfaffl, M.W., *A new mathematical model for relative quantification in real-time RT-PCR.* Nucleic Acids Res, 2001. **29**(9): p. e45.
94. Ni, Y., et al., *Biocatalytic properties of a recombinant aldo-keto reductase with broad substrate spectrum and excellent stereoselectivity.* Appl Microbiol Biotechnol, 2011. **89**(4): p. 1111-8.
95. Patti, J.M., et al., *MSCRAMM-mediated adherence of microorganisms to host tissues.* Annu Rev Microbiol, 1994. **48**: p. 585-617.
96. Krasteva, P.V., et al., *Vibrio cholerae VpsT regulates matrix production and motility by directly sensing cyclic di-GMP.* Science, 2010. **327**(5967): p. 866-8.
97. Kuchma, S.L., et al., *BifA, a cyclic-Di-GMP phosphodiesterase, inversely regulates biofilm formation and swarming motility by Pseudomonas aeruginosa PA14.* J Bacteriol, 2007. **189**(22): p. 8165-78.

98. Beloin, C., et al., *Global impact of mature biofilm lifestyle on Escherichia coli K-12 gene expression.* Mol Microbiol, 2004. **51**(3): p. 659-74.
99. Spangler, C., et al., *A liquid chromatography-coupled tandem mass spectrometry method for quantitation of cyclic di-guanosine monophosphate.* J Microbiol Methods, 2010. **81**(3): p. 226-31.
100. Krishnan, V. and S.V. Narayana, *Crystallography of gram-positive bacterial adhesins.* Adv Exp Med Biol, 2011. **715**: p. 175-95.
101. Rustan, E.B., *Biofilm formation in Bacillus thuringiensis*, in *Department of Pharmaceutical Biosciences*2010, University of Oslo.
102. Ellis, E.M., *Microbial aldo-keto reductases.* FEMS Microbiol Lett, 2002. **216**(2): p. 123-31.
103. Lei, J., et al., *Structural and biochemical analyses of YvgN and YtbE from Bacillus subtilis.* Protein Sci, 2009. **18**(8): p. 1792-800.
104. Minasov, G., et al., *Crystal structures of YkuI and its complex with second messenger cyclic Di-GMP suggest catalytic mechanism of phosphodiester bond cleavage by EAL domains.* J Biol Chem, 2009. **284**(19): p. 13174-84.